Kinetics of the S_N1 dissociation of ligands L (nitriles, phosphines) in the complexes $[CpFe(P\text{-}P)L]PF_6$ with variable chelate ring size. A surprising bimolecular substitution in the non-chelate complex $[CpFe(PPh_2Me)_2L]PF_6$

Henri Brunner,*[a] Hikaru Kitamura,[b] and Takashi Tsuno*[b]

[a]*Institut für Anorganische Chemie, Universität Regensburg, 93040 Regensburg, Germany.*
E-mail: henri.brunner@chemie-uni.regensburg.de
[b]*Department of Applied Molecular Chemistry, College of Industrial Technology,*
Nihon University, Chiba 275-8575, Japan.
E-mail: tsuno.takashi@nihon.-u.ac.jp

Contents

Table S1. Crystallographic Data for the Complexes (MoK_α radiation)

Complex	[CpFe(dppe)NCMe]PF_6	[CpFe(dppe)PPh_2-(OMe)]PF_6	[CpFe(dppe)PPh_2-(OEt)]PF_6	[CpFe(dppe)PPh_2-(O*i*Pr)]PF_6 $CHCl_3$	[CpFe(dppe)P$(OM)_3$] PF_6
Empirical formula	$C_{33}H_{32}FeNP_2$, F_6P	$C_{44}H_{42}FeOP_3$, F_6P	$C_{45}H_{44}FeP_3$, F_6P	$C_{46}H_{46}FeOP_3$, $CHCl_3$, F_6P	$C_{34}H_{38}FeO_3P_3$, F_6P
Formula weight	705.35	880.5	894.53	1027.93	788.37
Crystal system	monoclinic	monoclinic	Monoclinic	triclinic	monoclinic
Space group	$P2_1$/n	$C$2/c	$C$2/c	$P\bar{1}$	$P2_1$/c
a (Å)	12.4692(5)	38.785(13)	37.9260(12)	10.8369(8)	11.1635(4)
b (Å)	15.5620(6)	12.895(4)	12.6048(5)	12.6462(9)	16.6012(6)
c (Å)	16.9467(5)	16.767(4)	18.0209(6)	17.9320(14)	19.9065(7)
α (°)	90	90	90	77.660(2)	90
β (°)	99.3700(10)	104.747(10)	105.1740(10)	79.840(2)	107.2940(10)
γ (°)	90	90	90	75.172(2)	90
V (Å)^3	3244.6(2)	8109(4)	8314.4(5)	2301.4(3)	3522.4(2)
Z	4	8	8	2	4
ρcalcd (Mg/m^3)	1.4424	1.442	1.429	1.483	1.487
Abs coeff (mm^{-1})	0.672	0.592	0.579	0.702	0.676
Abs correct	multi-scan	multi-scan	multi-scan	multi-scan	multi-scan
Transmiss max/min	1.0000/0.7731	1.0000/0.5305	1.0000/0.5305	1.0000/0.6457	1.0000/0.4249
F (000)	1448	3632	3696	1056	1624
Crystal size (mm)	0.25 x 0.17 x 0.15	0.24 x 0.07 x 0.05	0.23 x 0.20 x 0.14	0.38 x 0.17 x 0.10	0.38 x 0.18 x 0.08
Θ range (°)	3.013-24.999	3.07-24.997	3.02-25	3.08-27.408	3.10-25
Rflns/unique	24949/5702	27894/6912	30802/7298	22240/10310	26969/6195
R_{int}	0.0528	0.1417	0.0835	0.0619	0.0745
Data/params	5702/398	6912/506	7298/514	10310/561	6195/436
Goodness of fit F^2	1.039	0.909	1.087	1.088	1.058
R_1/wR_2 (I>2σ(I))	0.0396/0.0850	0.084/0.1786	0.051/0.1182	0.0529/0.1133	0.0413/0.1009
R_1/wR_2 (all data)	0.0544/0.0916	0.1411/0.2155	0.0835/0.1382	0.0922/0.137	0.0549/0.1087
Abs. struct. param	-	-	-	-	-
Largest diff. peak and hole (e Å^{-3})	0.473/-0.321	0.424/-0.484	0.505/-0.427	0.709/-0.682	0.619/-0.47
CCDC No.	1535363	1535364	1535365	1535366	1535367

Table S1. Crystallographic Data for the Complexes (MoK_α radiation)

Complex	[CpFe(dppe)PPh-(OMe)$_2$]PF_6	[CpFe(PPh_2Me)$_2$NCMe]PF_6	[CpFe(PPh_2Me)$_2$-P(OMe)$_3$]PF_6 CH_2Cl_2	[CpFe(PPh_2Me)$_2$-PPh(OMe)$_2$]PF_6 CH_2Cl_2	[CpFe(PPh_2Me)$_2$I] CH_2Cl_2
Empirical formula	$C_{39}H_{40}FeO_2P_3$, F_6P	$C_{33}H_{34}NP_2Fe$, F_6P	$C_{34}H_{40}FeOP_2$, F_6P, CH_2Cl_2	$C_{39}H_{42}FeO_2P_3$, F_6P, CH_2Cl_2	$C_{31}H_{31}FeIP_2$, CH_2Cl_2
Formula weight	830.41	707.37	875.31	921.38	733.17
Crystal system	orthorhombic	triclinic	Monoclinic	monoclinic	triclinic
Space group	*Pbca*	$P\bar{1}$	$P2_1/c$	$P2_1/n$	$P\bar{1}$
a (Å)	12.2498(4)	9.493(5)	8.9902(2)	11.6214(11)	10.035(4)
b (Å)	19.1993(9)	12.392(5)	22.0037(6)	23.3763(19)	11.862(5)
c (Å)	31.6611(12)	14.053(5)	20.2720(5)	15.6475(13)	13.738(5)
α (°)	90	90.386(16)	90	90	70.821(16)
β (°)	90	93.909(16)	103.5440(10)	104.939(2)	86.016(13)
γ (°)	90	102.325(14)	90	90	83.341(15)
V (Å)^3	7446.3(5)	1611.0(12)	3974.32(18)	4107.2(6)	1533.3(11)
Z	8	2	4	4	2
ρcalcd (Mg/m^3)	1.481	1.458	1.491	1.490	1.588
Abs coeff (mm^{-1})	0.642	0.677	0.751	0.7160	1.798
Abs correct	multi-scan	multi-scan	multi-scan	multi-scan	multi-scan
Transmiss max/min	1.0000/0.9909	1.0000/0.7628	1.0000/0.7531	1.0000/0.52964	1.0000/0.5972
F (000)	3408	728	1800	1896	736
Crystal size (mm)	0.52 x 0.08 x 0.07	0.36 x 0.30 x 0.15	0.70 x 0.24 x 0.18	0.26 x 0.13 x 0.06	0.20 x 0.13 x 0.08
Θ range (°)	2.087-24.999	3.045-24.999	3.236-24.999	3.07-25.00	3.02-27.485
Rflns/unique	55723/6451	12799/5654	47138/6868	31695/7216	15116/6935
R_{int}	0.1841	0.0323	0.045	0.2042	0.0459
Data/params	6451/471	5654/400	6868/465	7216/496	6935/345
Goodness of fit F^2	1.047	1.069	0.962	1.035	1.057
R_1/wR_2 ($I>2\sigma(I)$)	0.0741/0.1462	0.0412/0.0881	0.0377/0.0917	0.0923/0.1442	0.0429/0.0838
R_1/wR_2 (all data)	0.1118/0.1674	0.053/0.0925	0.0464/0.0962	0.1735/0.1766	0.0555/0.0888
Abs. struct. param	-	-	-	-	-
Largest diff. peak and hole (e Å^{-3})	0.813/-0.691	0.511/-0.334	0.941/-0.608	0.526/-0.528	1.172/-0.843
CCDC No.	1535368	1535369	1535370	1535371	1535372

Table S1. Crystallographic Data for the Complexes (MoK_α radiation)

Complex	[CpFe(dppp)NCMe] PF_6 $CHCl_3$	[CpFe(dppp)-$P(OMe)_3$]PF_6	[CpFe(dppp)-$PPh(OMe)_2$]PF_6	[CpFe(dppp)-$PPh_2(OMe)PF_6$	[CpFe(dppp)-$PPh_2(OEt)$]PF_6
Empirical formula	$C_{34}H_{34}FeNP_2$, F_6P, $CHCl_3$	$C_{35}H_{40}FeO_3P_3$, F_6P	$C_{39}H_{40}FeO_2P_3$, F_6P	$C_{45}H_{44}FeOP_3$, F_6P	$C_{46}H_{46}FeOP_3$, F_6P
Formula weight	838.75	802.4	848.46	894.53	908.56
Crystal system	monoclinic	orthorhombic	Orthorhombic	orthorhombic	monoclinic
Space group	*C*2/c	*P*ca2_1	*P*na2_1	*P*n2_1a	*P*2_1/c
a (Å)	27.0808(19)	17.1671(6)	14.1022(4)	12.6131(14))	13.3871(10)
b (Å)	12.0515(8)	9.4816(3)	19.7486(4)	16.3705(19)	13.6101(9)
c (Å)	22.5312(16)	21.5862(6)	13.9570(6)	19.791(2)	25.3570(18)
α (^{o})	90	90	90	90	90
β (^{o})	92.450(2)	90	90	90	104.8700(10)
γ (^{o})	90	90	90	90	90
V (Å)^3	7346.7(9)	3513.6(3)	3887.0(2)	4086.4(8)	4465.3(5)
Z	8	4	4	4	4
ρcalcd (Mg/m^3)	1.517	1.517	1.45	1.454	1.351
Abs coeff (mm^{-1})	0.818	0.679	0.616	0.589	0.540
Abs correct	multi-scan	multi-scan	multi-scan	multi-scan	multi-scan
Transmiss max/min	1.0000/0.0938	1.0000/0.5765	1.0000/0.6350	1.0000/0.6262	1.0000/0.8813
F (000)	3424	1656	1752	1848	55402
Crystal size (mm)	0.24 x 0.18 x 0.17	0.19 x 0.11 x 0.10	0.30 x 0.14 x 0.11	0.24 x 0.24 x 0.11	0.41 x 0.36 x 0.35
Θ range (^{o})	2.992-27.456	3.032-27.431	3.068-24.987	3.009-24.999	2.993-25.00
Rflns/unique	34985/8360	53039/7954	47657/6811	30590/7182	55402/7852
R_{int}	0.176	0.1408	0.0826	0.0629	0.0443
Data/params	8360/443	7954/445	6811/471	7182/515	7852/582
Goodness of fit F^2	1.032	1.087	1.047	1.052	1.200
R_1/wR_2 ($I>2\sigma(I)$)	0.082/0.1862	0.0487/0.0945	0.0388/0.0888	0.0467/0.1136	0.1177/0.3143
R_1/wR_2 (all data)	0.1625/0.2365	0.0743/0.1071	0.0484/0.0938	0.053/0.1181	0.122/0.3163
Abs. struct. param	-	0.015(12)	0.011(10)	0.014(9)	-
Largest diff. peak and hole (e Å^{-3})	0.71/-0.836	0.468/-0.575	0.393/-0.327	0.915/-0.389	1.976/-1.093
CCDC No.	1535373	1535374	1535375	1535376	1535377

Table S1. Crystallographic Data for the Complexes (MoK_α radiation)

Complex	[CpFe(dppm)-P(OMe)$_3$]PF_6	[CpFe(dppb)-P(OMe)$_3$]PF_6, $CHCl_3$	[CpFe{PPh_2(OMe)}$_2$-NCMe]PF_6	[CpFe(PPh_2Me)-{PPh_2(OMe)}$_2$]PF_6, $2CH_2Cl_2$	[CpFe{PPh_2(OMe)}$_3$] PF_6, CH_2Cl_2
Empirical formula	$C_{33}H_{36}FeO_3P_3$, F_6P	2($C_{36}H_{42}FeO_3P_3$), 3($CHCl_3$), 2(F_6P)	$C_{33}H_{34}FeO_2P_3$, F_6P,	$C_{44}H_{44}FeO_2P_3$, F_6P, 2(CH_2Cl_2)	$C_{44}H_{44}FeO_3P_3$, F_6P, CH_2Cl_2
Formula weight	774.35	1990.95	739.37	1068.37	999.45
Crystal system	monoclinic	monoclinic	monoclinic	triclinic	triclinic
Space group	$P2_1/c$	$P2_1/a$	$P2_1/c$	$P\bar{1}$	$P\bar{1}$
a (Å)	19.3216(4)	14.7697(5)	9.6678(5)	12.1751(16)	12.4693(4)
b (Å)	18.9000(4)	31.5883(8)	28.7237(14)	12.9407(19)	13.1771(6)
c (Å)	19.6203(4)	18.7195(5)	12.8949(7)	17.154(2)	16.1150(6)
α (°)	90	90	90	68.006(4)	101.983(2)
β (°)	111.7630(10)	97.9320(10)	112.4920(10)	69.407(4)	102.7650(10)
γ (°)	90	90	90	82.255(4)	108.874(2)
V (Å)^3	6654.2 (2)	8650.0(4)	3308.5(3)	2345.9(6)	2329.12(16)
Z	8	4	4	2	2
ρcalcd (Mg/m^3)	1.546	1.529	1.484	1.513	1.425
Abs coeff (mm^{-1})	0.714	0.837	0.667	0.748	0.639
Abs correct	multi-scan	multi-scan	multi-scan	multi-scan	multi-scan
Transmiss max/min	1.0000/ 0.8467	1.0000/0.8227	1.0000/0.8698	1.0000/0.7954	1.0000/0.8063
F (000)	3184	4072	1520	1096	1028
Crystal size (mm)	0.50 x 0.14 x 0.13	0.55 x 0.16 x 0.10	0.32 x 0.25 x 0.24	0.49 x 0.38 x 0.26	0.42 x 0.39 x 0.04
Θ range (°)	3.009-25.00	3.046-24.999	3.109-24.996	3.181-25	3.18-25
Rflns/unique	77137/11683	107735/15210	41814/5824	29577/8225	18459/8220
R_{int}	0.0752	0.0832	0.0402	0.0568	0.0296
Data/params	11688/853	15210/1027	5825/418	8225/572	8220/562
Goodness of fit F^2	1.036	1.045	1.033	1.077	1.044
R_1/wR_2 ($I>2\sigma(I)$)	0.0431/0.087	0.078/0.1986	0.0449/0.1095	0.0811/0.2378	0.0856/0.2547
R_1/wR_2 (all data)	0.0752/0.0979	0.1122/0.2221	0.0537/0.1152	0.1099/0.2763	0.0979/0.2691
Largest diff. peak and hole (e Å^{-3})	0.49/-0.399	1.495/-0.966	1.058/-1.028	1.545/-1.112	4.179/-1.231
Abs. struct. param	-	-	-	-	-
CCDC No.	1535378	1535379	1549806	1549807	1550539

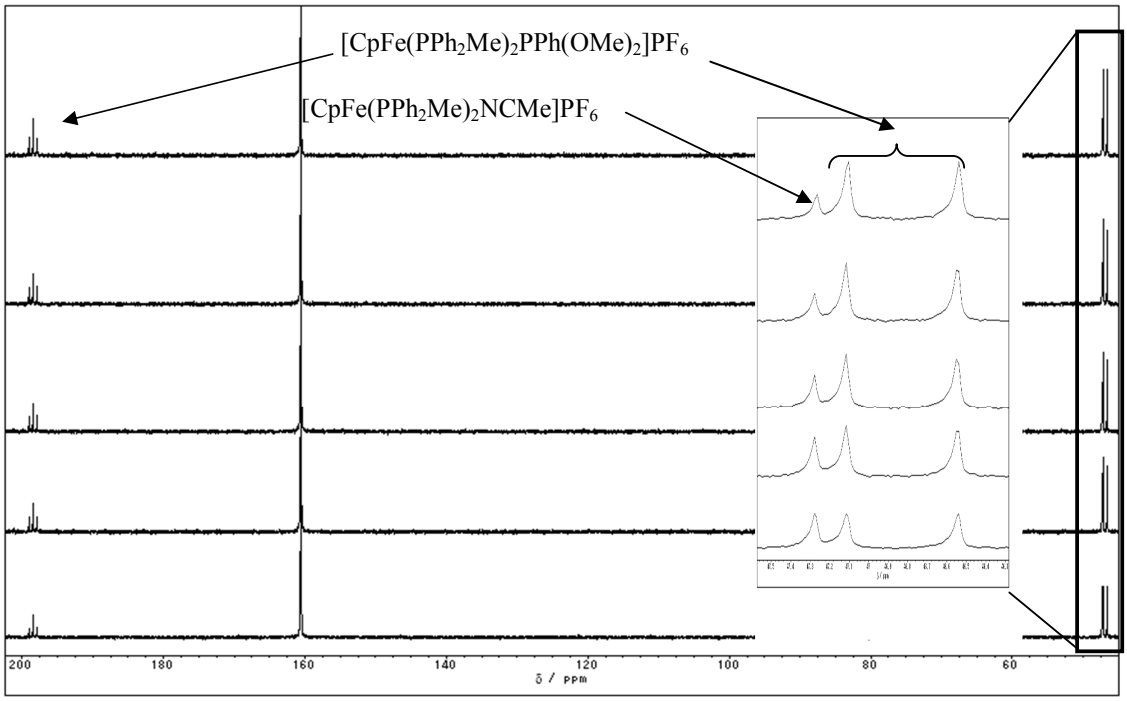

Figure S1. Time-resolved $^{31}P\{^{1}H\}$ NMR spectra of the ligand exchange of $[CpFe(PPh_2Me)NCMe]PF_6$ with $PPh(OMe)_2$ (10 eq.) at 293 K in $CDCl_3$.

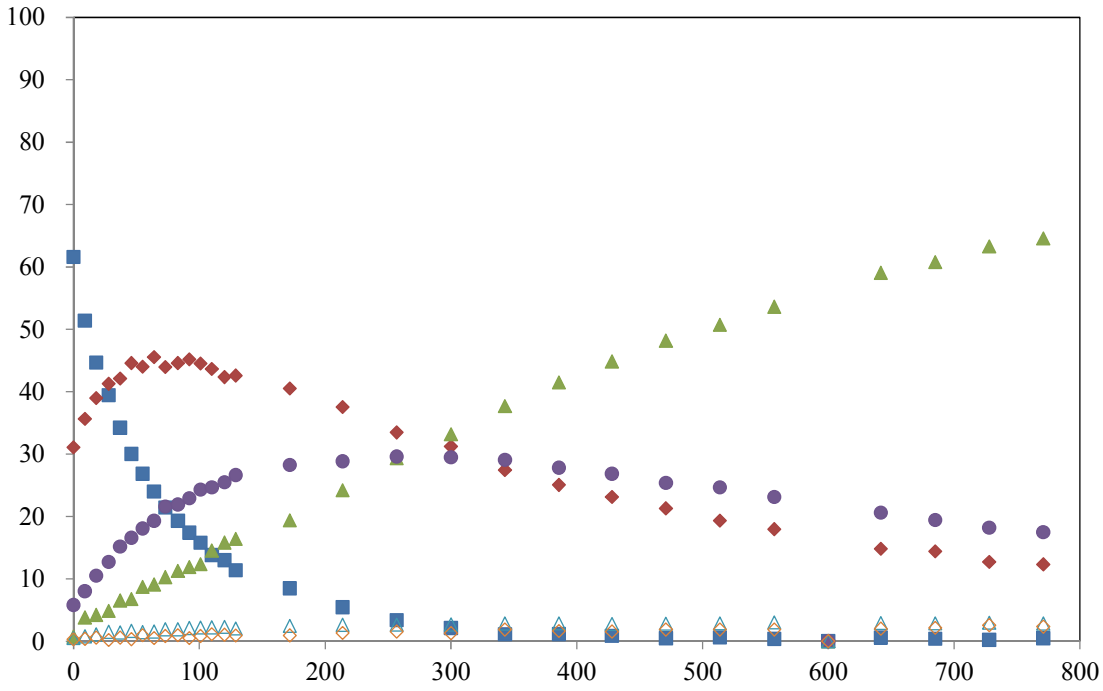

Figure S2. Time dependence of the concentrations of reactants and products in the reaction of $[CpFe(PPh_2Me)_2NCMe]PF_6$ with 5 equivalents of $PPh_2(OMe)$ in $CDCl_3$ at 293 K: $[CpFe(PPh_2Me)_2NCMe]PF_6$ (■), $[CpFe(PPh_2Me)_2PPh_2(OMe)]PF_6$ (◆), $[CpFe(PPh_2Me)\{PPh_2(OMe)\}_2]PF_6$ (▲), $[CpFe(PPh_2Me)\{PPh_2(OMe)\}NCMe]PF_6$ (●), $[CpFe\{PPh_2(OMe)\}_2NCMe]$ (△), and $[CpFe\{PPh_2(OMe)\}_3]$ (◇).

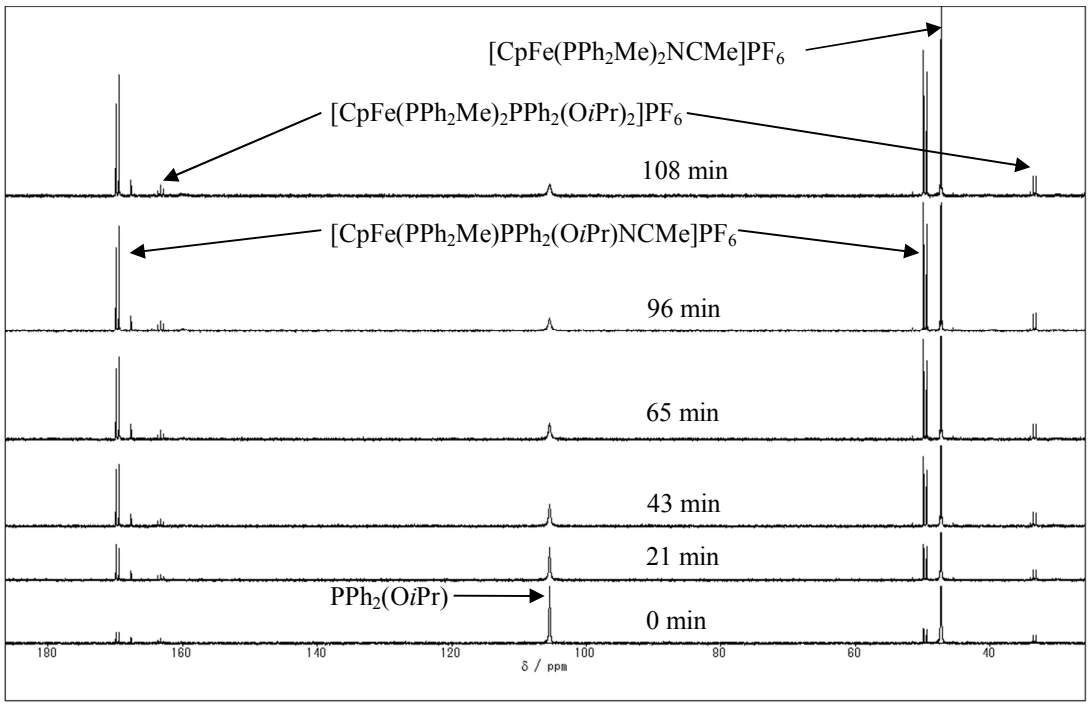

Figure S3. Time-resolved $^{31}P\{^{1}H\}$ NMR spectra of the ligand exchange of $[CpFe(PPh_2Me)NCMe]PF_6$ with $PPh_2(OiPr)$ (1 eq.) at 293 K in $CDCl_3$.

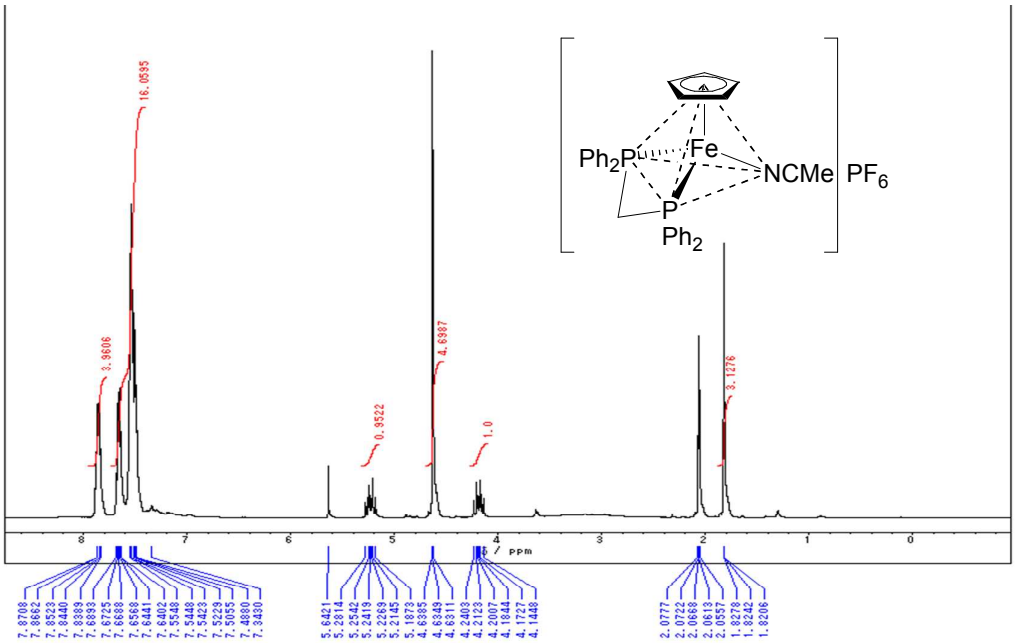

Figure S4-1. ^{1}H NMR Spectrum of [CpFe(dppm)NCMe]PF_6 in acetone-d_6 at 293 K.

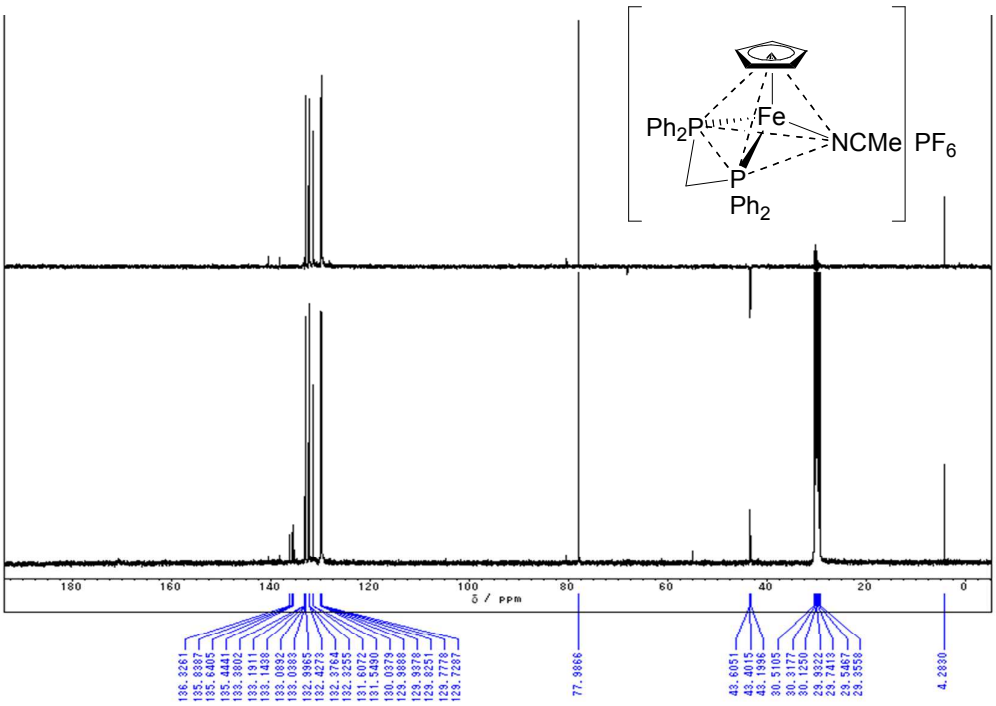

Figure S4-2. ^{13}C NMR Spectra of [CpFe(dppm)NCMe]PF_6 in acetone-d_6 at 293 K (top: DEPT135, bottom: decoupling).

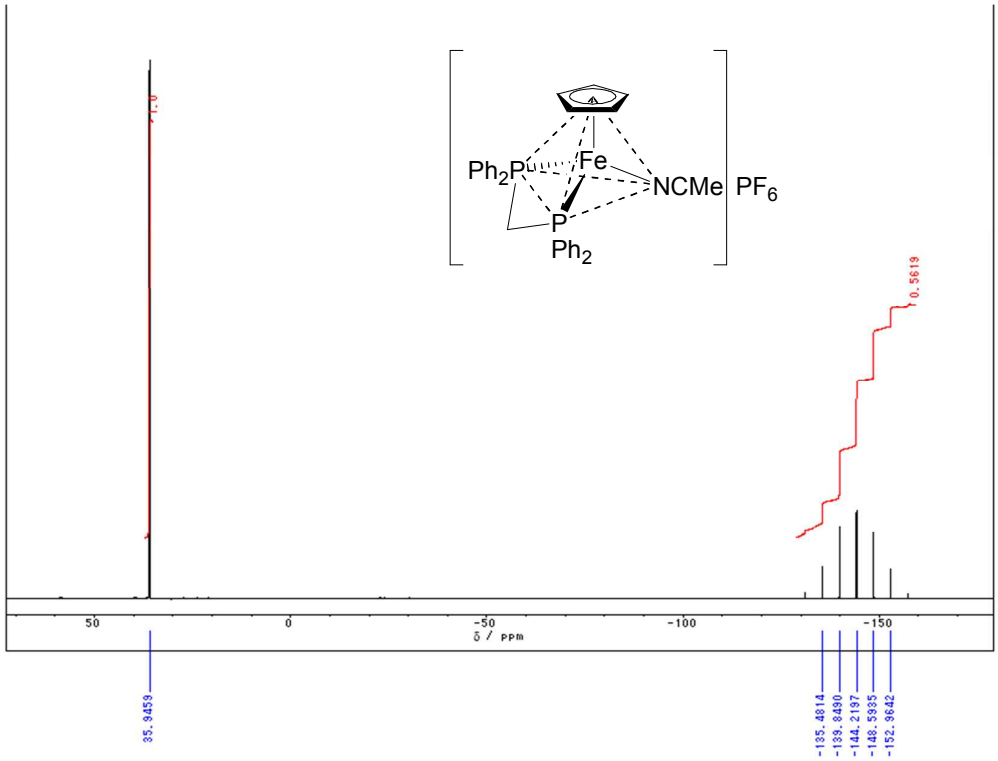

Figure S4-3. $^{31}P\{^{1}H\}$ NMR Spectrum of [CpFe(dppm)NCMe]PF_6 in acetone-d_6 at 293 K.

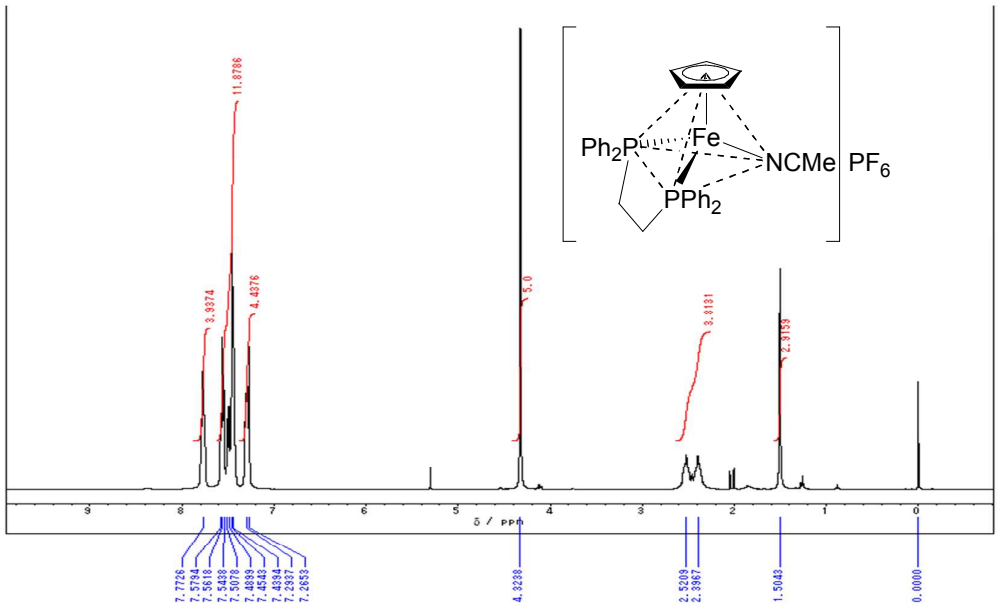

Figure S5-1. ^{1}H NMR Spectrum of [CpFe(dppe)NCMe]PF_6 in $CDCl_3$ at 293 K.

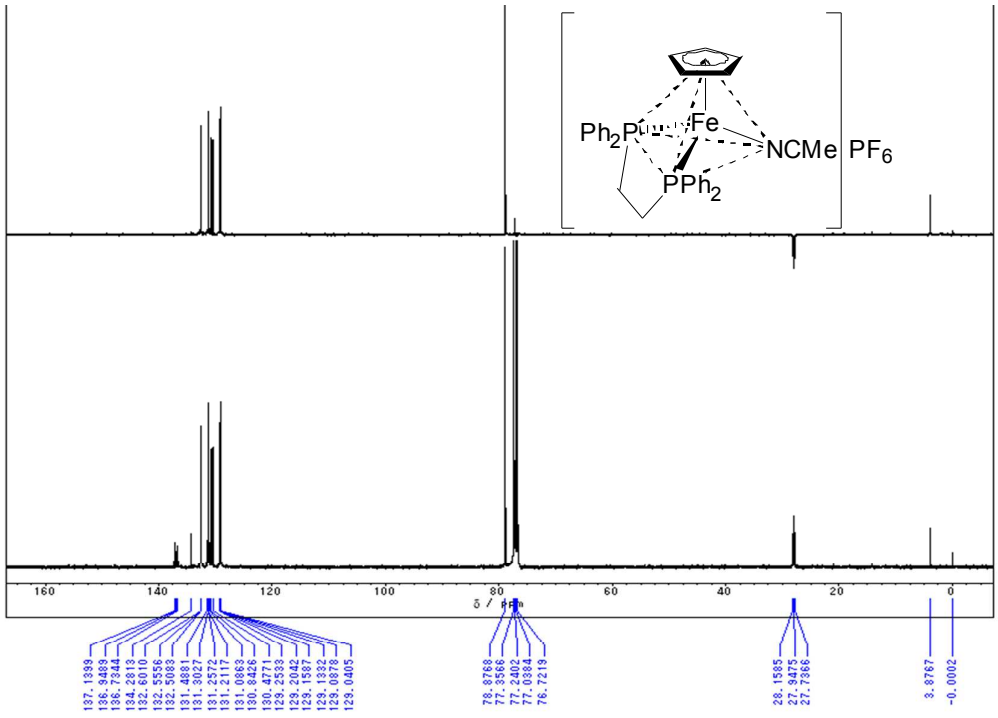

Figure S5-2. ^{13}C NMR Spectra of [CpFe(dppe)NCMe]PF_6 in $CDCl_3$ at 293 K (top: DEPT135, bottom: decoupling).

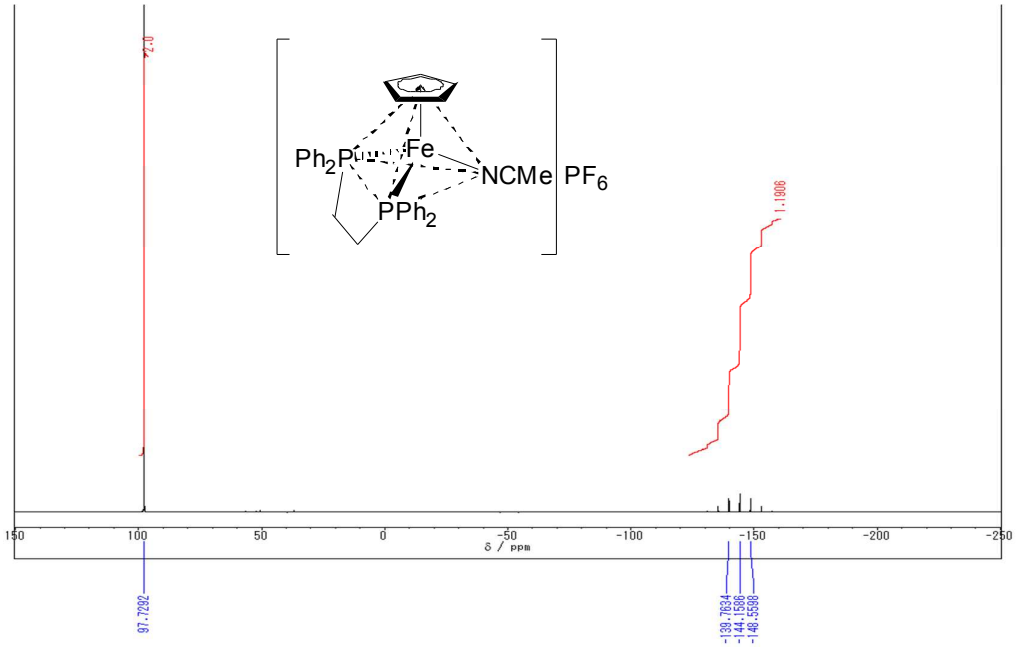

Figure S5-3. $^{31}P\{^{1}H\}$ NMR Spectrum of [CpFe(dppe)NCMe]PF_6 in $CDCl_3$ at 293 K.

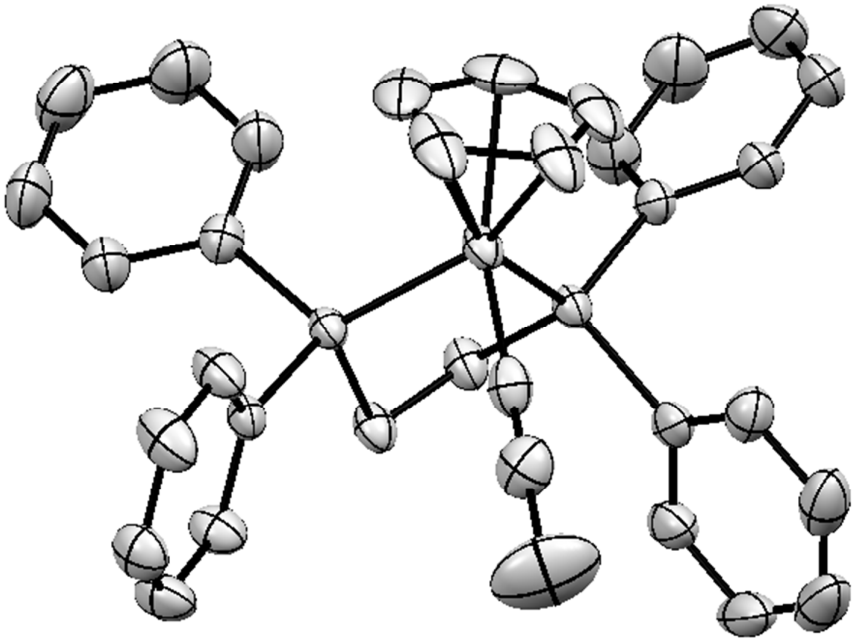

Figure S5-4. ORTEP drawing of [CpFe(dppe)NCMe]PF_6. Hydrogen atoms and hexafluorophosphate anion are omitted for clarity.

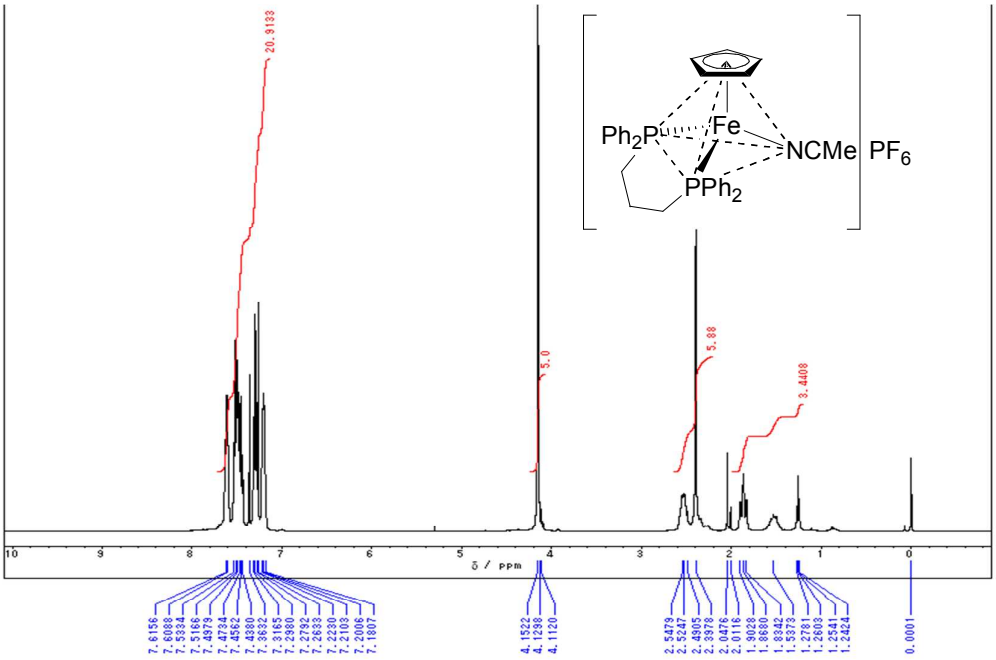

Figure S6-1. ^{1}H NMR Spectrum of [CpFe(dppp)NCMe]PF_6 in $CDCl_3$ at 293 K.

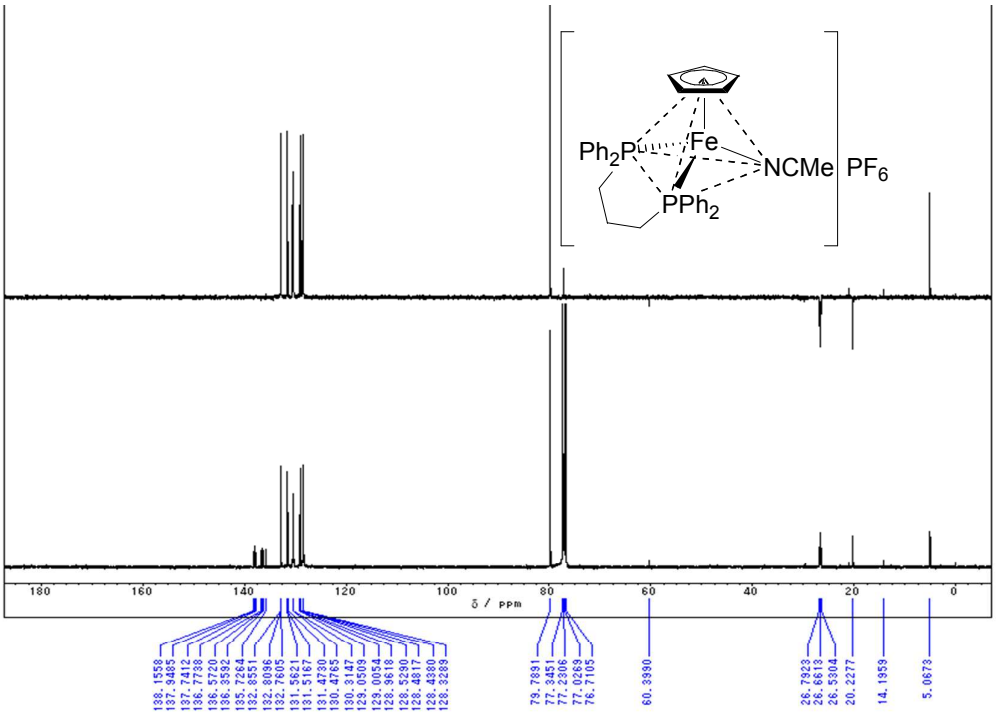

Figure S6-2. ^{13}C NMR Spectra of [CpFe(dppp)NCMe]PF_6 in $CDCl_3$ at 293 K (top: DEPT135, bottom: decoupling).

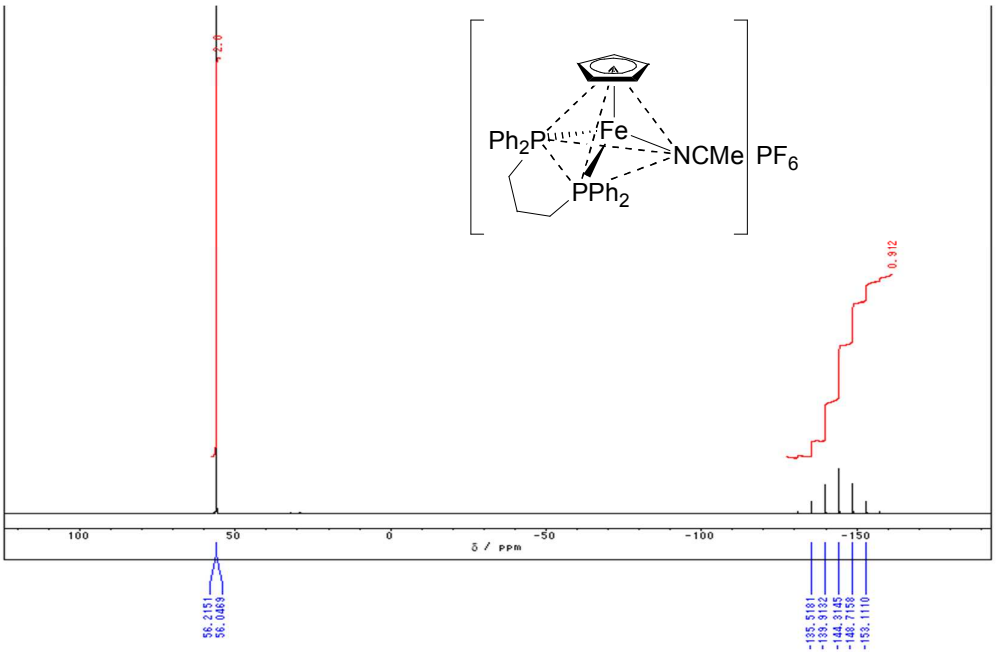

Figure S6-3. $^{31}P\{^{1}H\}$ NMR Spectrum of [CpFe(dppp)NCMe]PF_6 in $CDCl_3$ at 293 K.

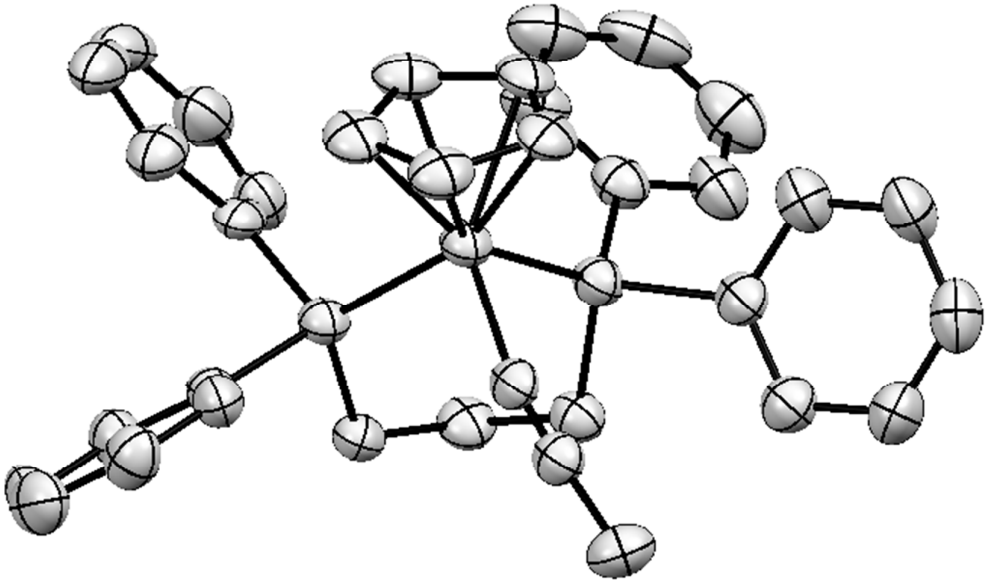

Figure S6-4. ORTEP drawing of [CpFe(dppp)NCMe]PF_6· $CHCl_3$. Hydrogen atoms, hexafluorophosphate anion, and one $CHCl_3$ molecule are omitted for clarity.

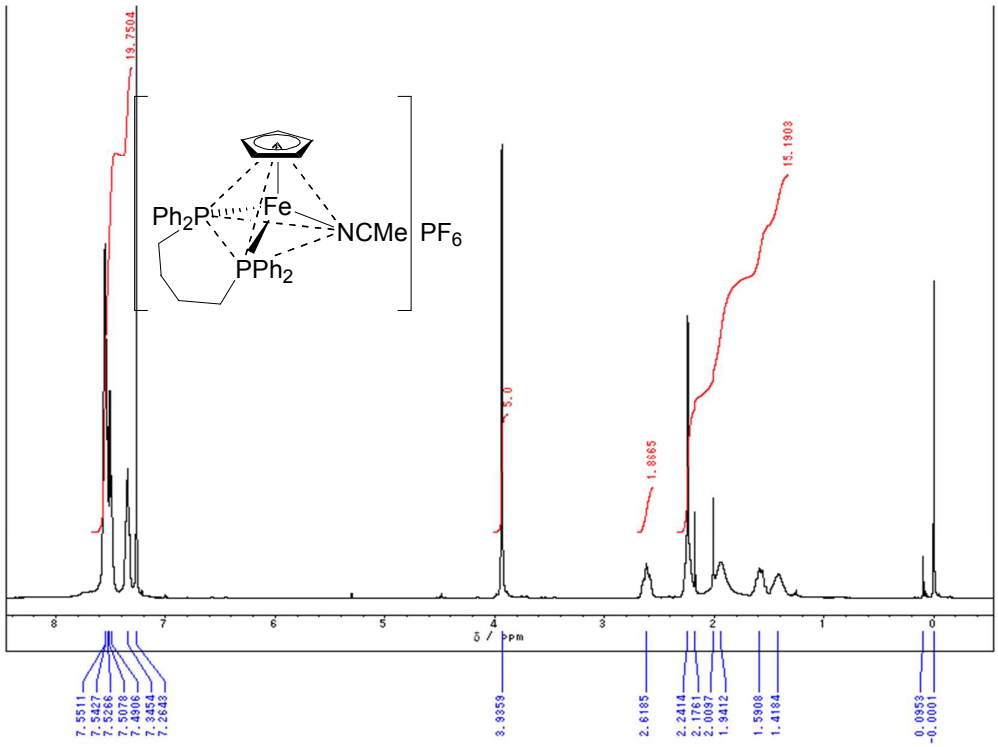

Figure S7-1. ^1H NMR Spectrum of [CpFe(dppb)NCMe]PF_6 in $CDCl_3$ at 293 K.

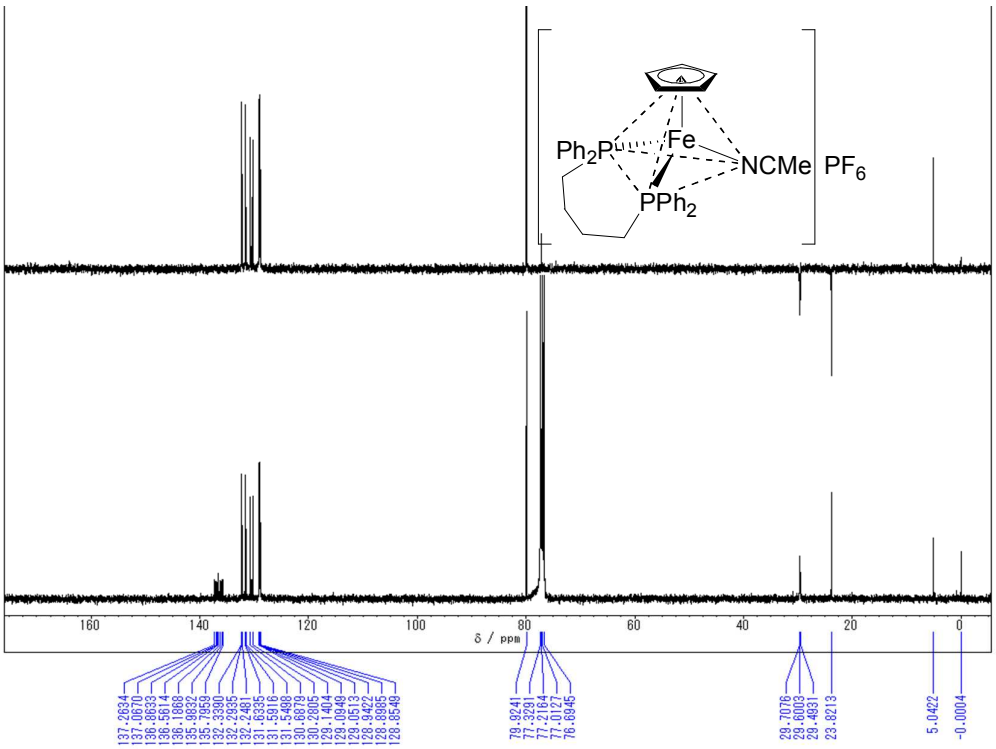

Figure S7-2. ^{13}C NMR Spectra of [CpFe(dppb)NCMe]PF_6 in $CDCl_3$ at 293 K (top: DEPT135, bottom: decoupling).

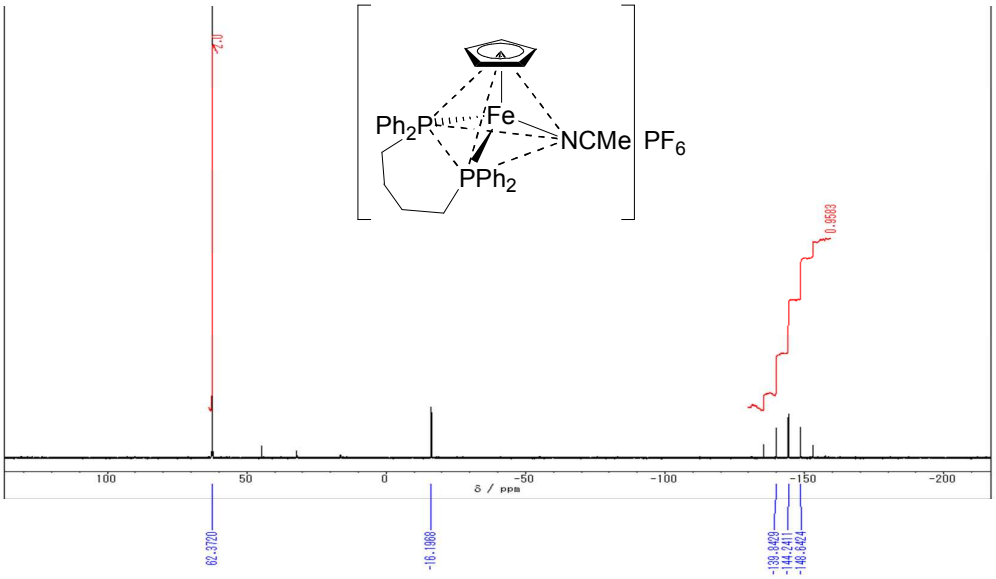

Figure S7-3. $^{31}P\{^{1}H\}$ NMR Spectrum of [CpFe(dppb)NCMe]PF_6 in $CDCl_3$ at 293 K.

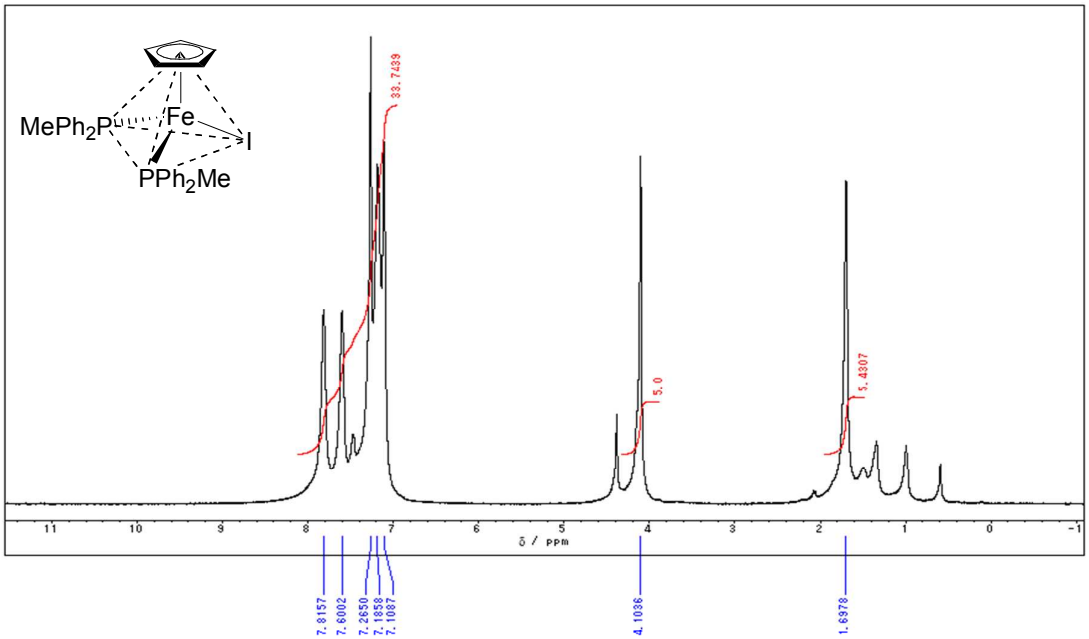

Figure S8-1. ^{1}H NMR Spectrum of [CpFe(PPh$_2$Me)$_2$I] in benzene-d_6 at 293 K.

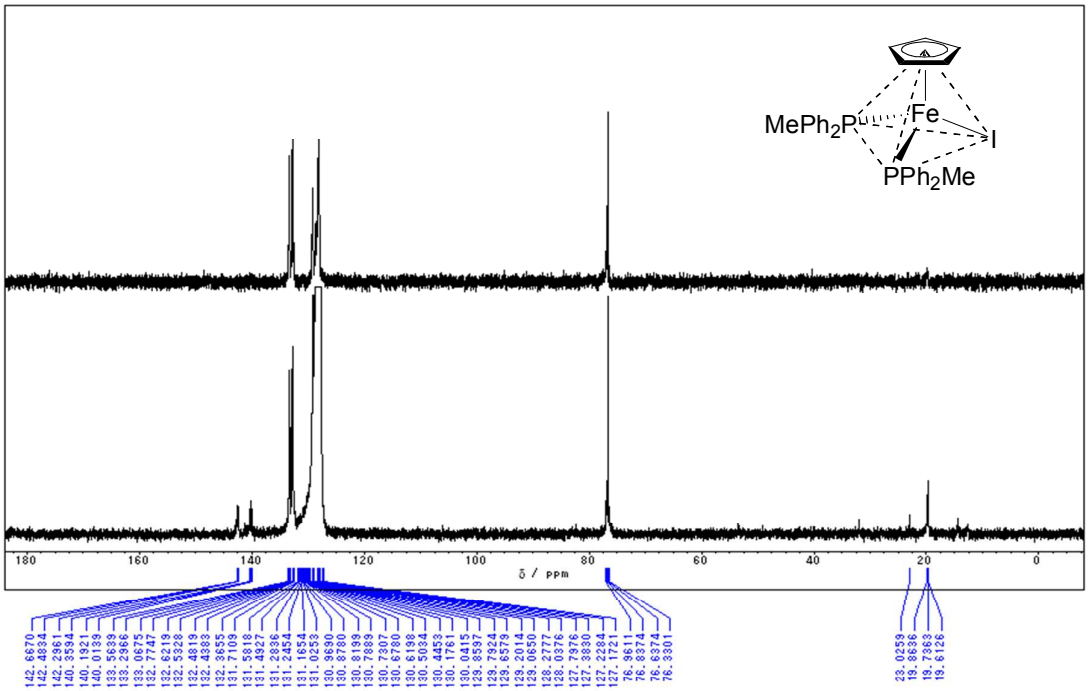

Figure S8-2. ^{13}C NMR Spectra of [CpFe(PPh$_2$Me)$_2$I] in benzene-d_6 at 293 K (top: DEPT135, bottom: decoupling).

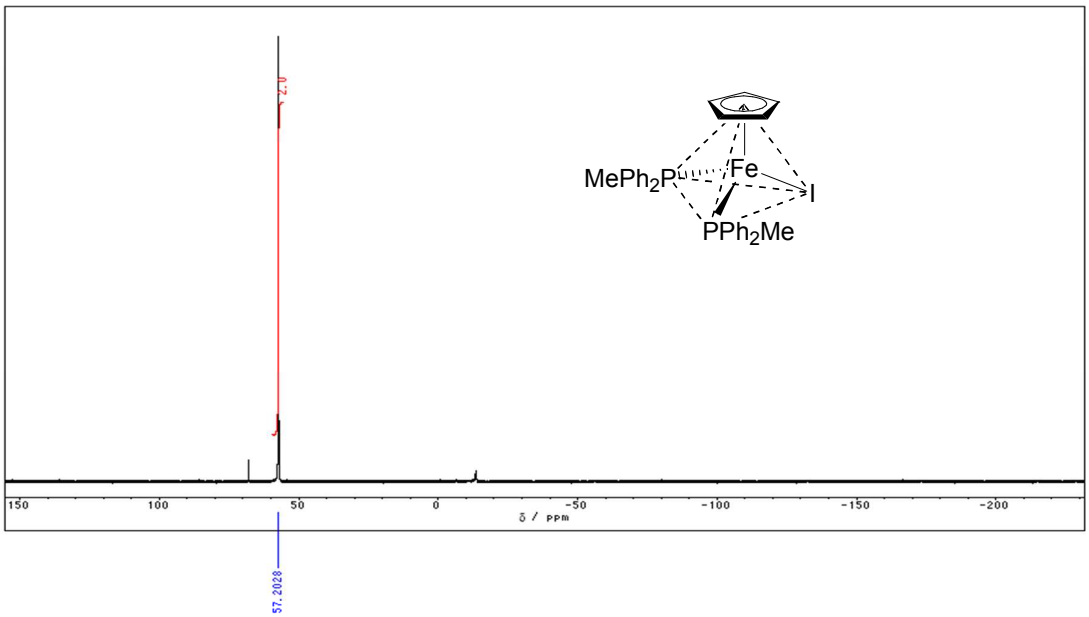

Figure S8-3. $^{31}P\{^{1}H\}$ NMR Spectrum of $[CpFe(PPh_2Me)_2I]$ in benzene-d_6 at 293 K.

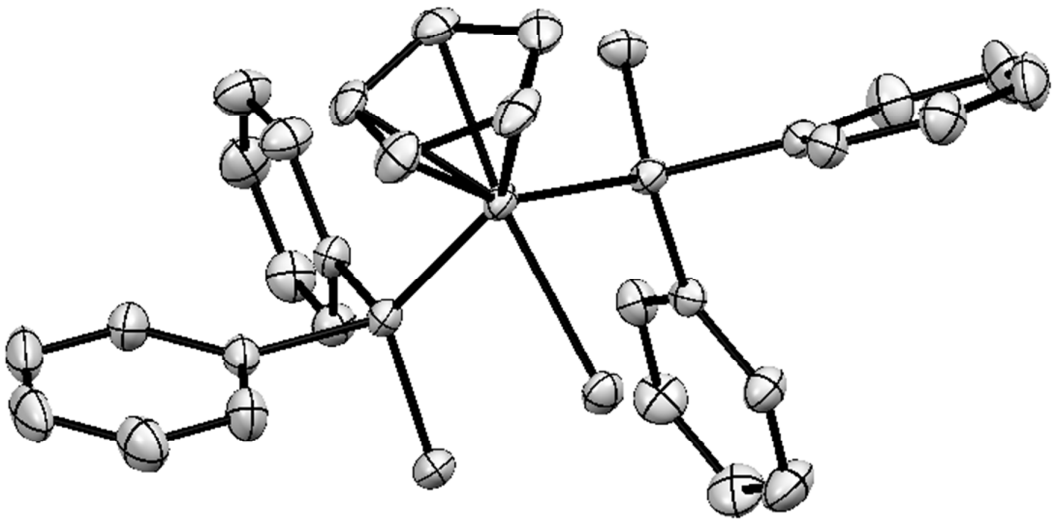

Figure S8-4. ORTEP drawing of $[CpFe(PPh_2Me)_2I]\cdot CH_2Cl_2$. Hydrogen atoms and one CH_2Cl_2 molecule are omitted for clarity.

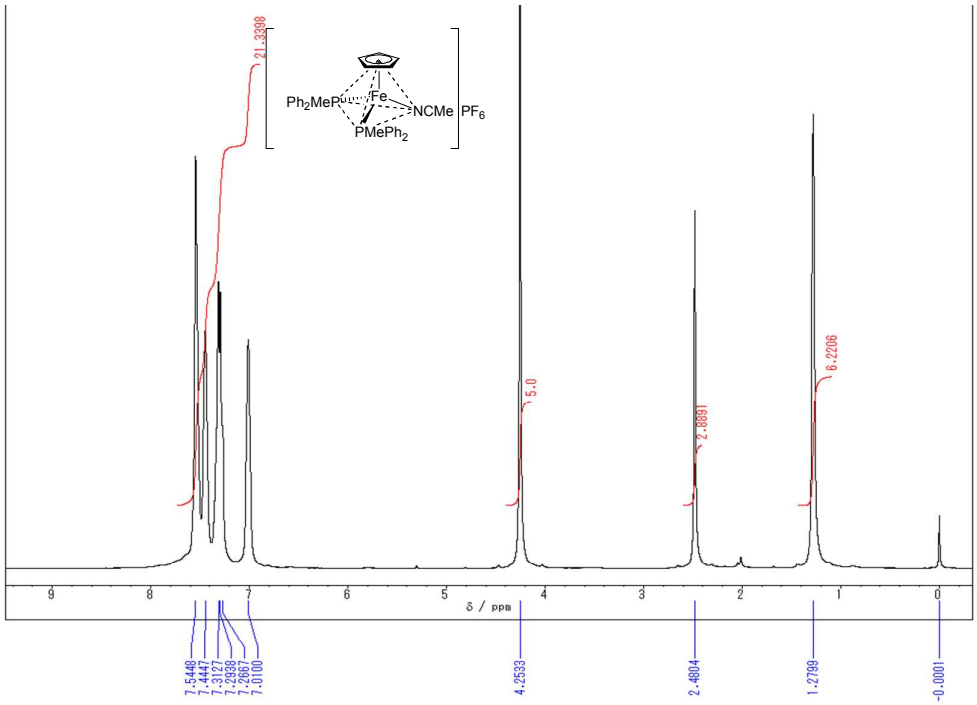

Figure S9-1. ^{1}H NMR Spectrum of [CpFe(PPh_2Me)$_2$NCMe]PF_6 in $CDCl_3$ at 293 K.

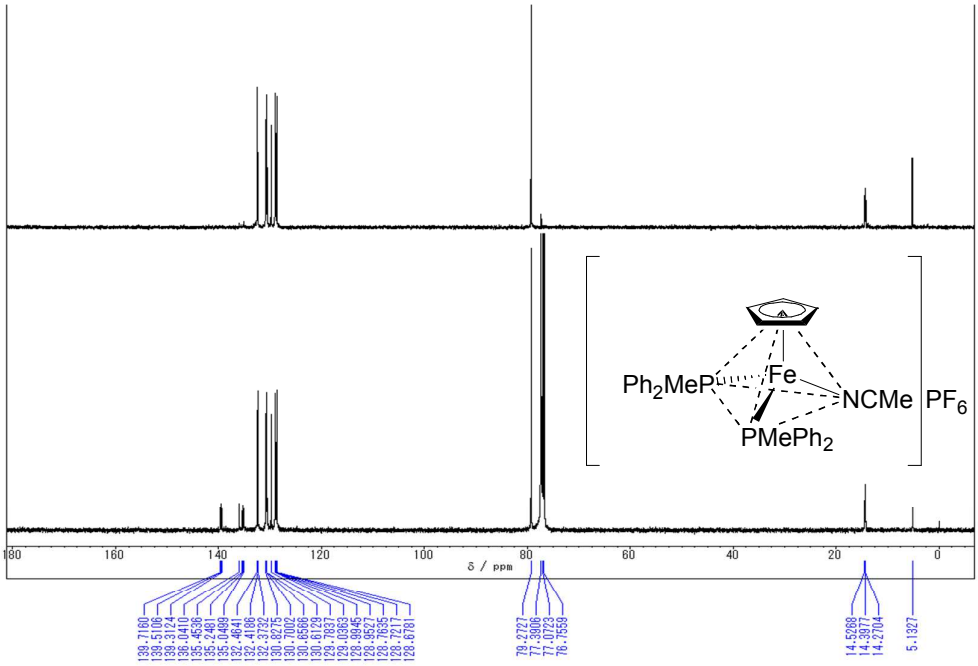

Figure S9-2. ^{13}C NMR Spectra of [CpFe(PPh_2Me)$_2$NCMe]PF_6 in $CDCl_3$ at 293 K (top: DEPT135, bottom: decoupling).

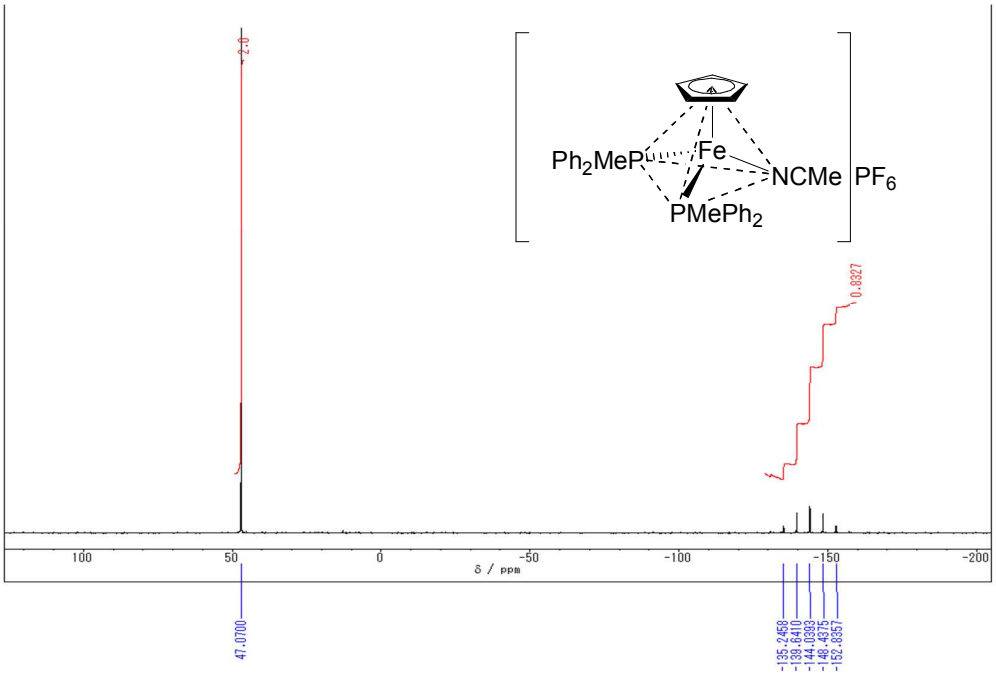

Figure S9-3. $^{31}P\{^{1}H\}$ NMR Spectrum of $[CpFe(PPh_2Me)_2NCMe]PF_6$ in $CDCl_3$ at 293 K.

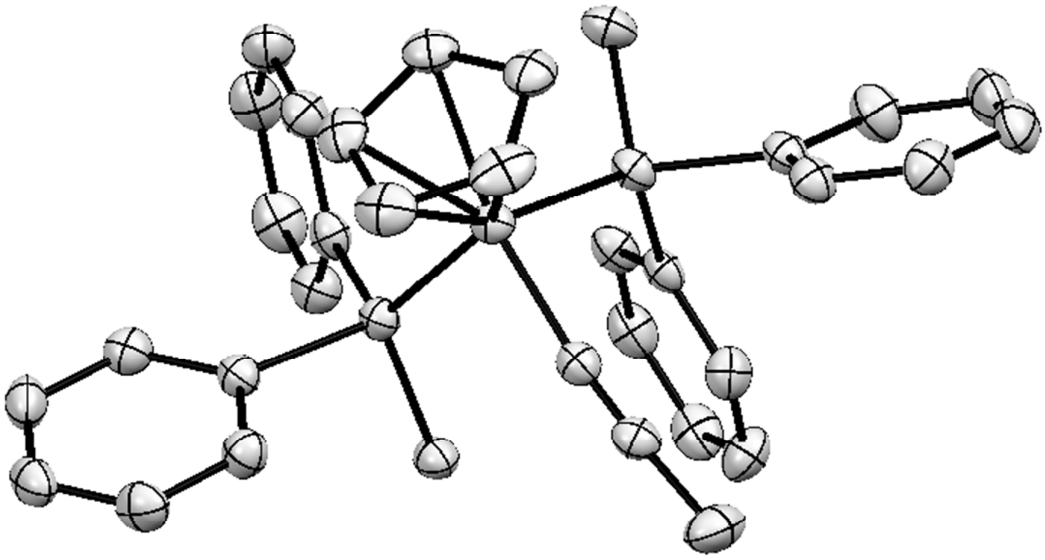

Figure S9-4. ORTEP drawing of $[CpFe(PPh_2Me)_2NCMe]PF_6$. Hydrogen atoms and hexafluorophosphate anion are omitted for clarity.

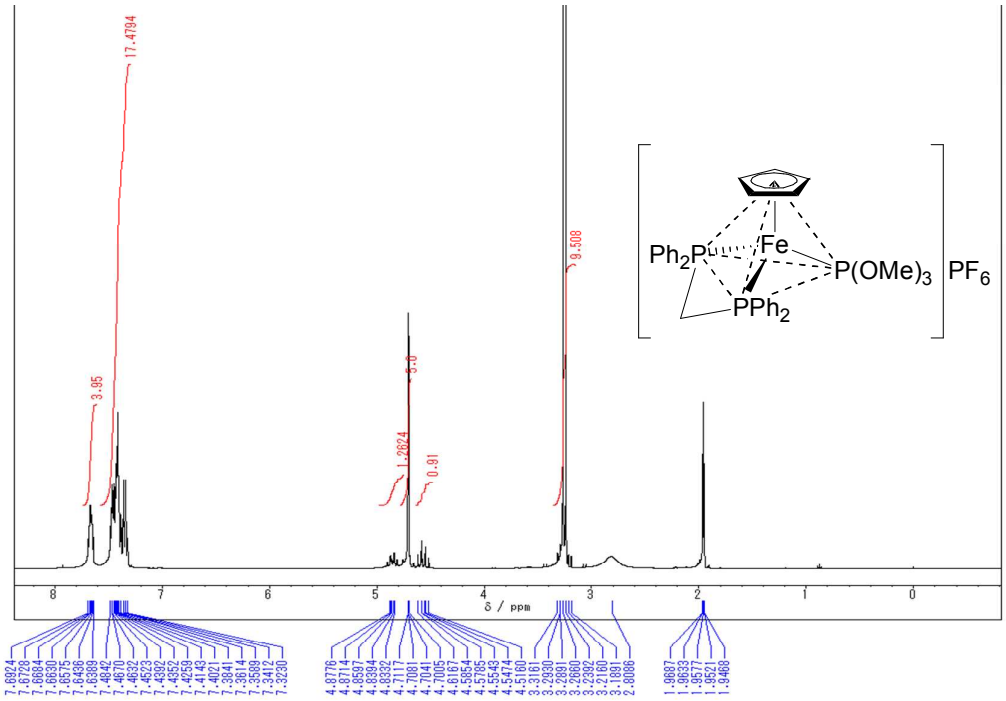

Figure S10-1. ^{1}H NMR Spectrum of [CpFe(dppm)P(OMe)$_3$]PF$_6$ in acetone-d_6 at 293 K.

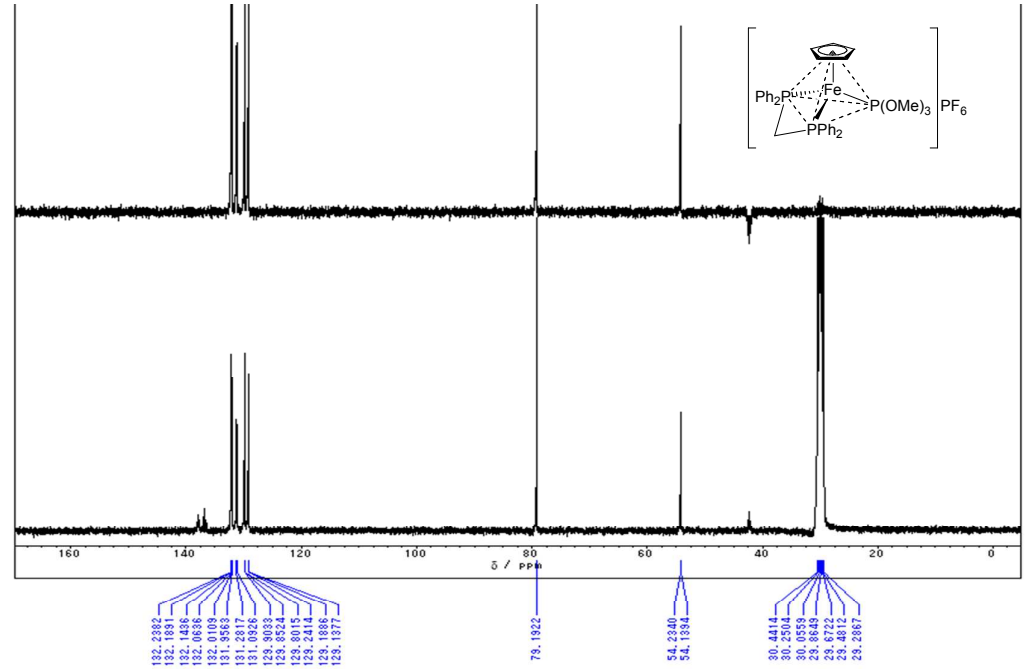

Figure S10-2. ^{13}C NMR Spectra of [CpFe(dppm)P(OMe)$_3$]PF$_6$ in acetone-d_6 at 293 K (top: DEPT135, bottom: decoupling).

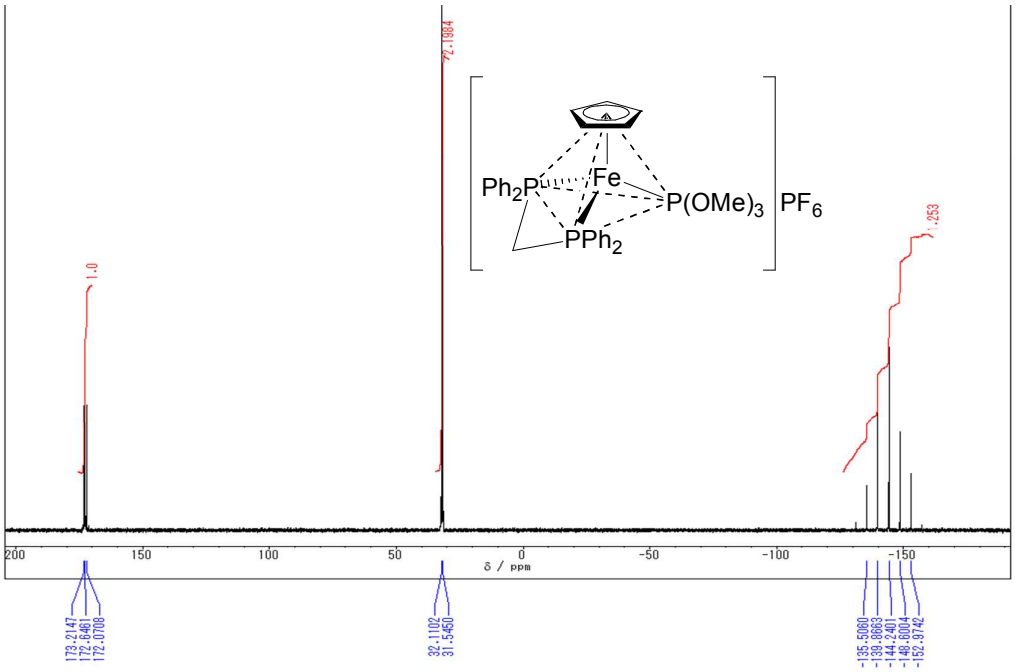

Figure S10-3. $^{31}P\{^{1}H\}$ NMR Spectrum of $[CpFe(dppm)P(OMe)_3]PF_6$ in acetone-d_6 at 293 K.

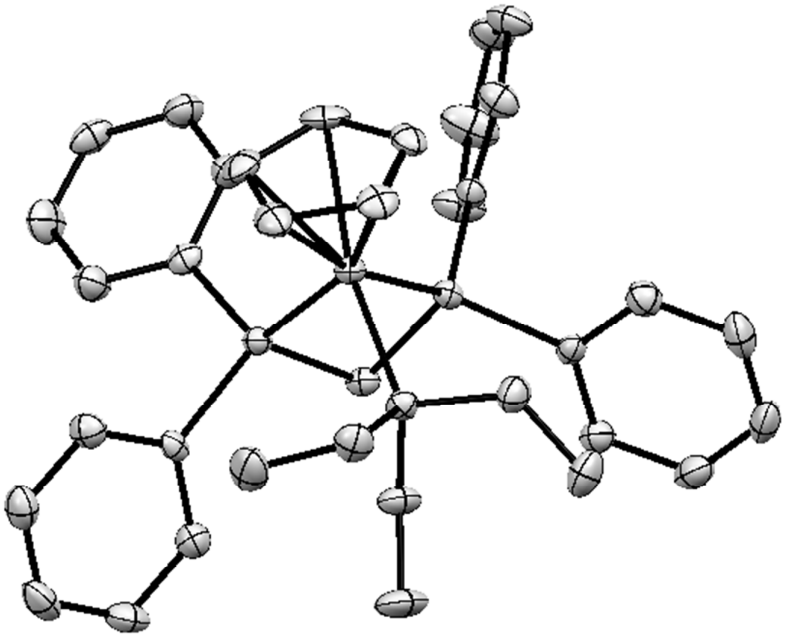

Figure S10-4. ORTEP drawing of $[CpFe(dppm)P(OMe)_3]PF_6$. Hydrogen atoms and hexafluorophosphate anion are omitted for clarity.

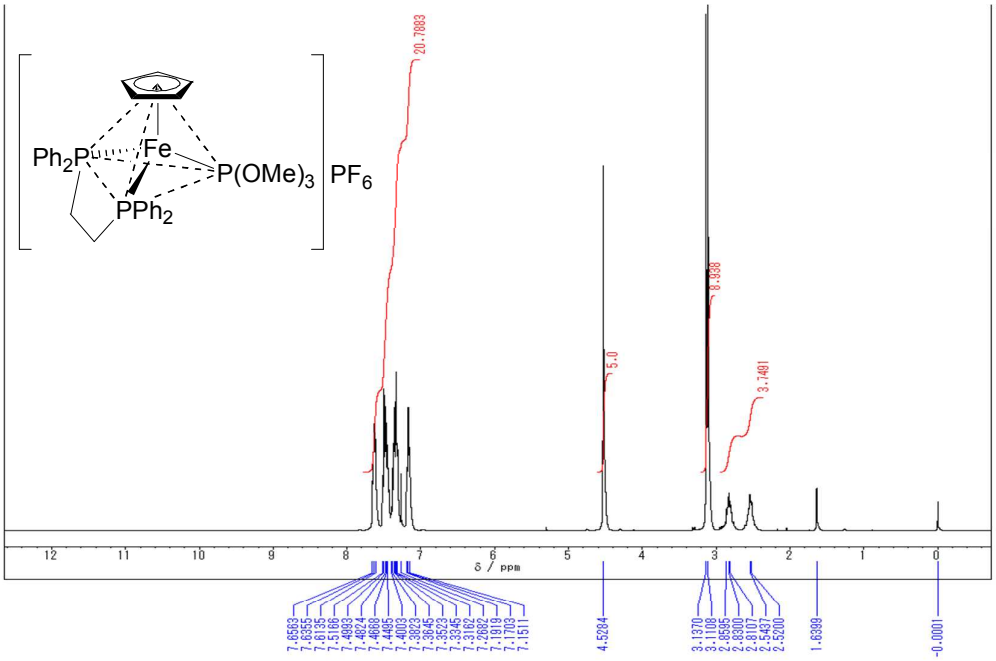

Figure S11-1. ^{1}H NMR Spectrum of [CpFe(dppe)P(OMe)$_3$]PF$_6$ in CDCl$_3$ at 293 K.

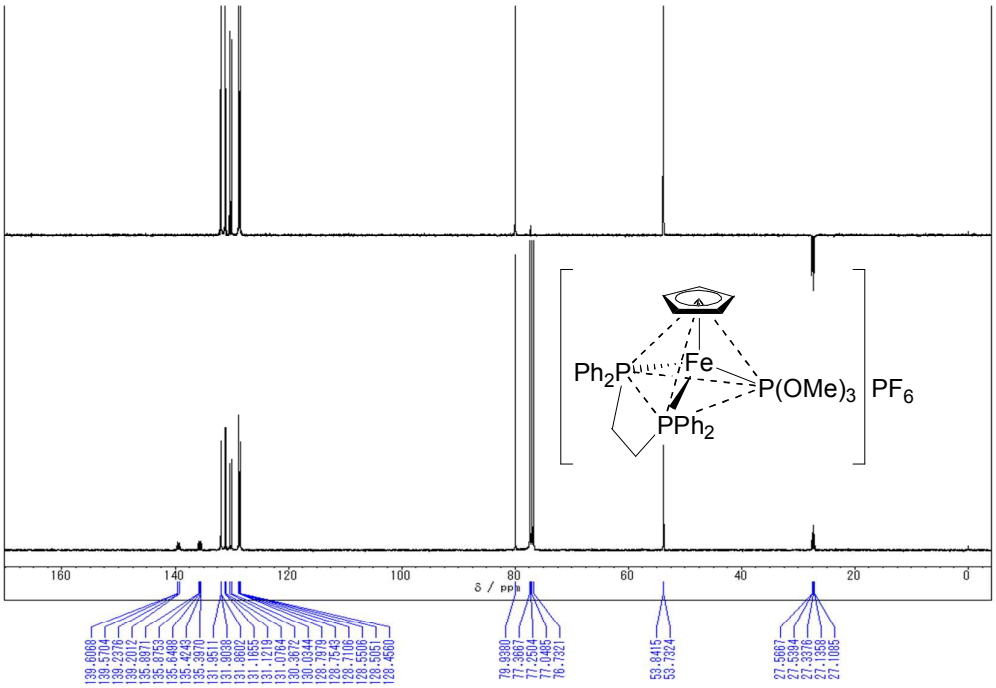

Figure S11-2. ^{13}C NMR Spectra of [CpFe(dppe)P(OMe)$_3$]PF$_6$ in CDCl$_3$ at 293 K (top: DEPT135, bottom: decoupling).

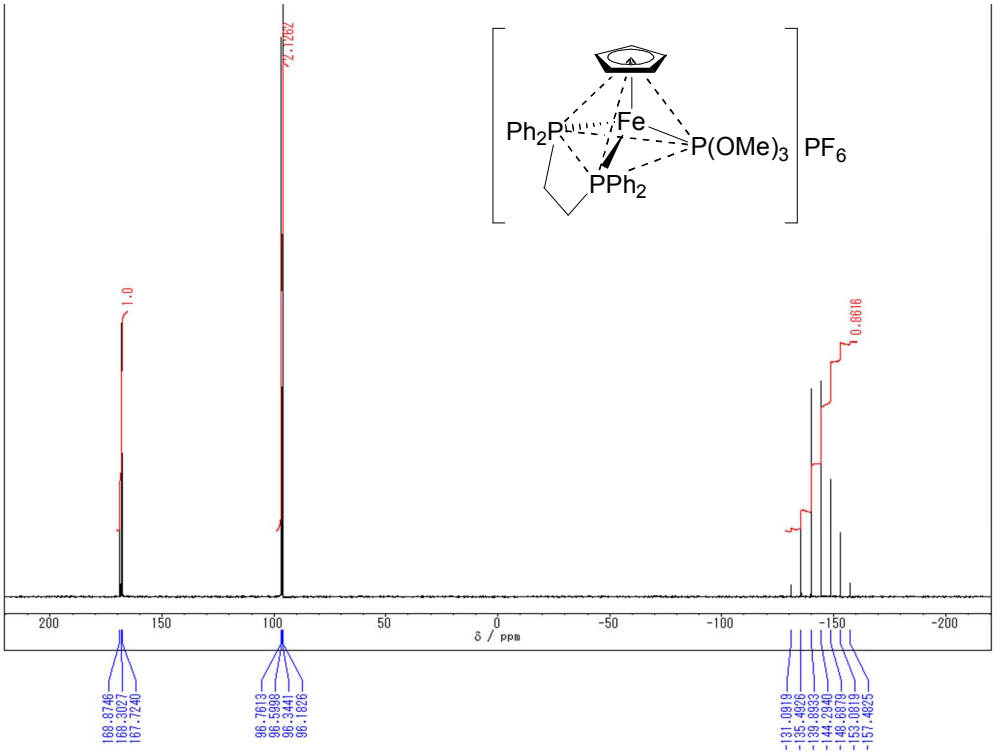

Figure S11-3. $^{31}P\{^{1}H\}$ NMR Spectrum of $[CpFe(dppe)P(OMe)_3]PF_6$ in $CDCl_3$ at 293 K.

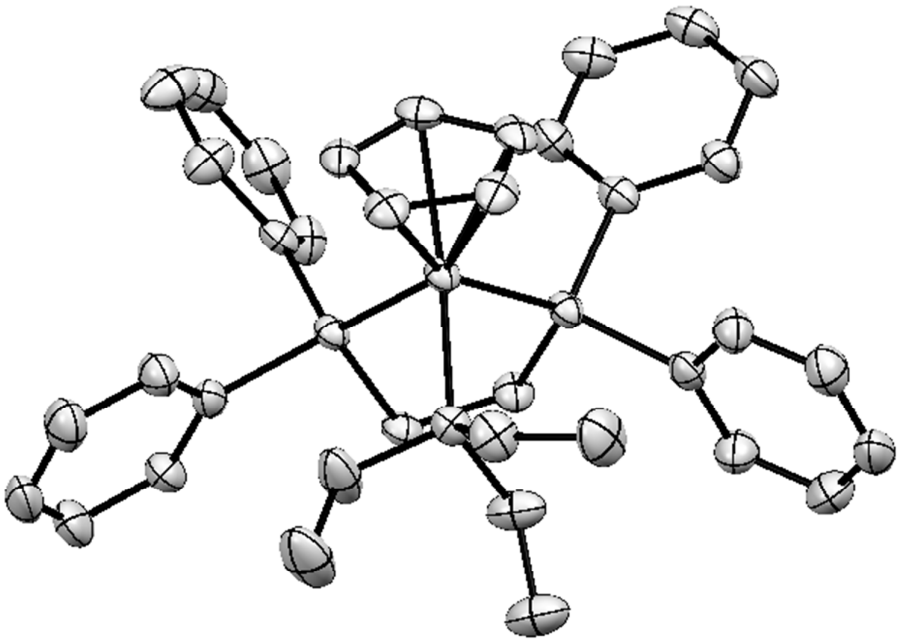

Figure S11-4. ORTEP drawing of $[CpFe(dppe)P(OMe)_3]PF_6$. Hydrogen atoms and hexafluorophosphate anion are omitted for clarity.

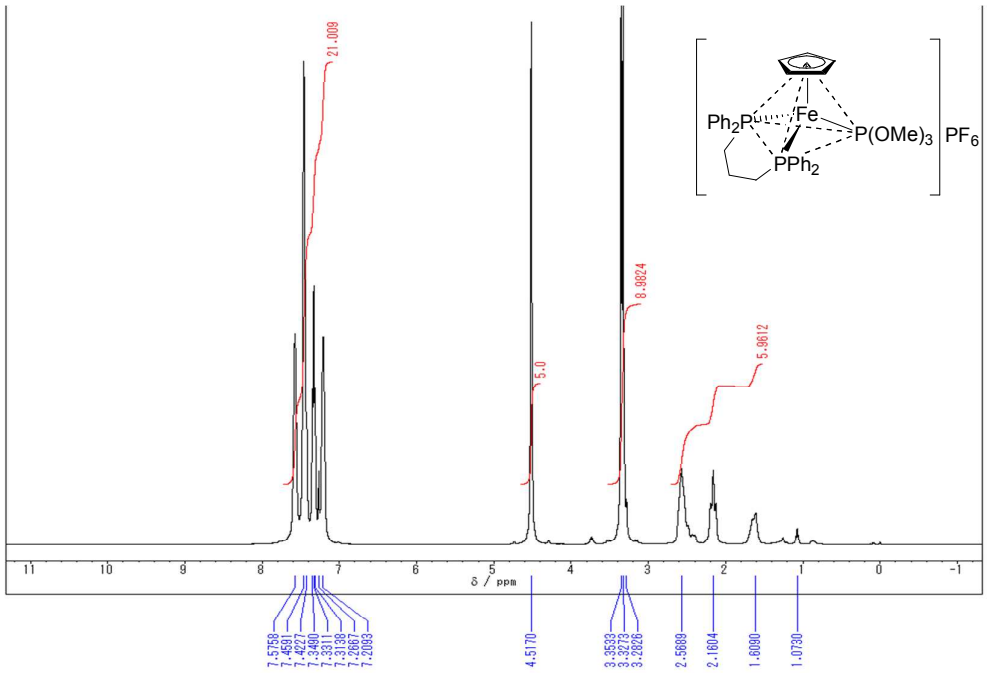

Figure S12-1. ^{1}H NMR Spectrum of [CpFe(dppp)P(OMe)$_3$]PF$_6$ in CDCl$_3$ at 293 K.

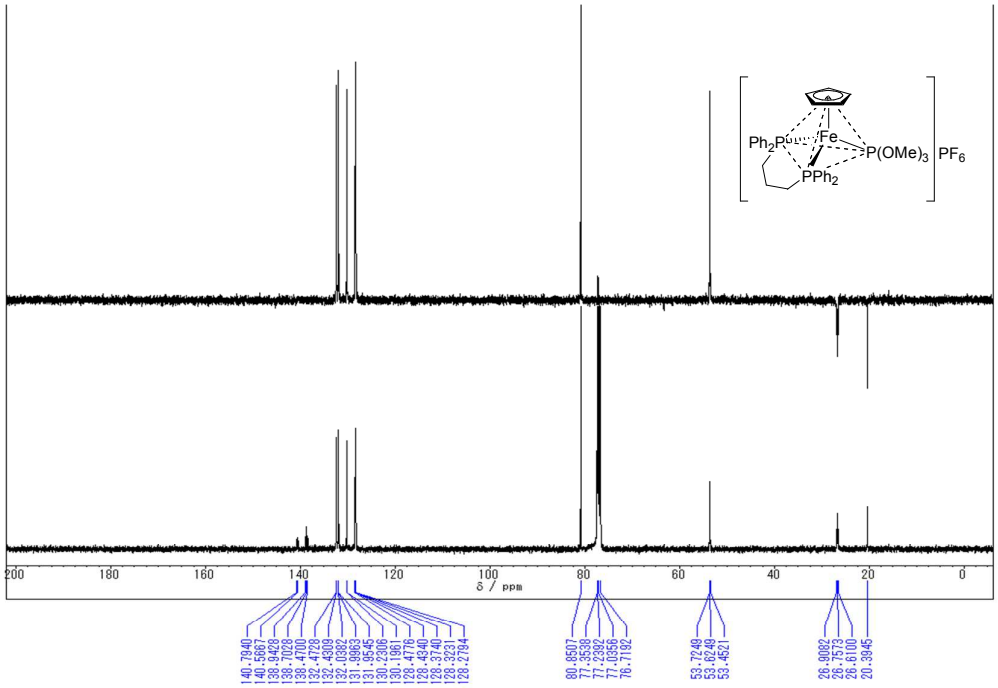

Figure S12-2. ^{13}C NMR Spectra of [CpFe(dppp)P(OMe)$_3$]PF$_6$ in CDCl$_3$ at 293 K (top: DEPT135, bottom: decoupling).

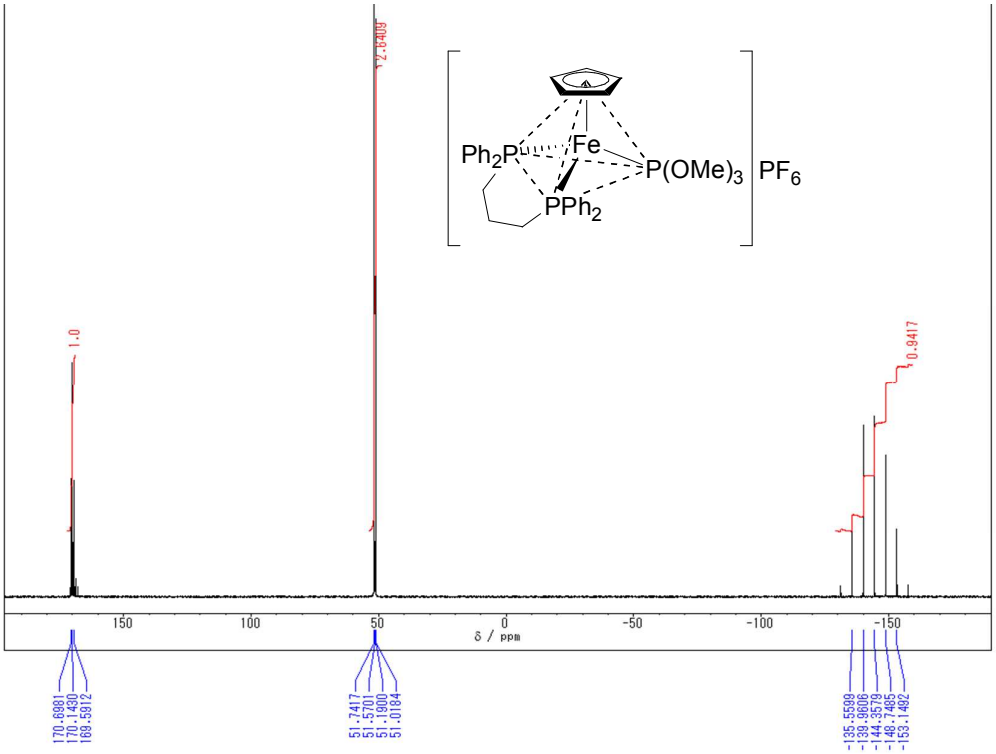

Figure S12-3. $^{31}P\{^{1}H\}$ NMR Spectrum of $[CpFe(dppp)P(OMe)_3]PF_6$ in $CDCl_3$ at 293 K.

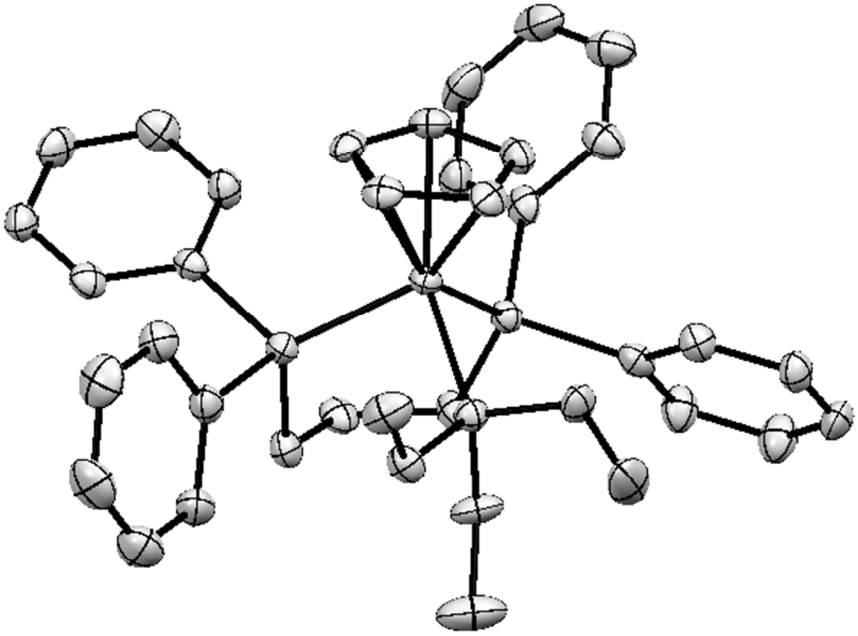

Figure S12-4. ORTEP drawing of $[CpFe(dppp)P(OMe)_3]PF_6$. Hydrogen atoms and hexafluorophosphate anion are omitted for clarity.

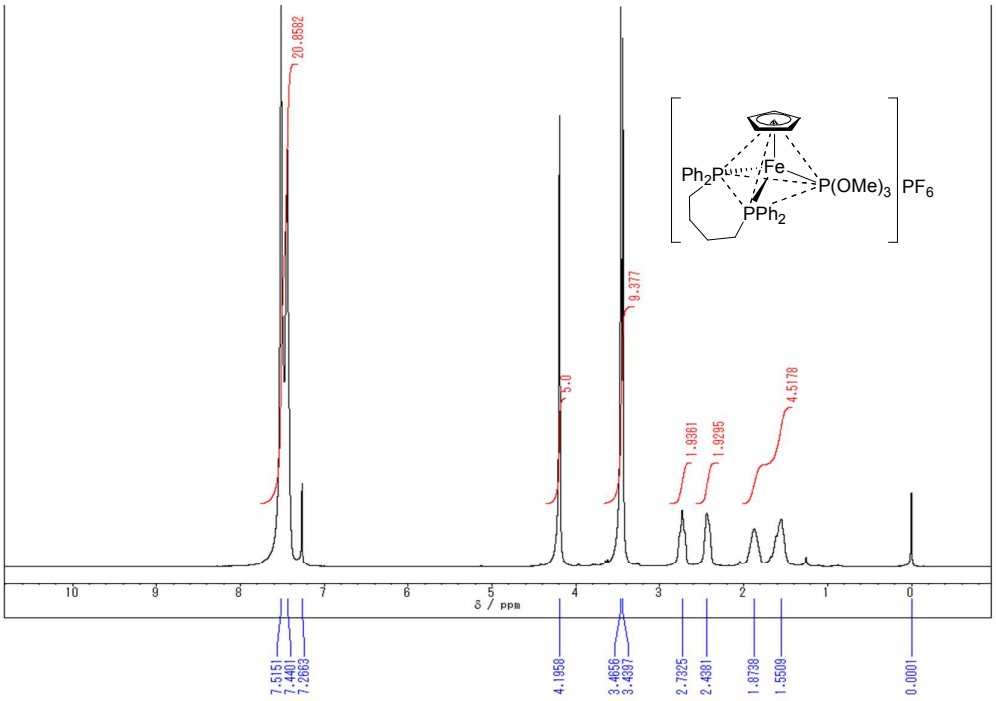

Figure S13-1. ^{1}H NMR Spectrum of [CpFe(dppb)P(OMe)$_3$]PF$_6$ in CDCl$_3$ at 293 K.

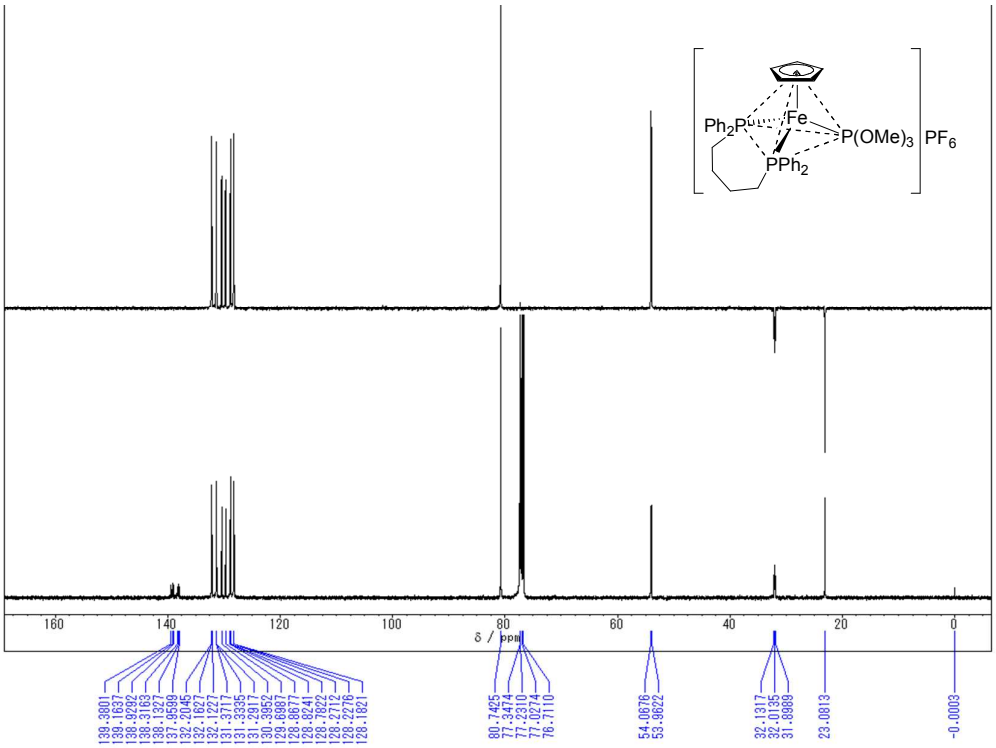

Figure S13-2. ^{13}C NMR Spectra of [CpFe(dppb)P(OMe)$_3$]PF$_6$ in CDCl$_3$ at 293 K (top: DEPT135, bottom: decoupling).

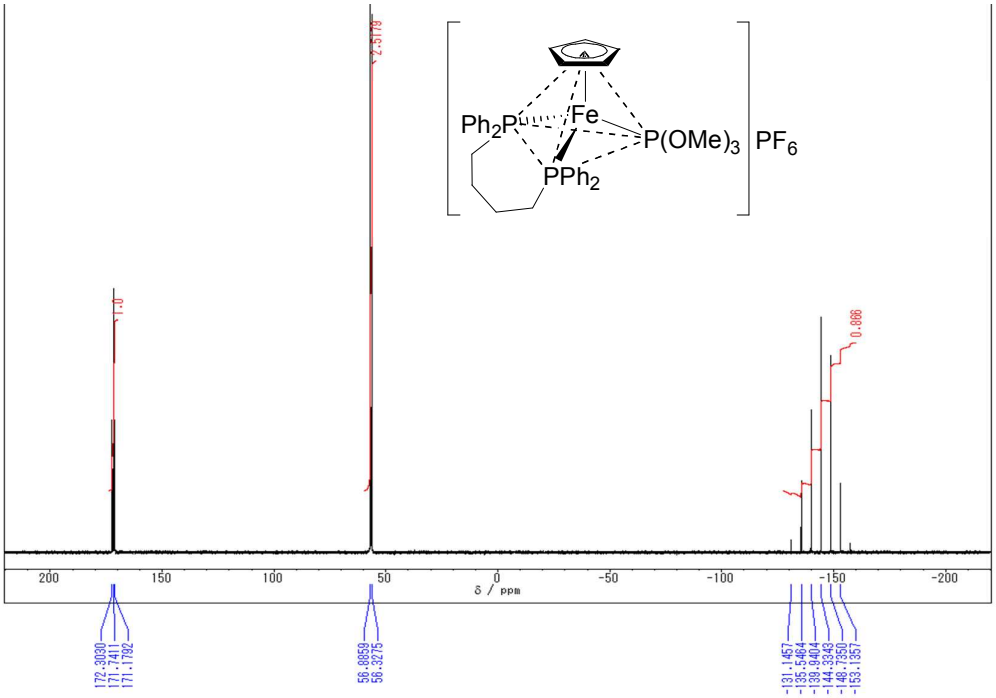

Figure S13-3. $^{31}P\{^{1}H\}$ NMR Spectrum of $[CpFe(dppb)P(OMe)_3]PF_6$ in $CDCl_3$ at 293 K.

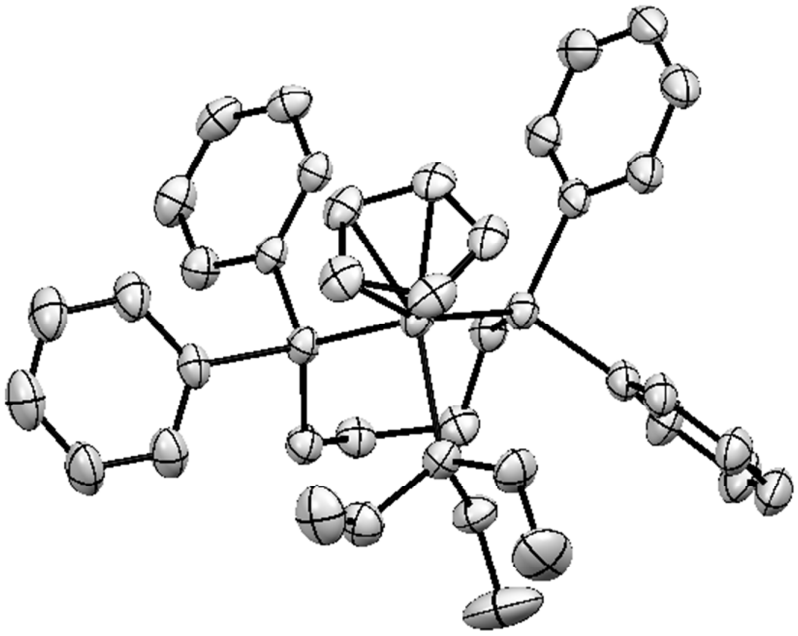

Figure S13-4. ORTEP drawing of $2([CpFe(dppp)P(OMe)_3]PF_6) \cdot 3CHCl_3$. Hydrogen atoms, hexafluorophosphate anion, and three $CHCl_3$ molecules are omitted for clarity.

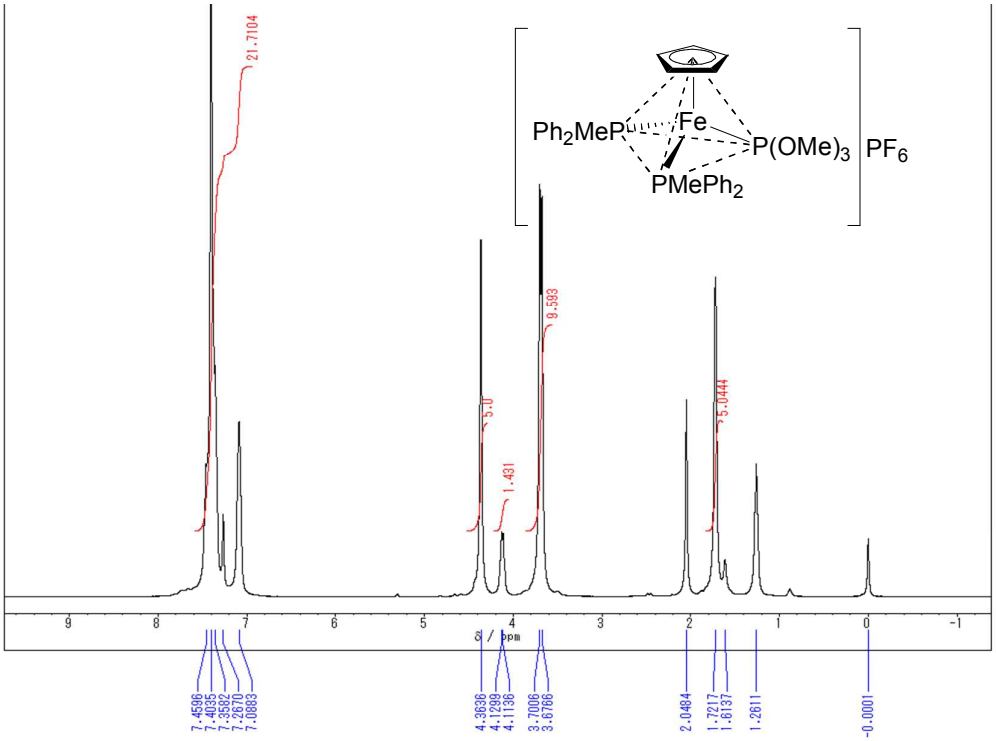

Figure S14-1. ^{1}H NMR Spectrum of $[CpFe(PPh_2Me)_2P(OMe)_3]PF_6$ in $CDCl_3$ at 293 K.

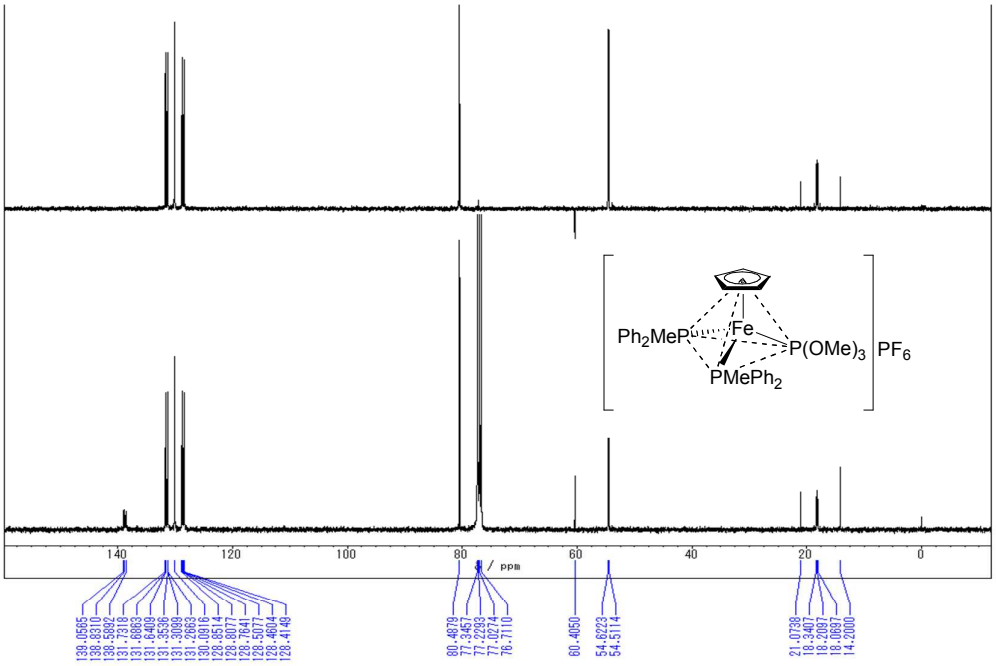

Figure S14-2. ^{13}C NMR Spectra of $[CpFe(PPh_2Me)_2P(OMe)_3]PF_6$ in $CDCl_3$ at 293 K (top: DEPT135, bottom: decoupling).

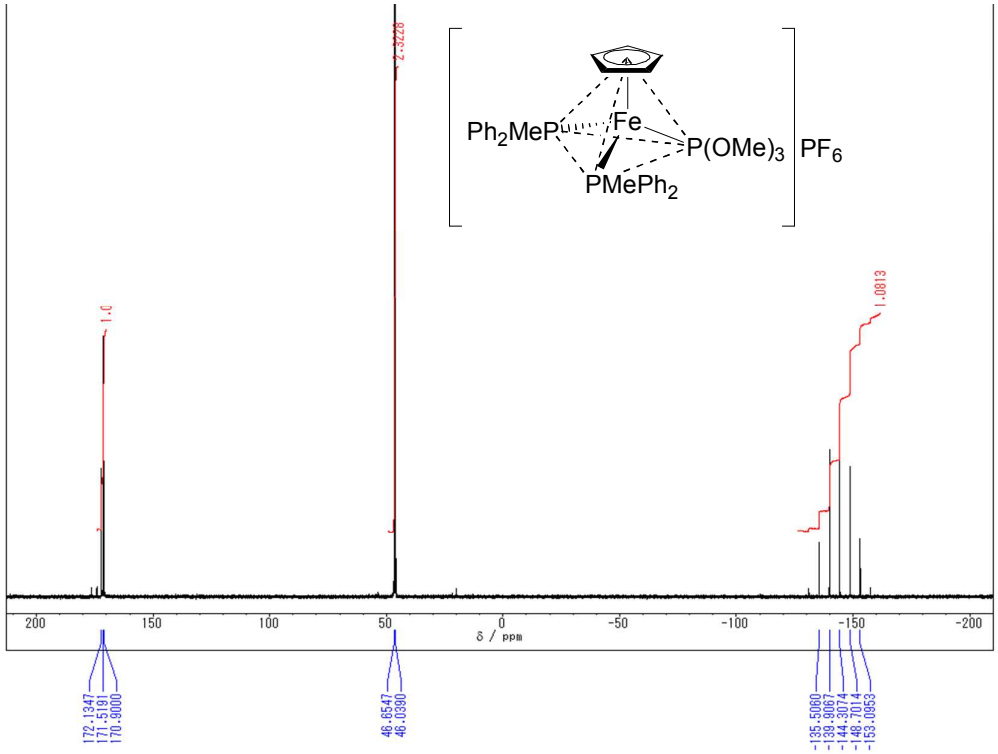

Figure S14-3. $^{31}P\{^{1}H\}$ NMR Spectrum of $[CpFe(PPh_2Me)_2P(OMe)_3]PF_6$ in $CDCl_3$ at 293 K.

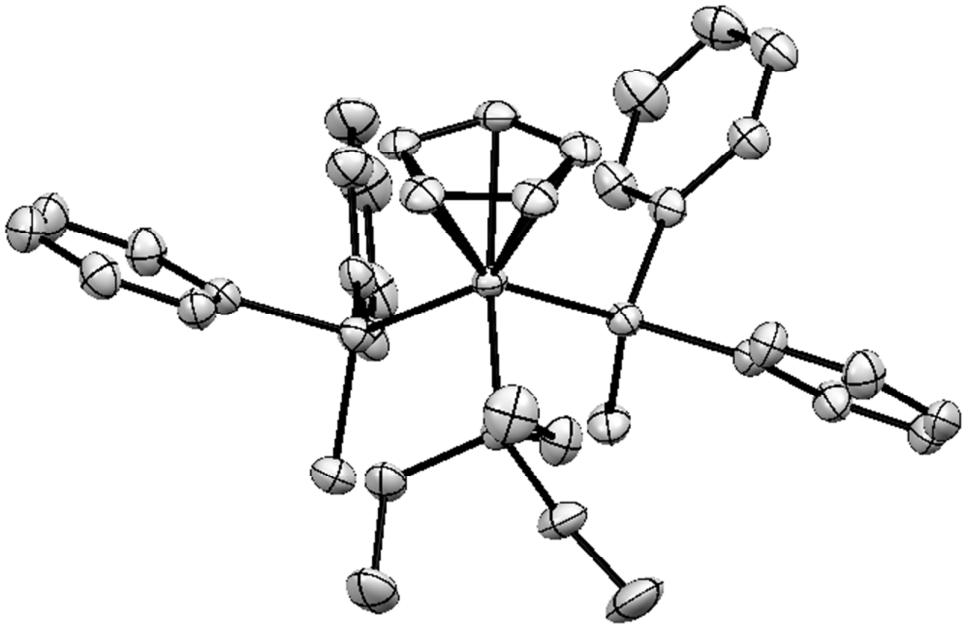

Figure S14-4. ORTEP drawing of $[CpFe(PPh_2Me)_2P(OMe)_3]PF_6 \cdot CH_2Cl_2$. Hydrogen atoms, hexafluorophosphate anion, and one CH_2Cl_2 molecule are omitted for clarity.

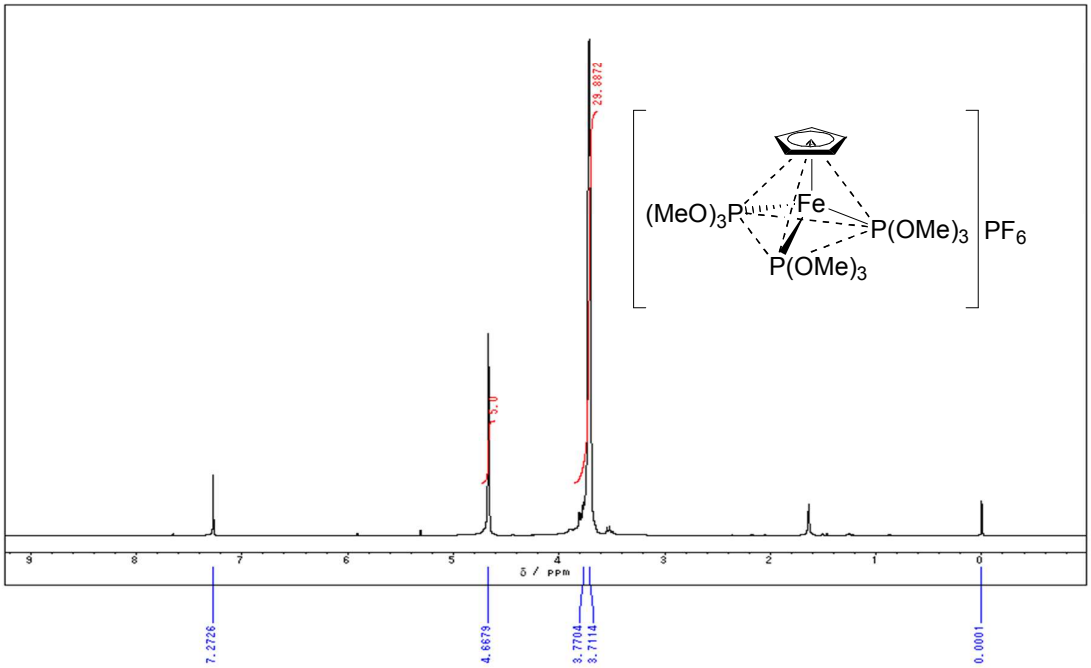

Figure S15-1. ^{1}H NMR Spectrum of [CpFe{P(OMe)$_3$}$_3$]PF$_6$ in CDCl$_3$ at 293 K.

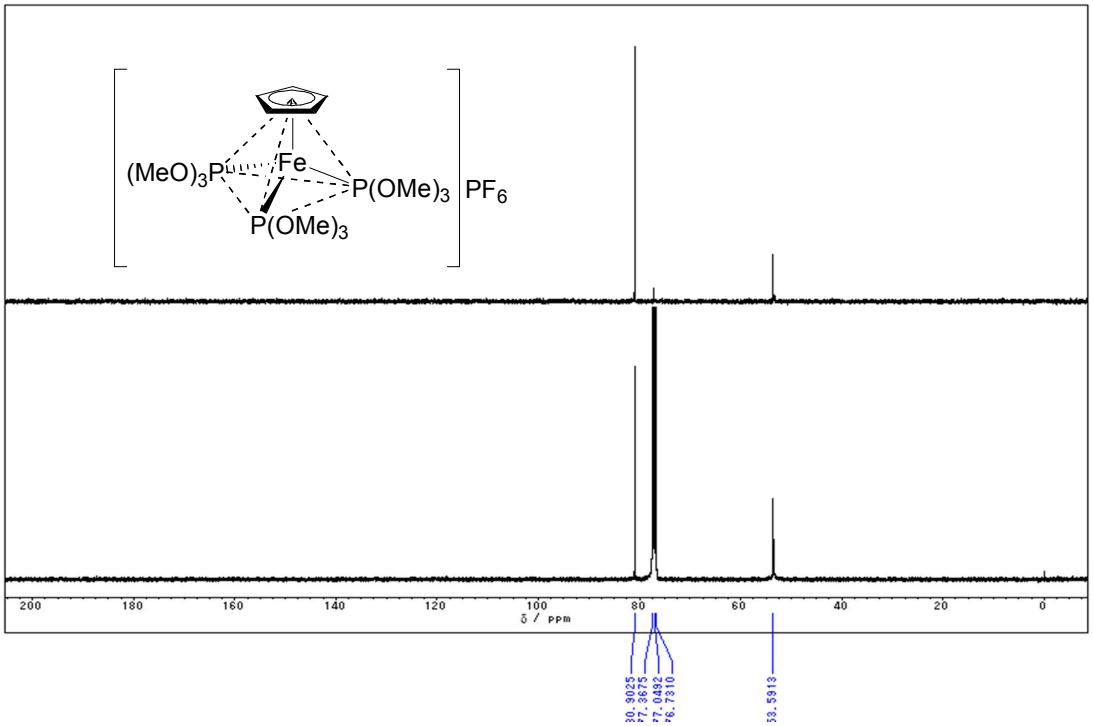

Figure S15-2. ^{13}C NMR Spectra of [CpFe{P(OMe)$_3$}$_3$]PF$_6$ in CDCl$_3$ at 293 K (top: DEPT135, bottom: decoupling).

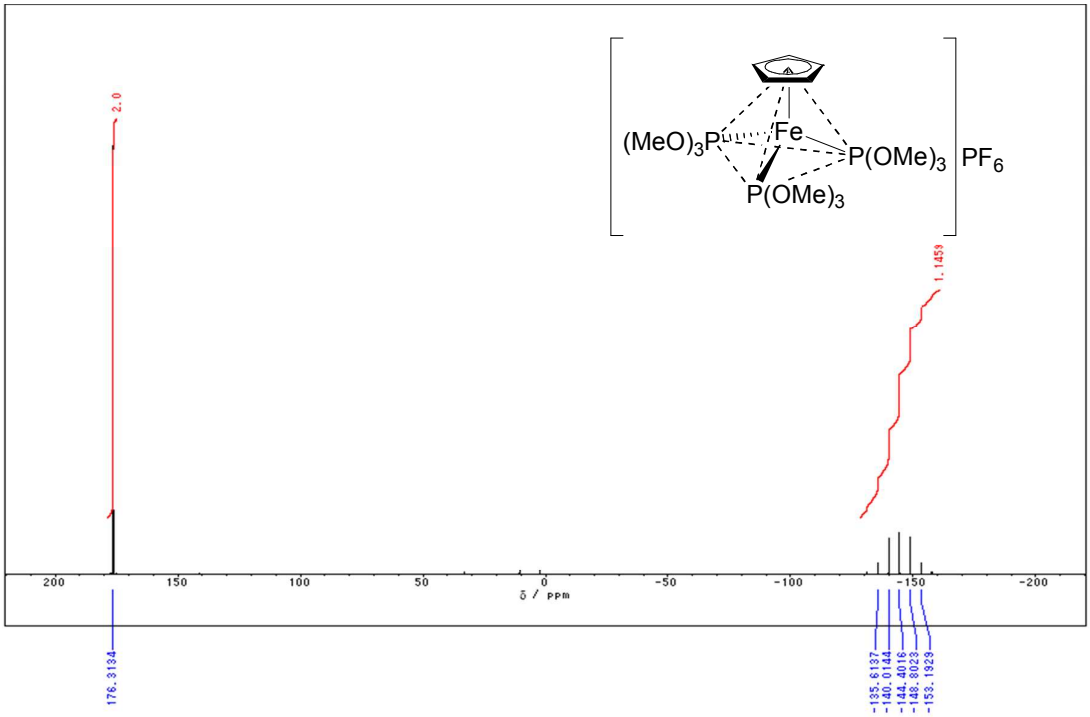

Figure S15-3. $^{31}P\{^{1}H\}$ NMR Spectrum of $[CpFe\{P(OMe)_3\}_3]PF_6$ in $CDCl_3$ at 293 K

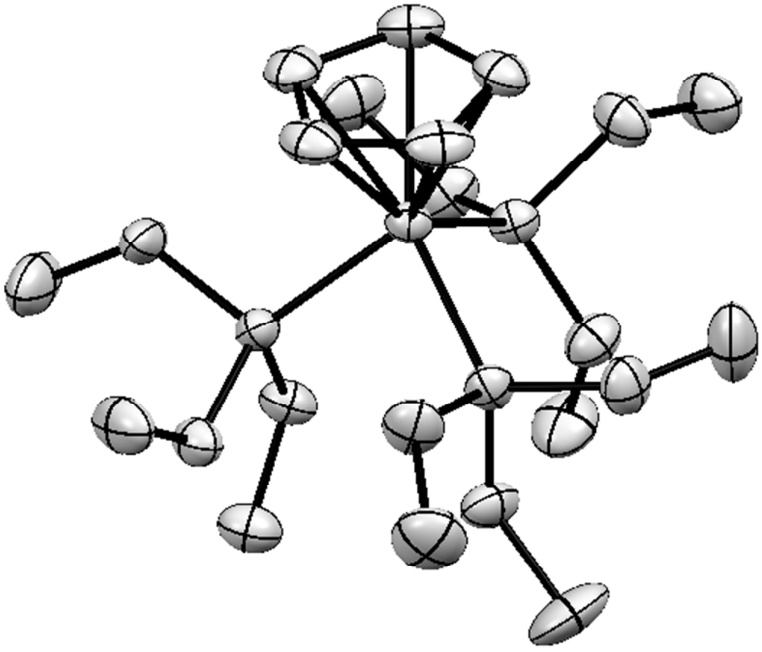

Figure S15-4. ORTEP drawing of $[CpFe\{P(OMe)_3\}_3]PF_6$. Hydrogen atoms and hexafluorophosphate anion are omitted for clarity.

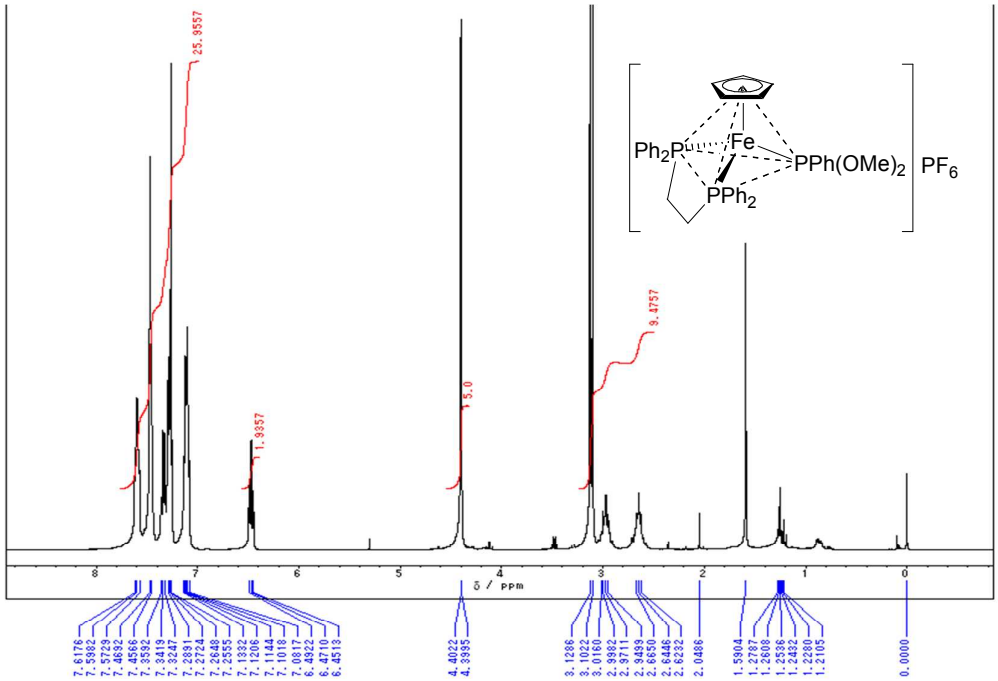

Figure S16-1. ^{1}H NMR Spectrum of [CpFe(dppe)PPh(OMe)$_2$]PF$_6$ in CDCl$_3$ at 293 K.

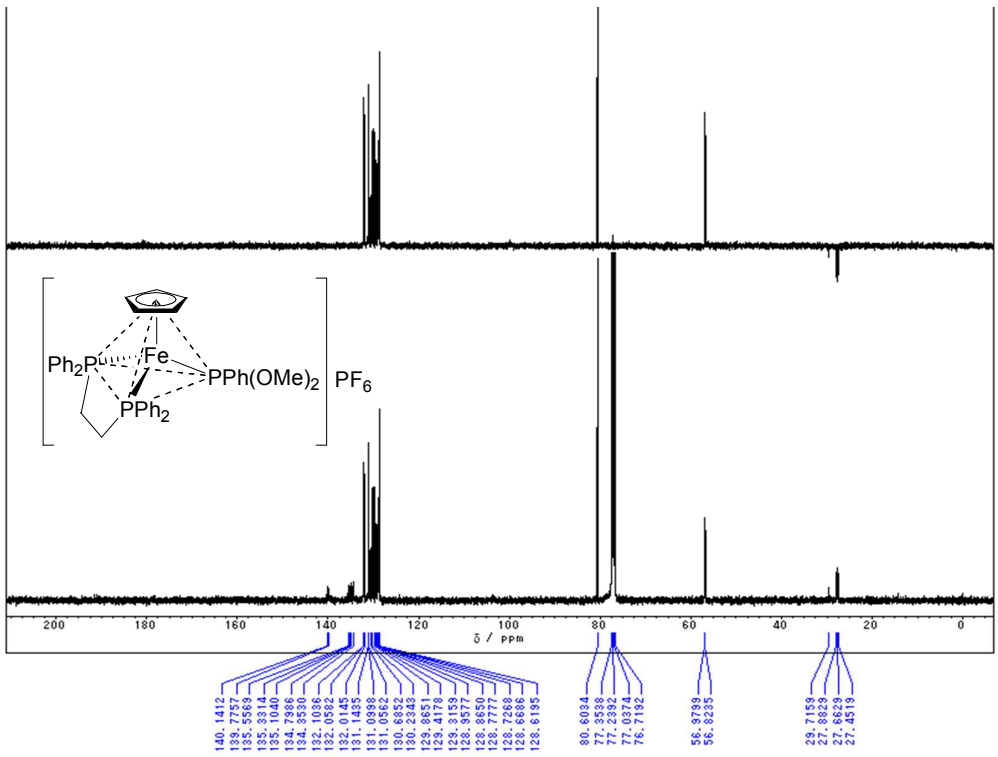

Figure S16-2. ^{13}C NMR Spectra of [CpFe(dppe)PPh(OMe)$_2$]PF$_6$ in CDCl$_3$ at 293 K (top: DEPT135, bottom: decoupling).

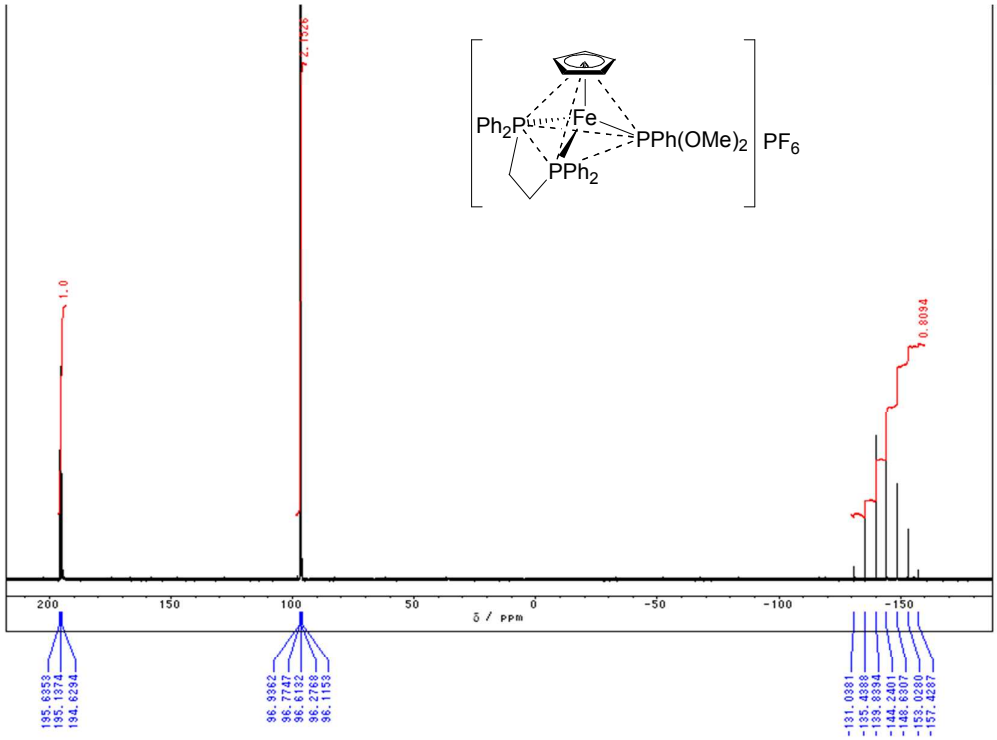

Figure S16-3. $^{31}P\{^{1}H\}$ NMR Spectrum of $[CpFe(dppe)PPh(OMe)_2]PF_6$ in $CDCl_3$ at 293 K.

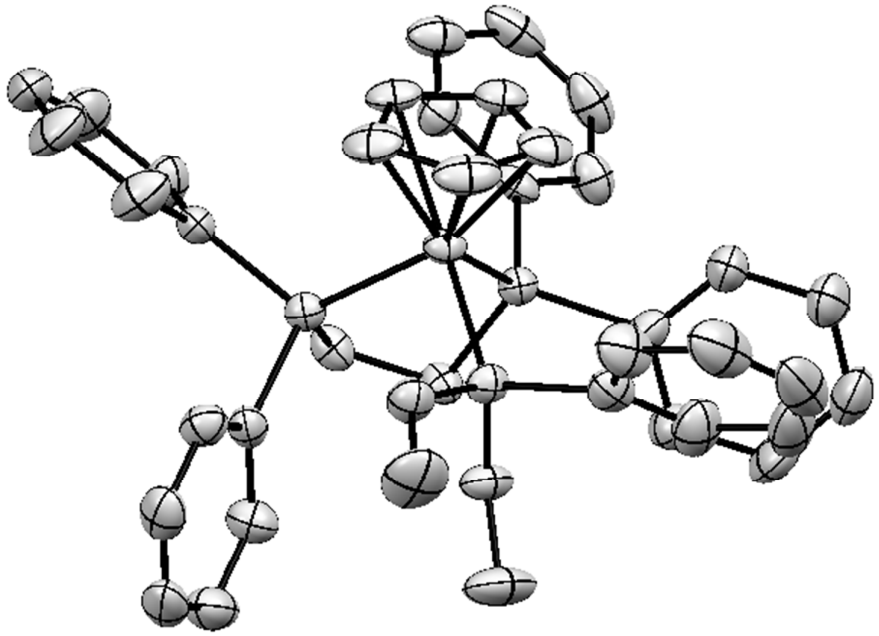

Figure S16-4. ORTEP drawing of $[CpFe(dppe)PPh(OMe)_2]PF_6$. Hydrogen atoms and hexafluorophosphate anion are omitted for clarity.

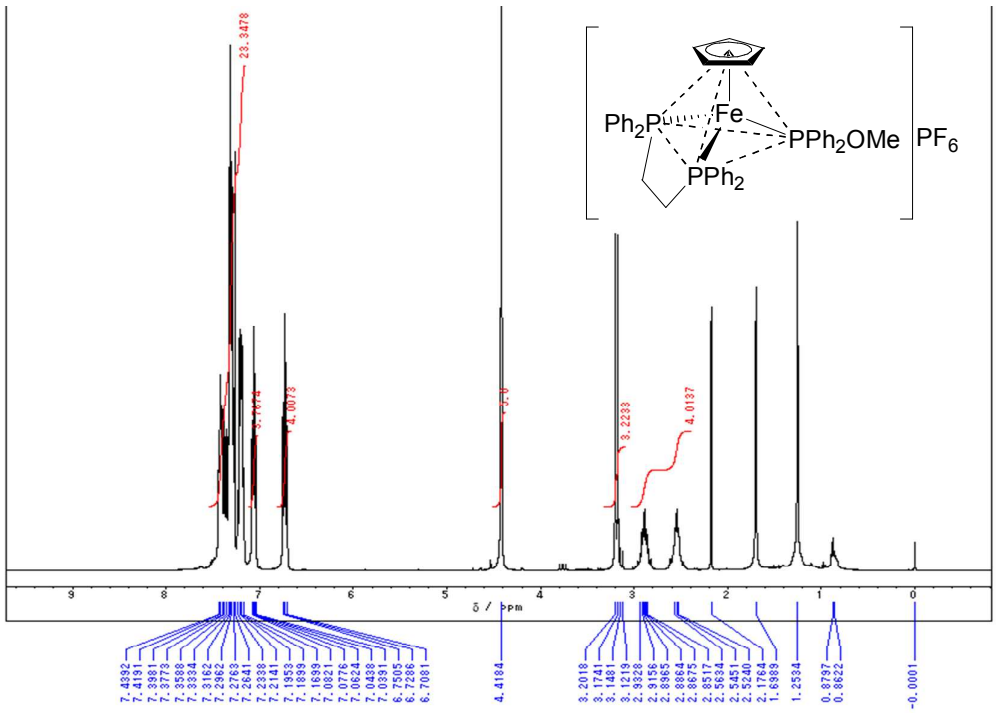

Figure S17-1. ^{1}H NMR Spectrum of [CpFe(dppe)PPh$_2$(OMe)]PF$_6$ in CDCl$_3$ at 293 K.

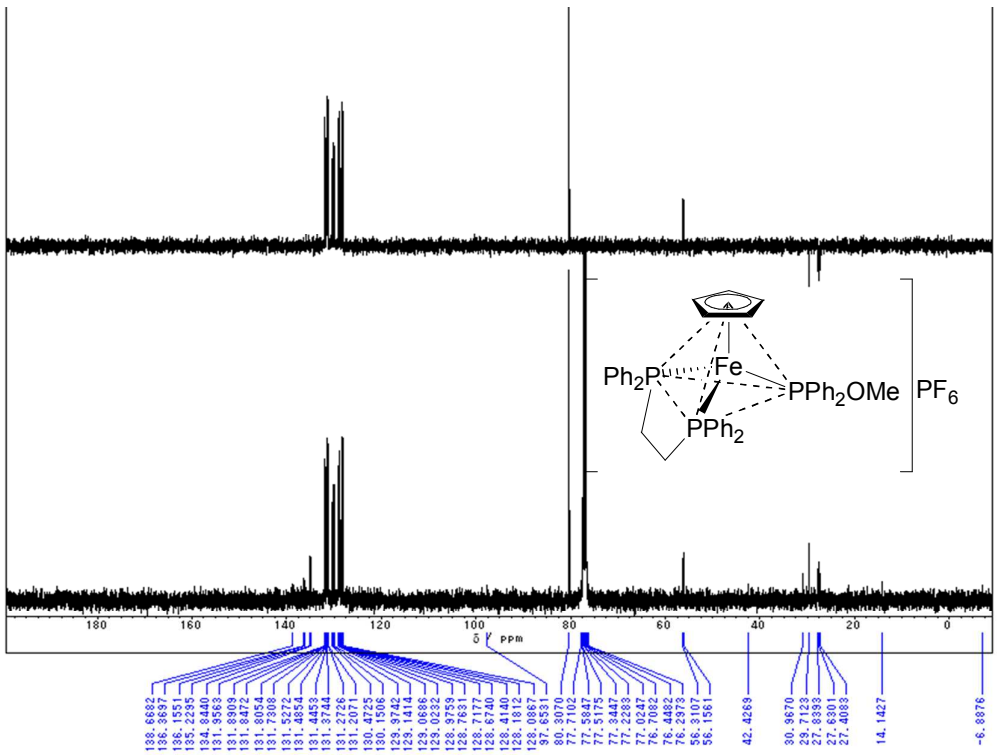

Figure S17-2. ^{13}C NMR Spectra of [CpFe(dppe)PPh$_2$(OMe)]PF$_6$ in CDCl$_3$ at 293 K (top: DEPT135, bottom: decoupling).

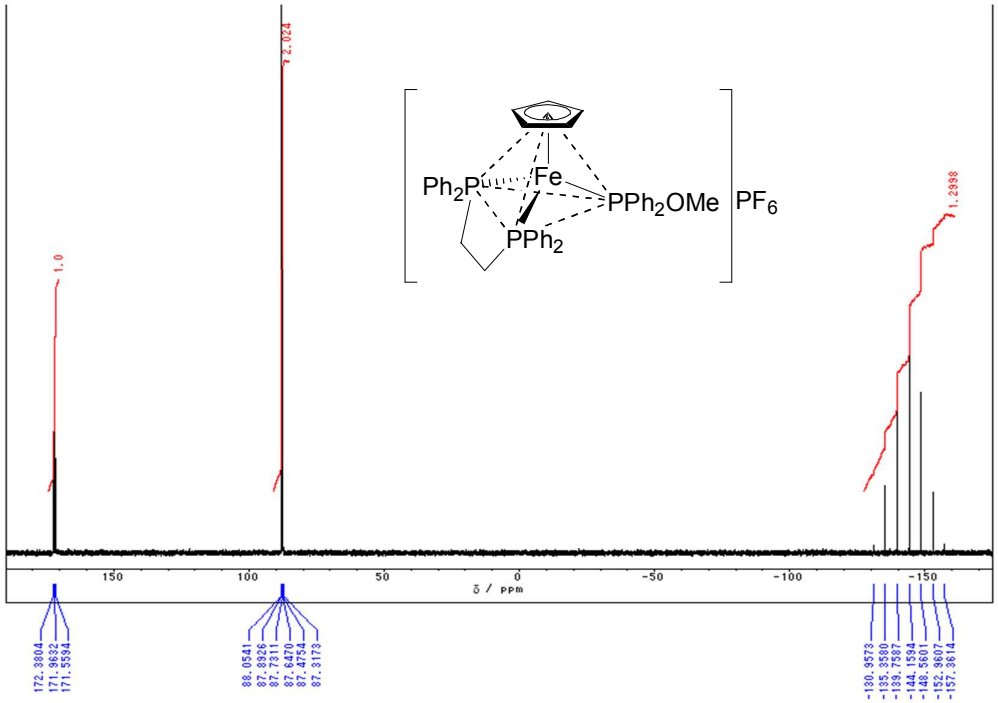

Figure S17-3. $^{31}P\{^{1}H\}$ NMR Spectrum of $[CpFe(dppe)PPh_2(OMe)]PF_6$ in $CDCl_3$ at 293 K.

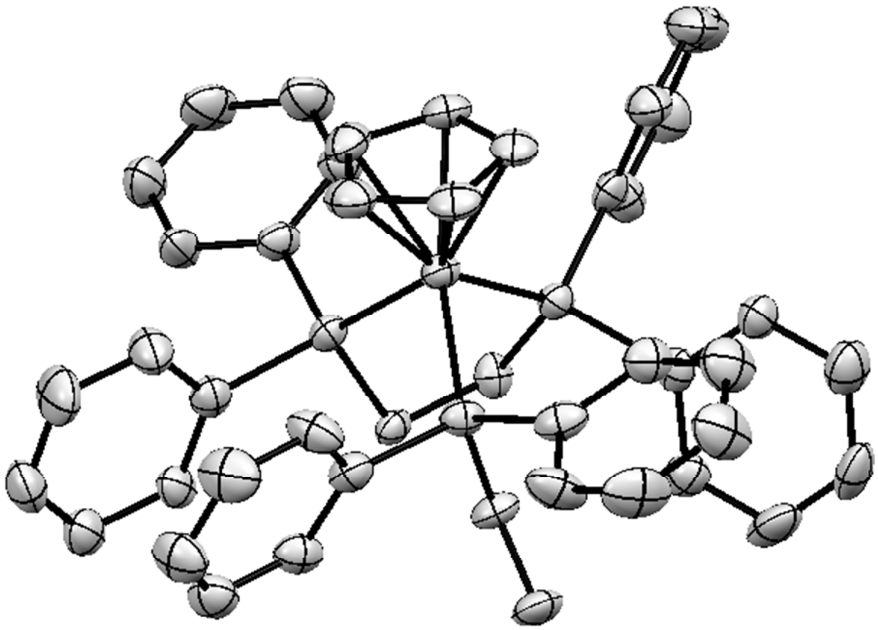

Figure S17-4. ORTEP drawing of $[CpFe(dppe)PPh_2(OMe)]PF_6$. Hydrogen atoms and hexafluorophosphate anion are omitted for clarity.

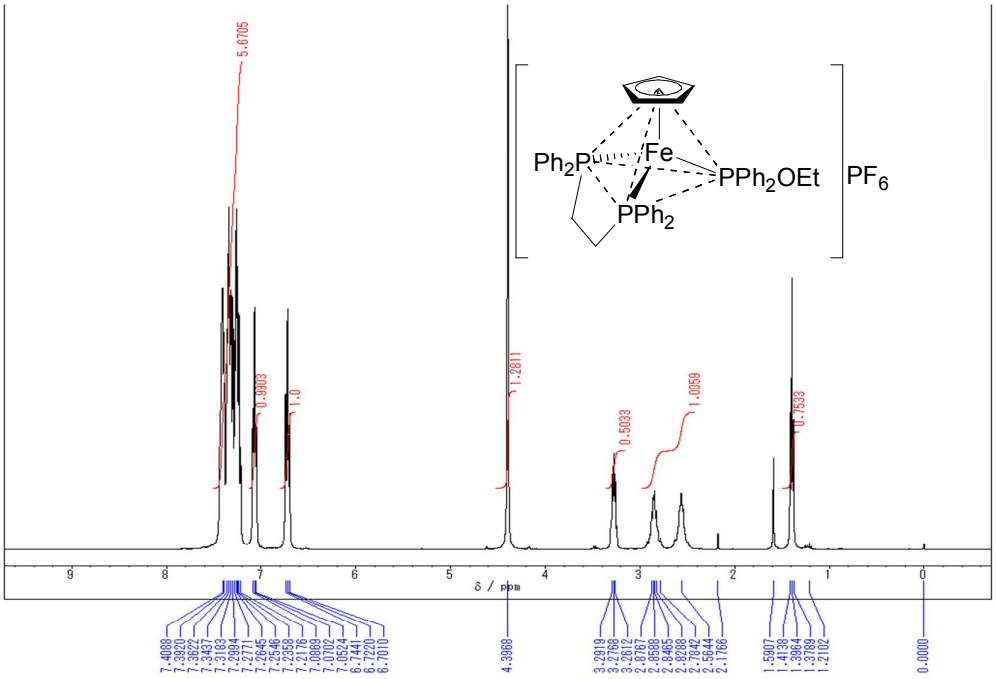

Figure S18-1. ^{1}H NMR Spectrum of [CpFe(dppe)PPh_2(OEt)]PF_6 in $CDCl_3$ at 293 K.

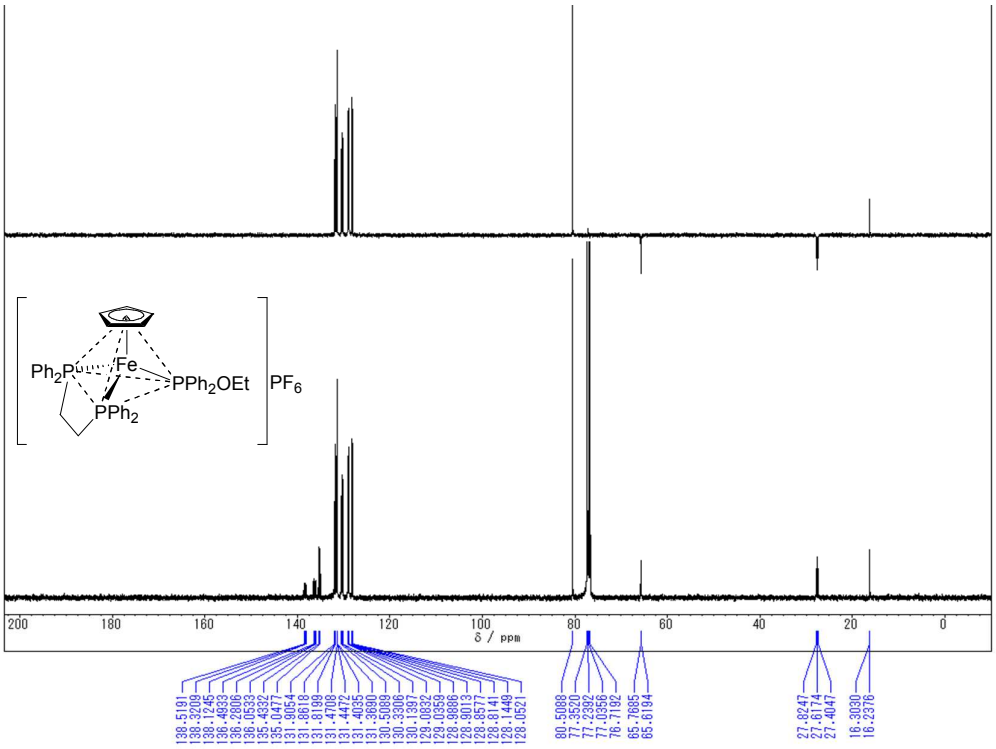

Figure S18-2. ^{13}C NMR Spectra of [CpFe(dppe)PPh_2(OEt)]PF_6 in $CDCl_3$ at 293 K (top: DEPT135, bottom: decoupling).

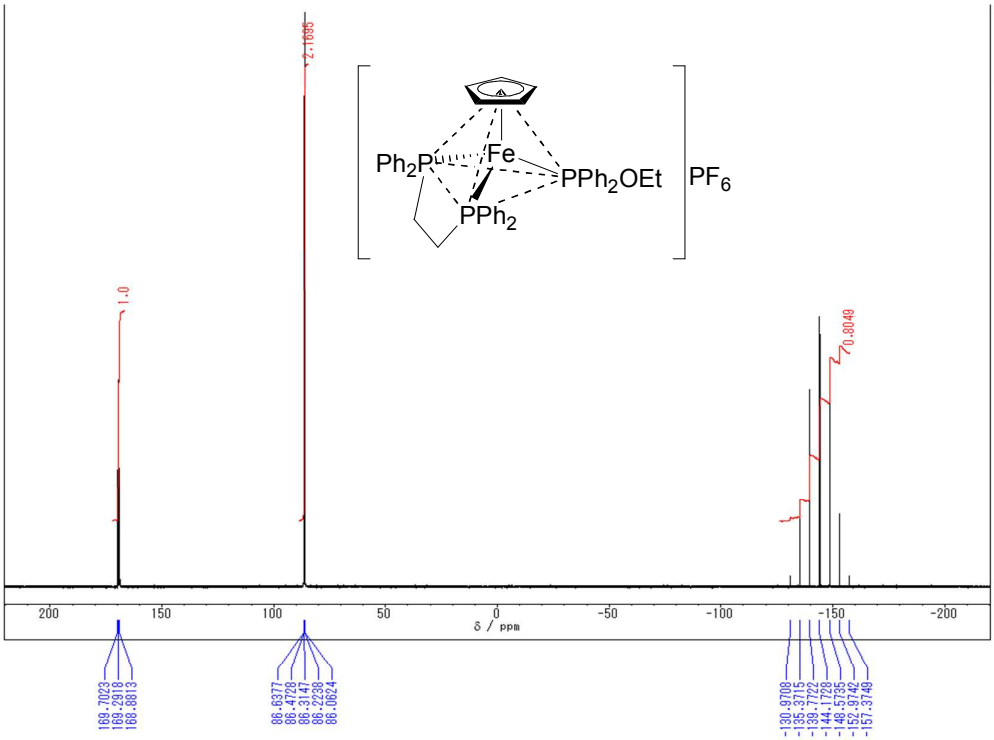

Figure S18-3. $^{31}P\{^{1}H\}$ NMR Spectrum of $[CpFe(dppe)PPh_2(OEt)]PF_6$ in $CDCl_3$ at 293 K.

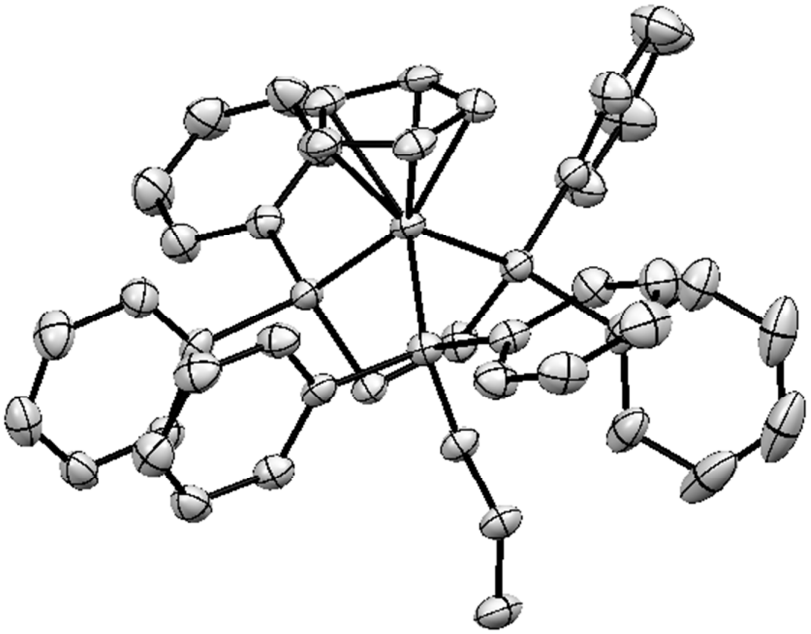

Figure S18-4. ORTEP drawing of $[CpFe(dppe)PPh_2(OEt)]PF_6$. Hydrogen atoms and hexafluorophosphate anion are omitted for clarity.

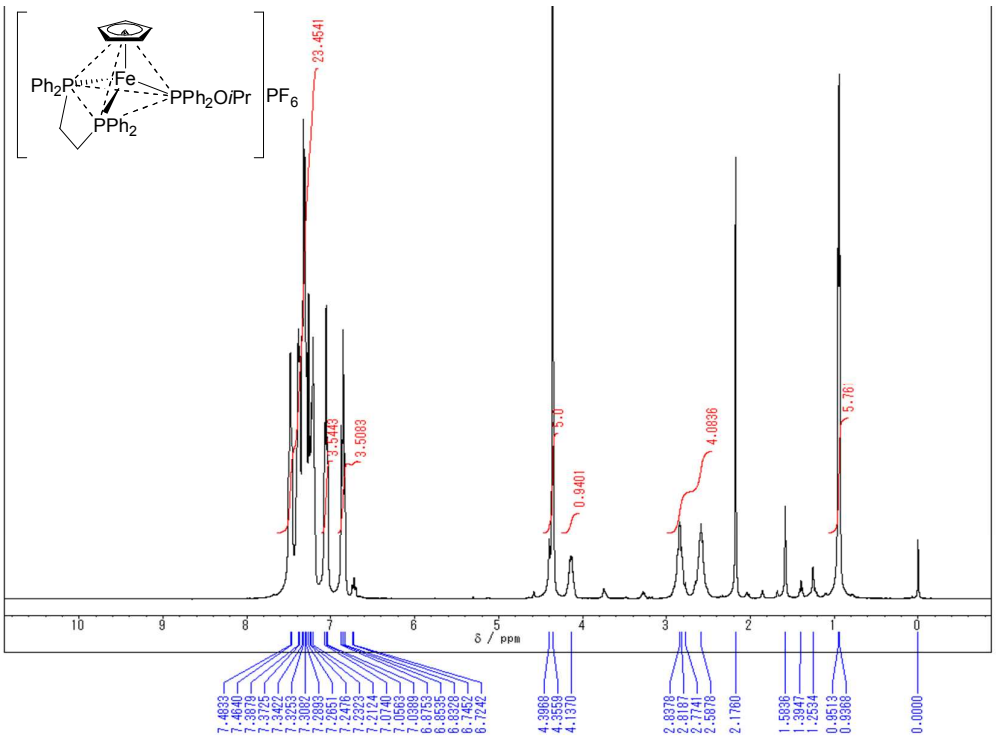

Figure S19-1. ^{1}H NMR Spectrum of [CpFe(dppe)PPh$_2$(O*i*Pr)]PF$_6$ in CDCl$_3$ at 293 K.

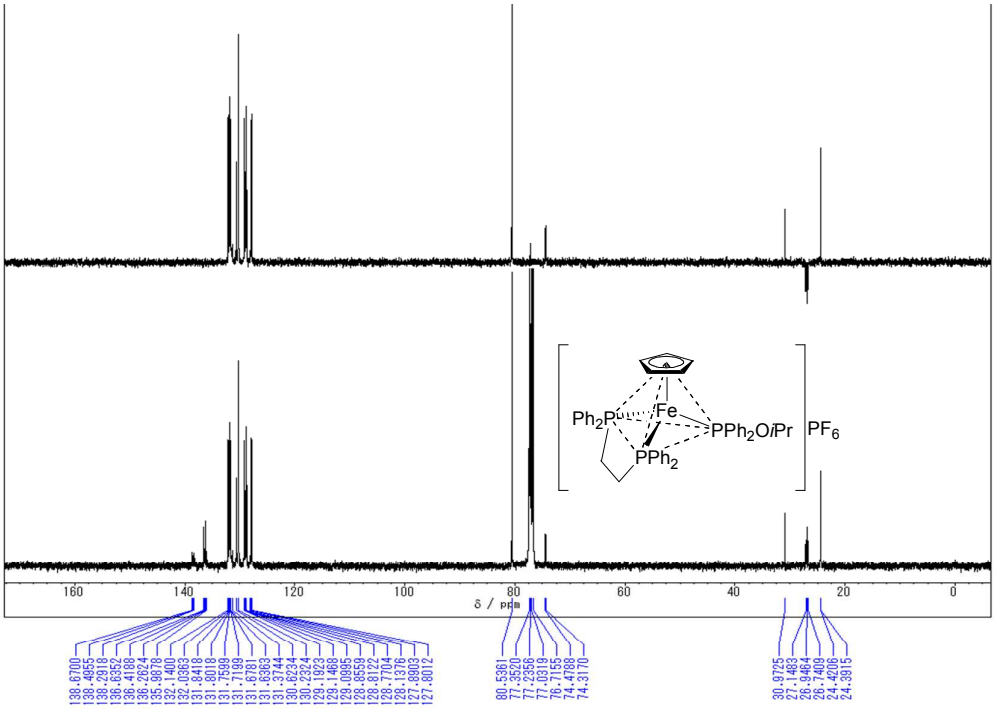

Figure S19-2. ^{13}C NMR Spectra of [CpFe(dppe)PPh$_2$(O*i*Pr)]PF$_6$ in CDCl$_3$ at 293 K (top: DEPT135, bottom: decoupling).

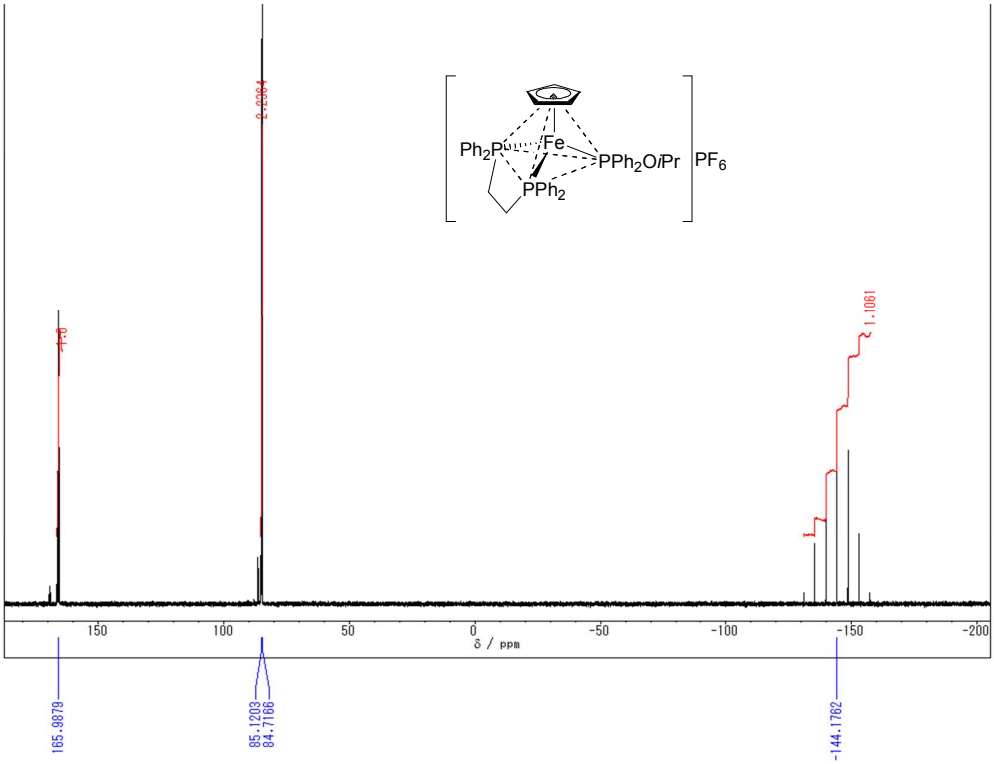

Figure S19-3. $^{31}P\{^{1}H\}$ NMR Spectrum of [CpFe(dppe)PPh_2(O*i*Pr)]PF_6 in $CDCl_3$ at 293 K.

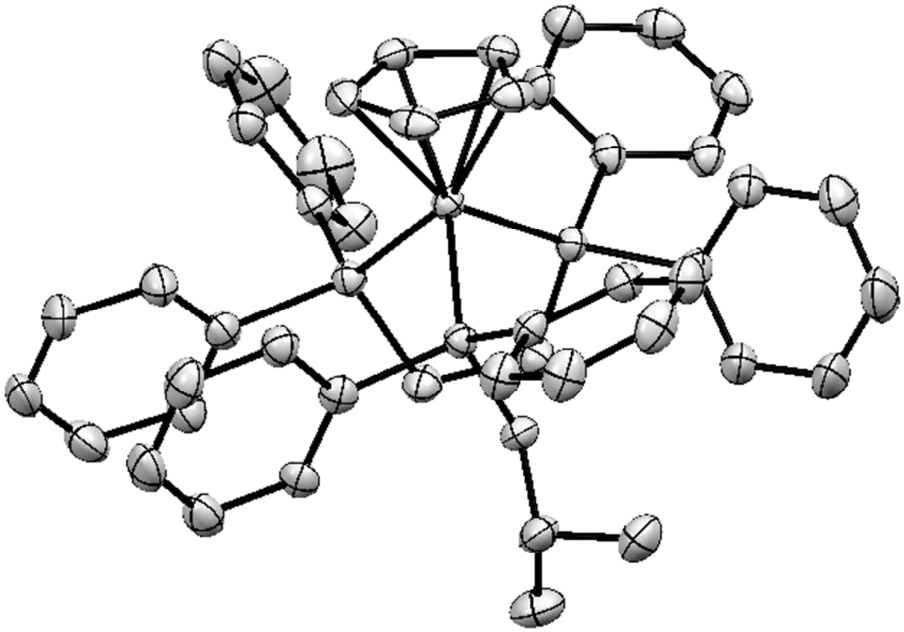

Figure S19-4. ORTEP drawing of [CpFe(dppe)PPh_2(O*i*Pr)]PF_6· $CHCl_3$. Hydrogen atoms, hexafluorophosphate anion, and one $CHCl_3$ molecule are omitted for clarity.

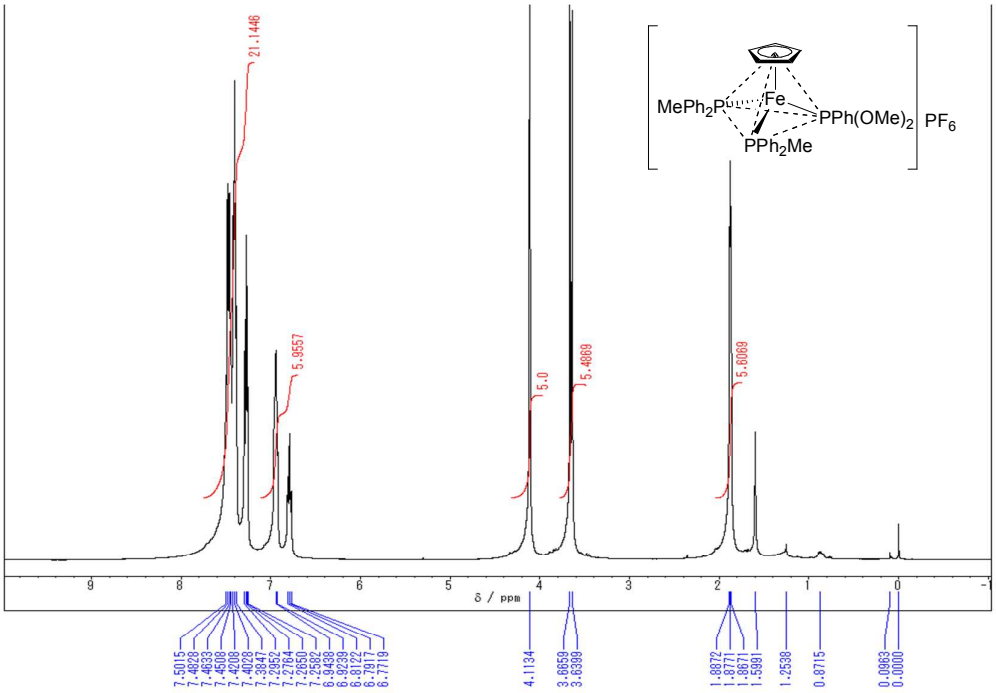

Figure S20-1. ^{1}H NMR Spectrum of [CpFe(PPh$_2$Me)PPh(OMe)$_2$]PF$_6$ in CDCl$_3$ at 293 K.

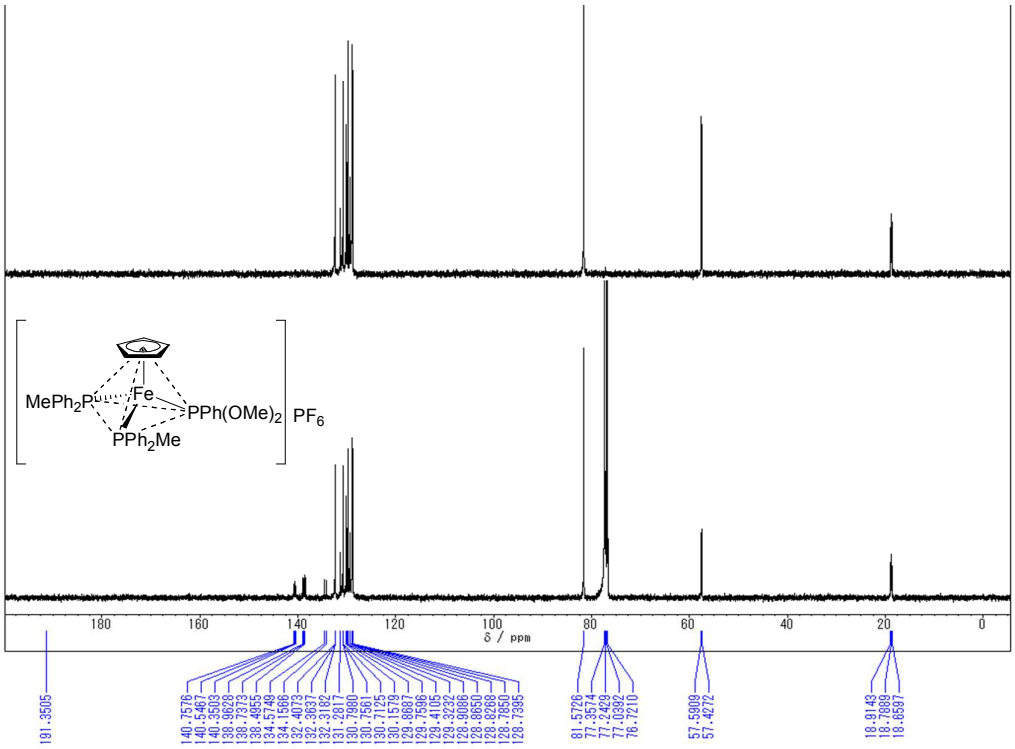

Figure S20-2. ^{13}C NMR Spectra of [CpFe(PPh$_2$Me)$_2$PPh(OMe)$_2$]PF$_6$ in CDCl$_3$ at 293 K (top: DEPT135, bottom: decoupling).

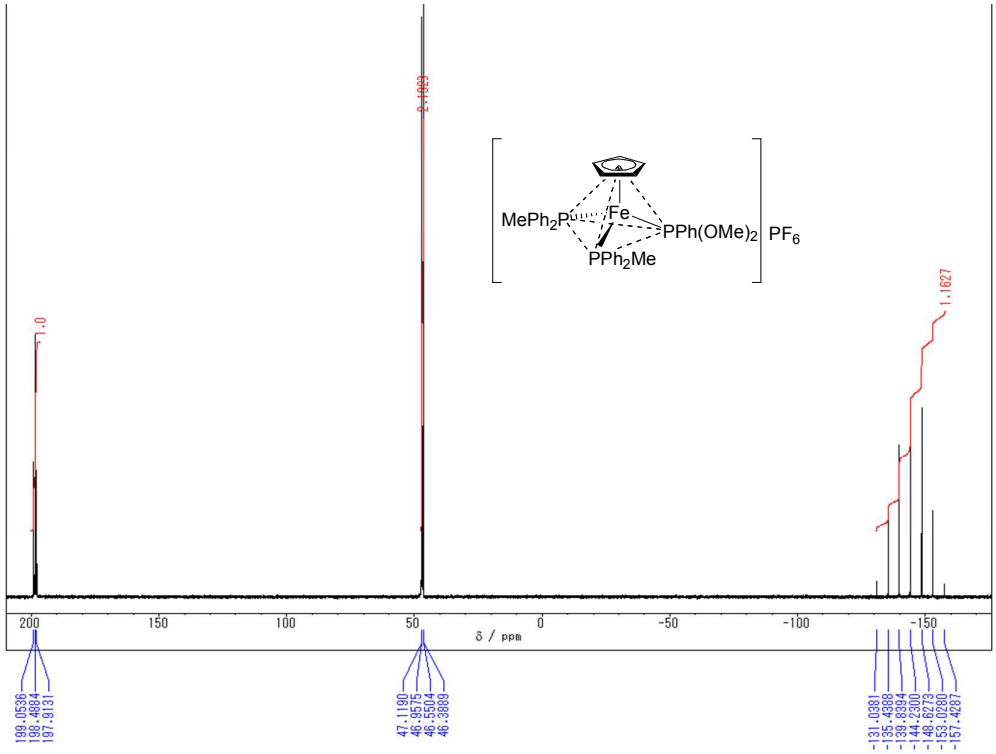

Figure S20-3. $^{31}P\{^{1}H\}$ NMR Spectrum of $[CpFe(PPh_2Me)_2PPh(OMe)_2]PF_6$ in $CDCl_3$ at 293 K.

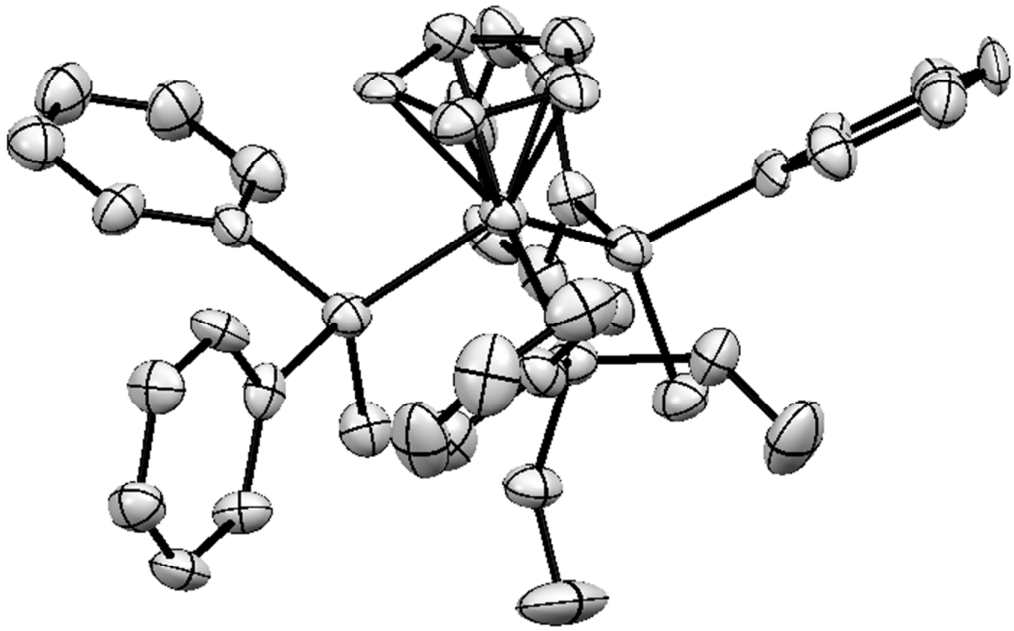

Figure S20-4. ORTEP drawing of $[CpFe(PPh_2Me)_2PPh(OMe)_2]PF_6 \cdot CH_2Cl_2$. Hydrogen atoms, hexafluorophosphate anion, and one CH_2Cl_2 molecule are omitted for clarity.

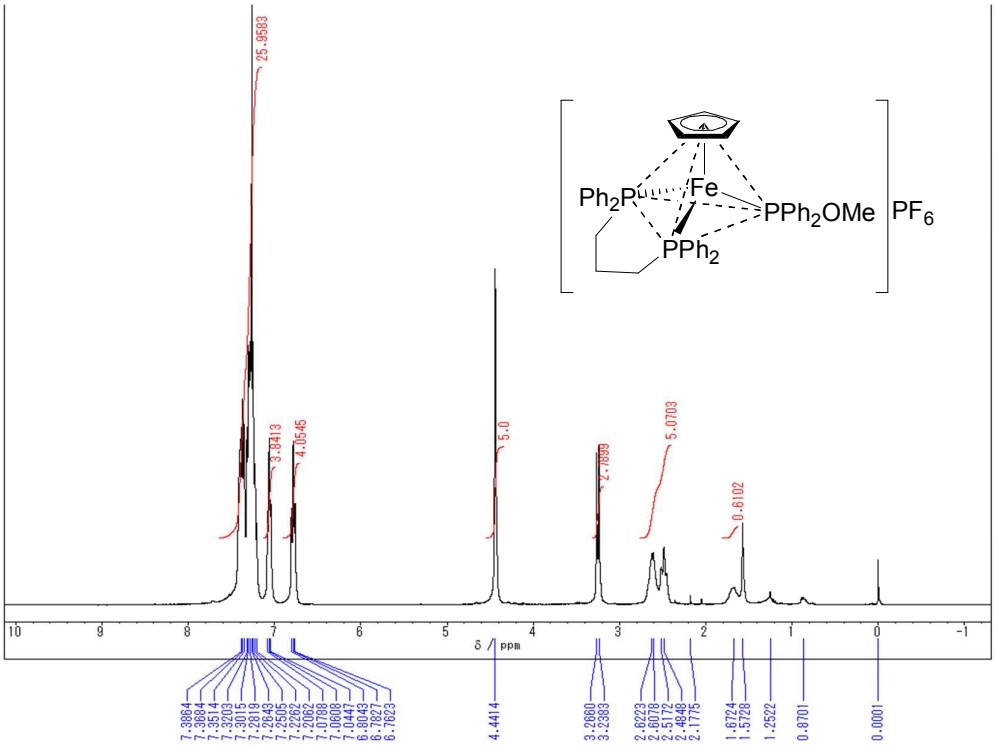

Figure S21-1. ^{1}H NMR Spectrum of [CpFe(dppp)PPh$_2$(OMe)]PF$_6$ in CDCl$_3$ at 293 K.

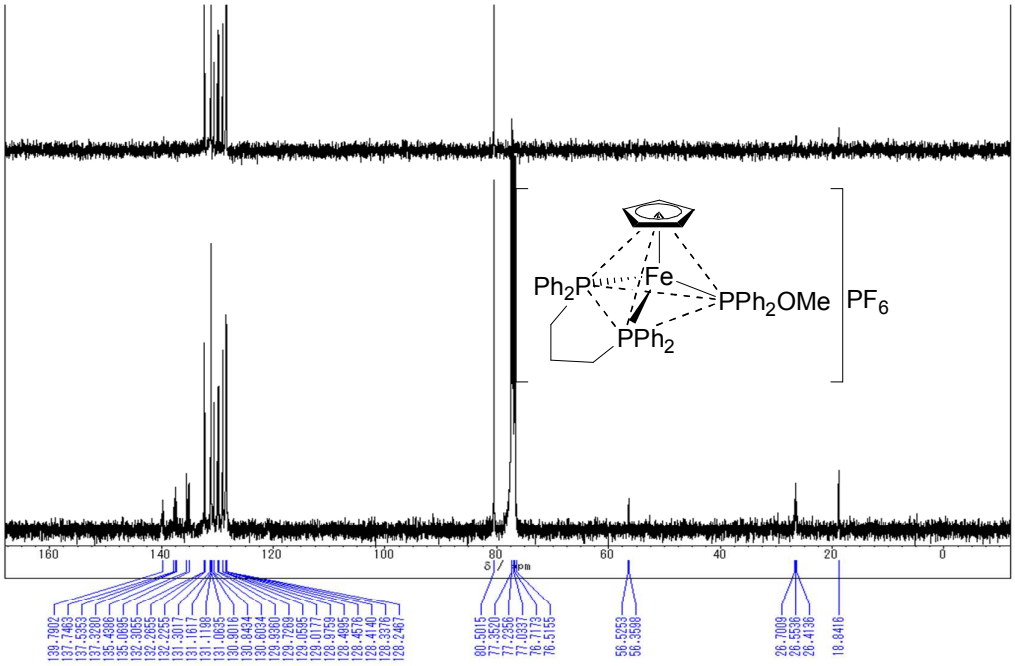

Figure S21-2. ^{13}C NMR Spectra of [CpFe(dppp)PPh$_2$(OMe)]PF$_6$ in CDCl$_3$ at 293 K (top: DEPT135, bottom: decoupling).

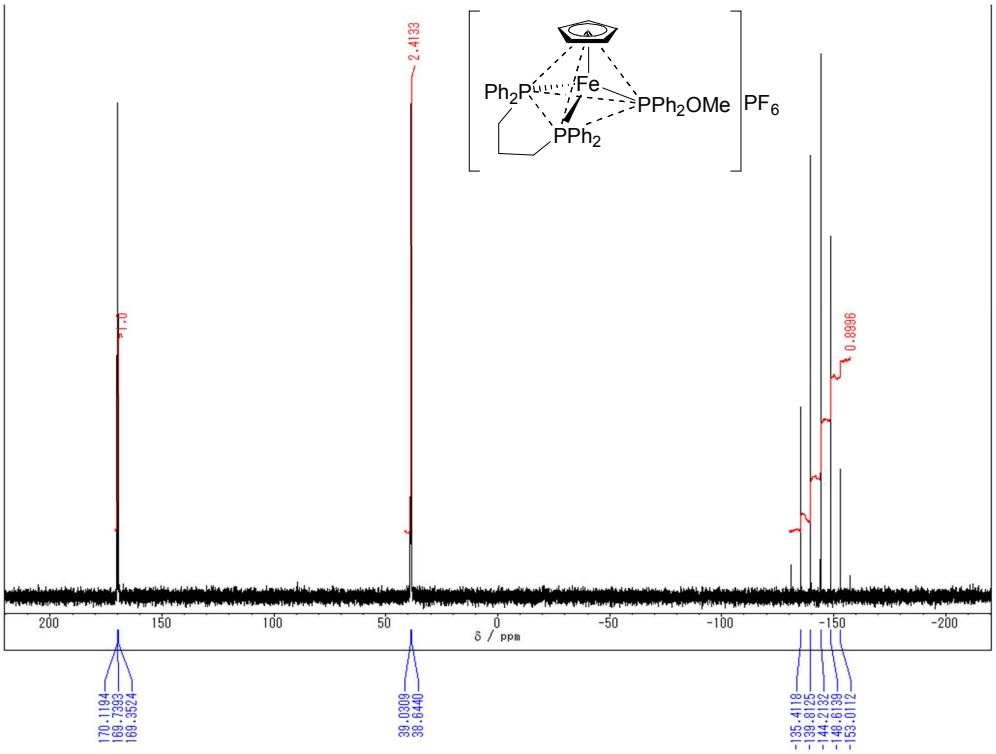

Figure S21-3. $^{31}P\{^{1}H\}$ NMR Spectrum of $[CpFe(dppp)PPh_2(OMe)]PF_6$ in $CDCl_3$ at 293 K.

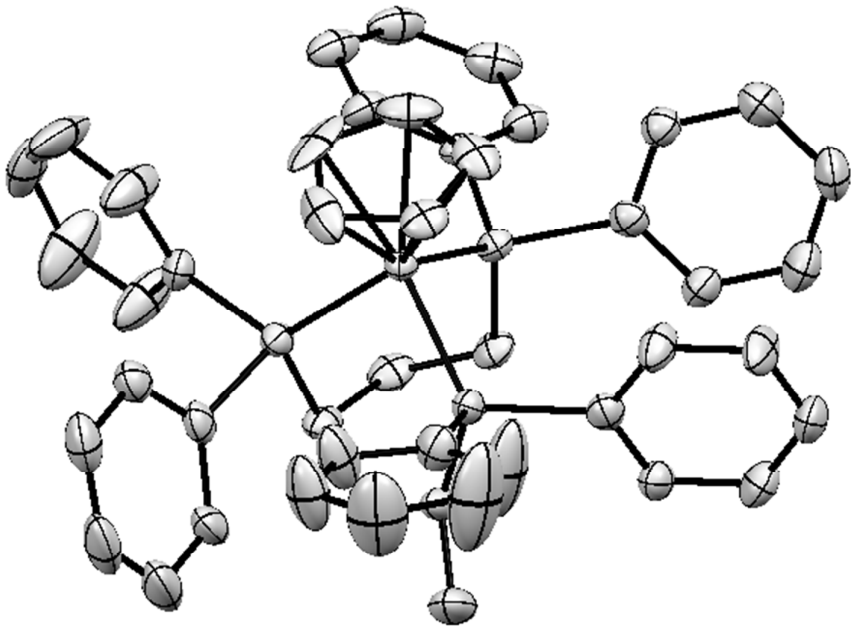

Figure S21-4. ORTEP drawing of $[CpFe(dppp)PPh_2(OMe)]PF_6$. Hydrogen atoms and hexafluorophosphate anion are omitted for clarity.

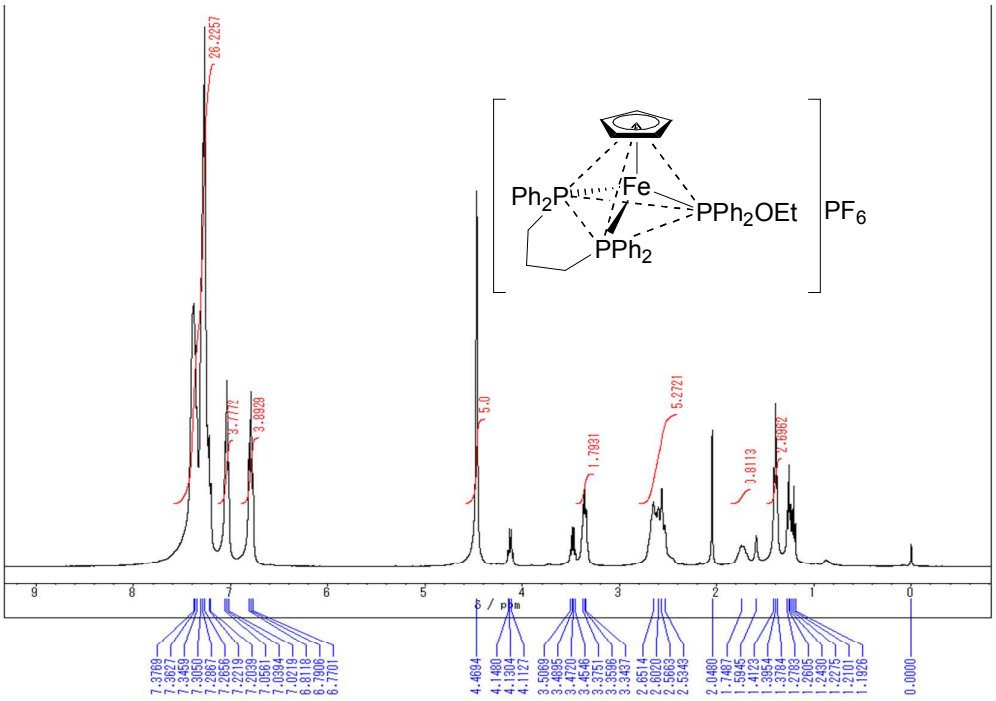

Figure S22-1. ^{1}H NMR Spectrum of [CpFe(dppp)PPh$_2$(OEt)]PF$_6$ in CDCl$_3$ at 293 K.

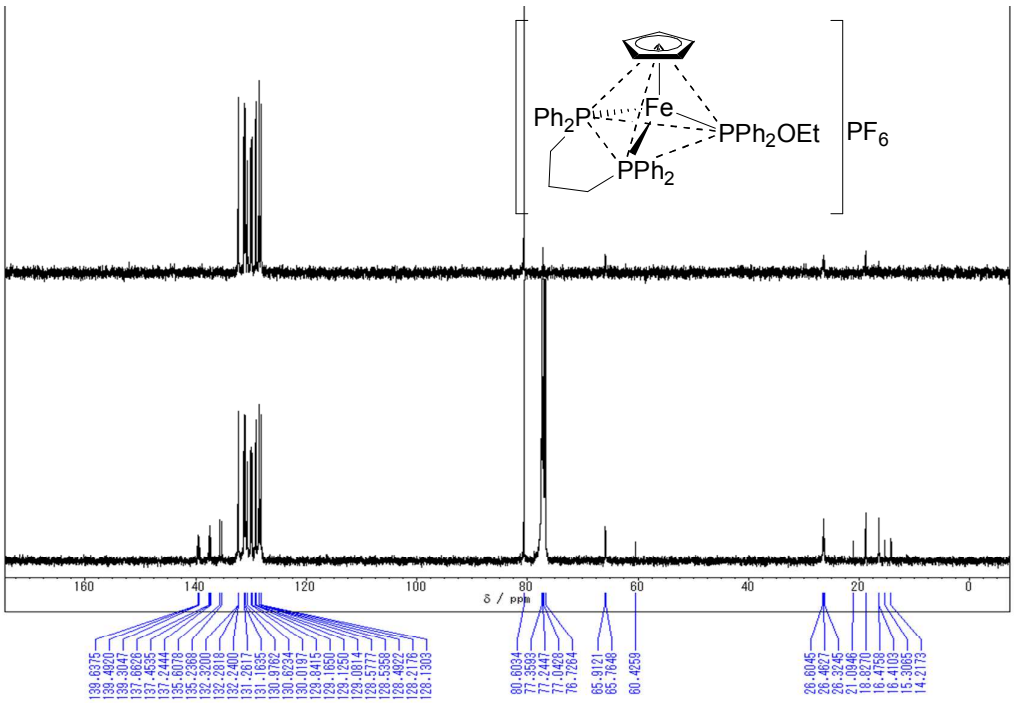

Figure S22-2. ^{13}C NMR Spectra of [CpFe(dppp)PPh$_2$(OEt)]PF$_6$ in CDCl$_3$ at 293 K (top: DEPT135, bottom: decoupling).

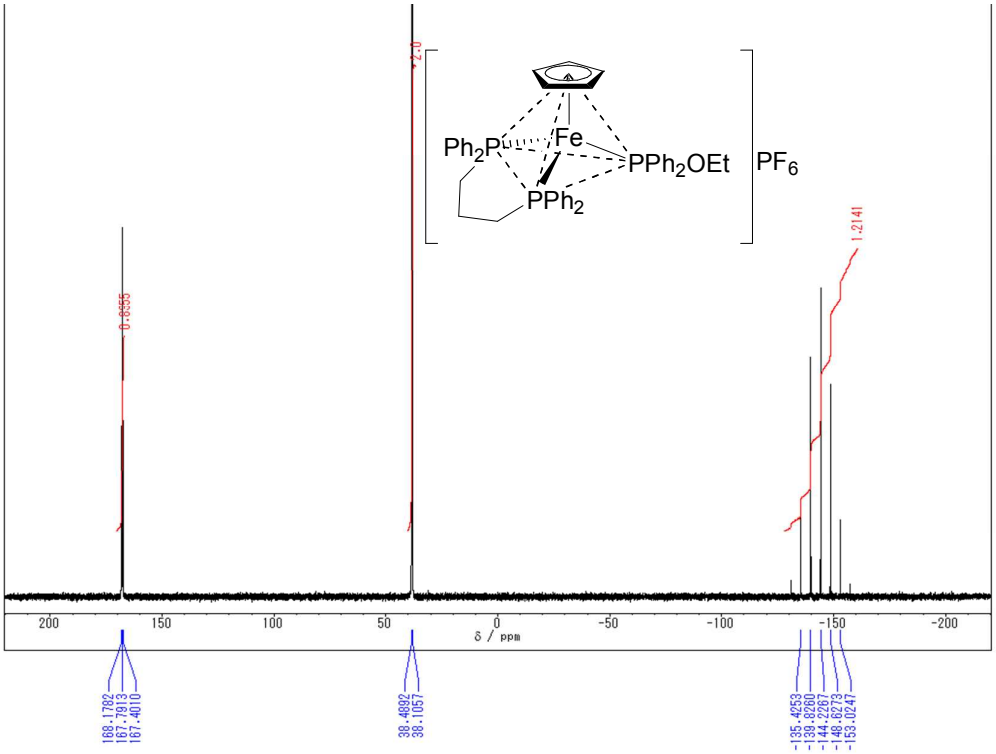

Figure S22-3. $^{31}P\{^{1}H\}$ NMR Spectrum of $[CpFe(dppp)PPh_2(OEt)]PF_6$ in $CDCl_3$ at 293 K.

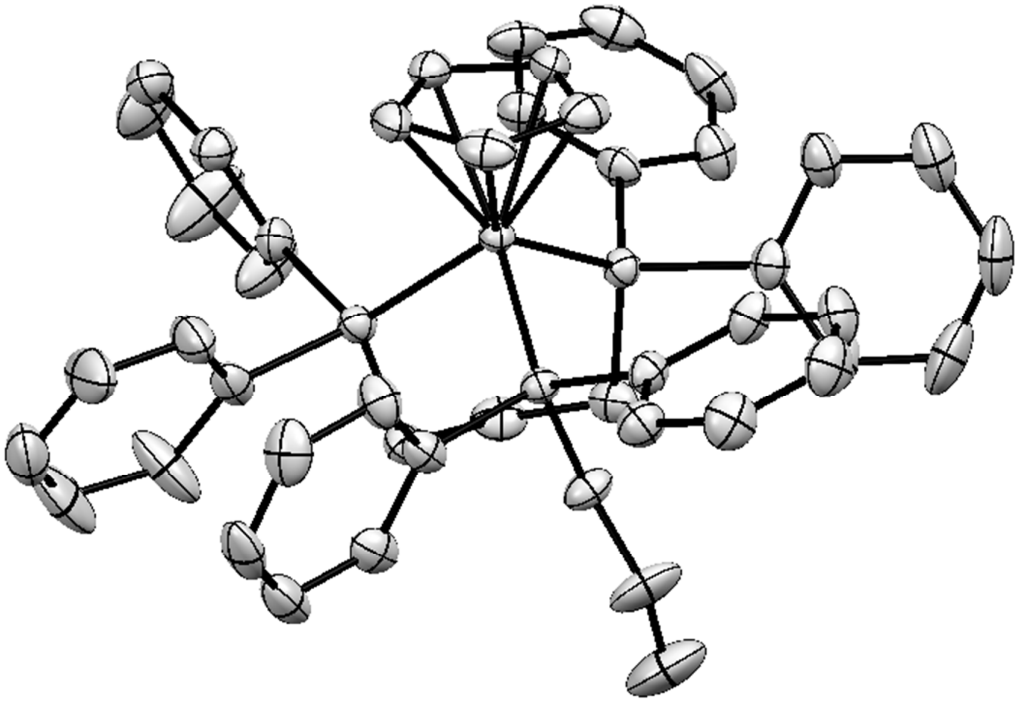

Figure S22-4. ORTEP drawing of $[CpFe(dppp)PPh_2(OEt)]PF_6$. Hydrogen atoms and hexafluorophosphate anion are omitted for clarity.

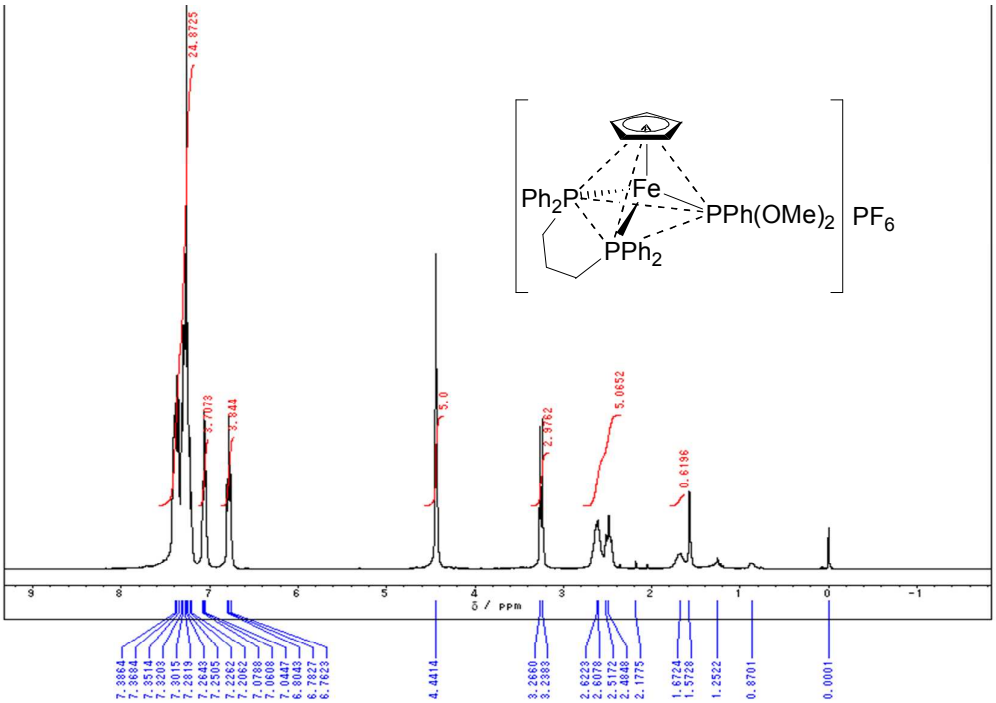

Figure S23-1. ^{1}H NMR Spectrum of [CpFe(dppp)PPh(OMe)$_2$]PF$_6$ in CDCl$_3$ at 293 K.

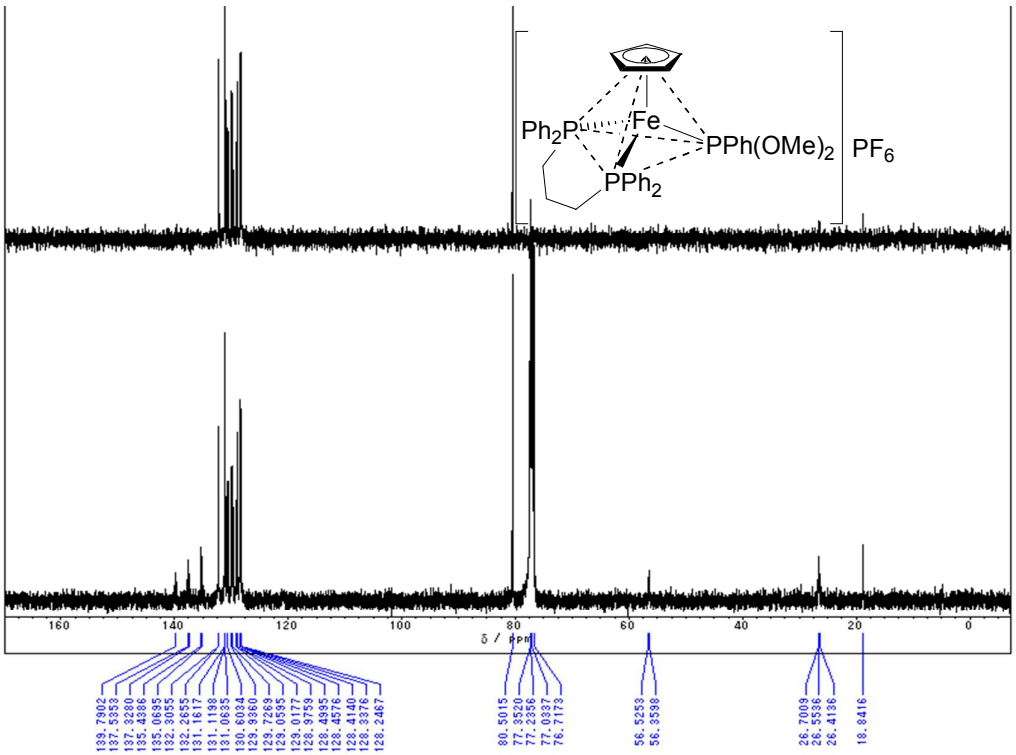

Figure S23-2. ^{13}C NMR Spectra of [CpFe(dppp)PPh(OMe)$_2$]PF$_6$ in CDCl$_3$ at 293 K (top: DEPT135, bottom: decoupling).

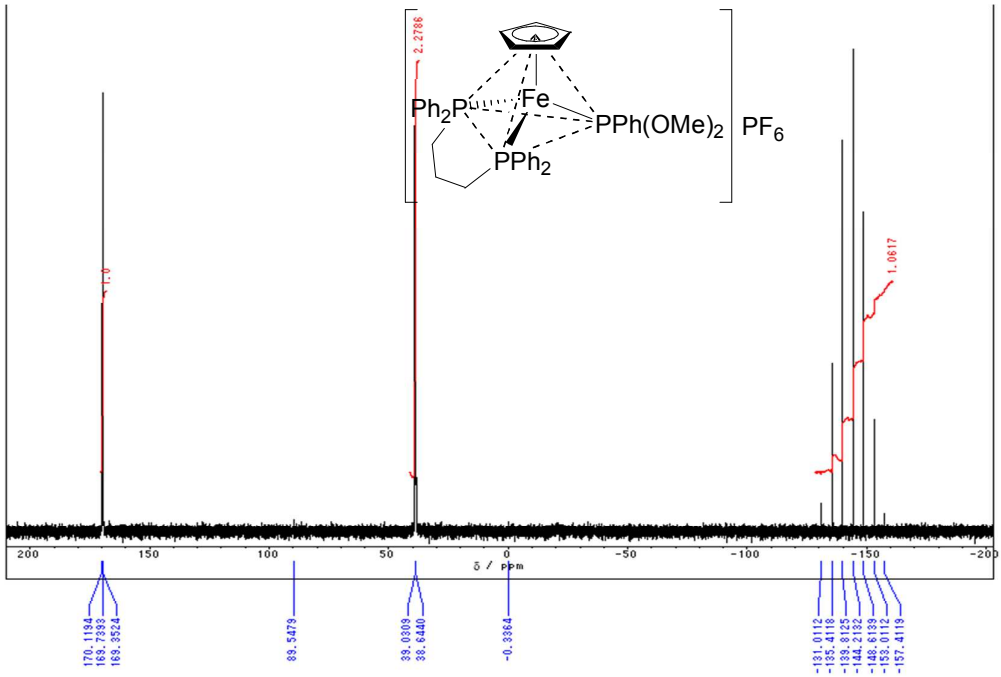

Figure S23-3. $^{31}P\{^{1}H\}$ NMR Spectrum of $[CpFe(dppp)PPh(OMe)_2]PF_6$ in $CDCl_3$ at 293 K.

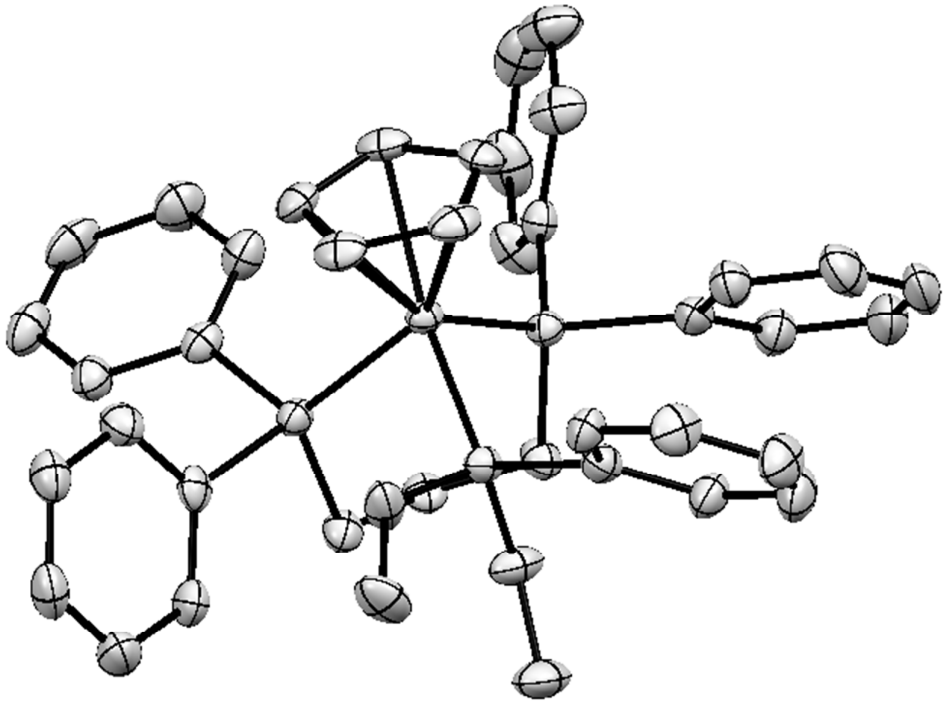

Figure S23-4. ORTEP drawing of $[CpFe(dppp)PPh(OMe)_2]PF_6$. Hydrogen atoms and hexafluorophosphate anion are omitted for clarity.

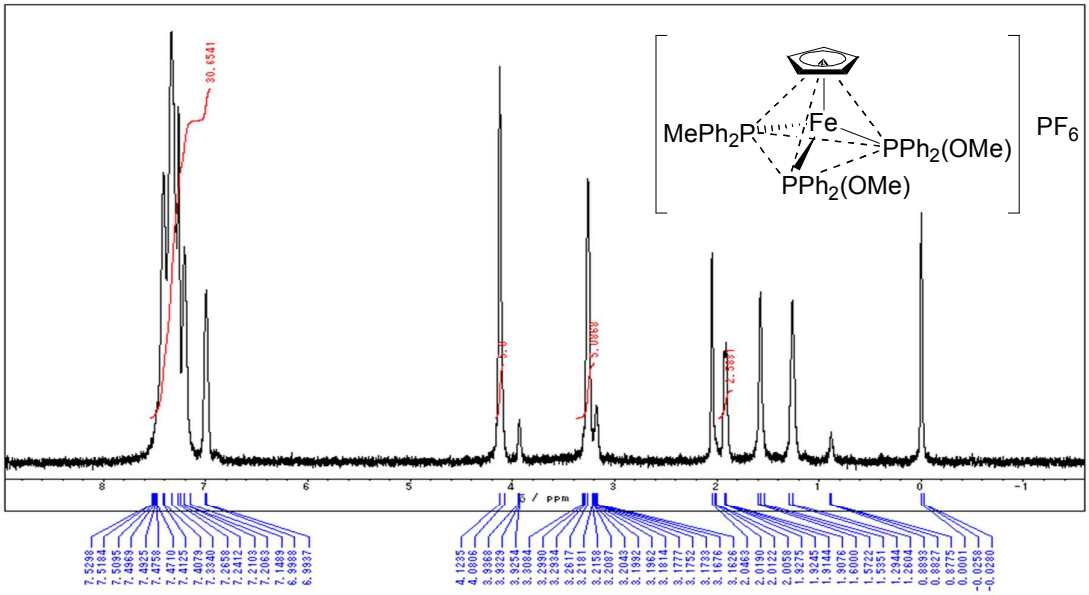

Figure S24-1. ^{1}H NMR Spectrum of $[CpFe(PPh_2Me)\{PPh_2(OMe)\}_2]PF_6$ in $CDCl_3$ at 293 K.

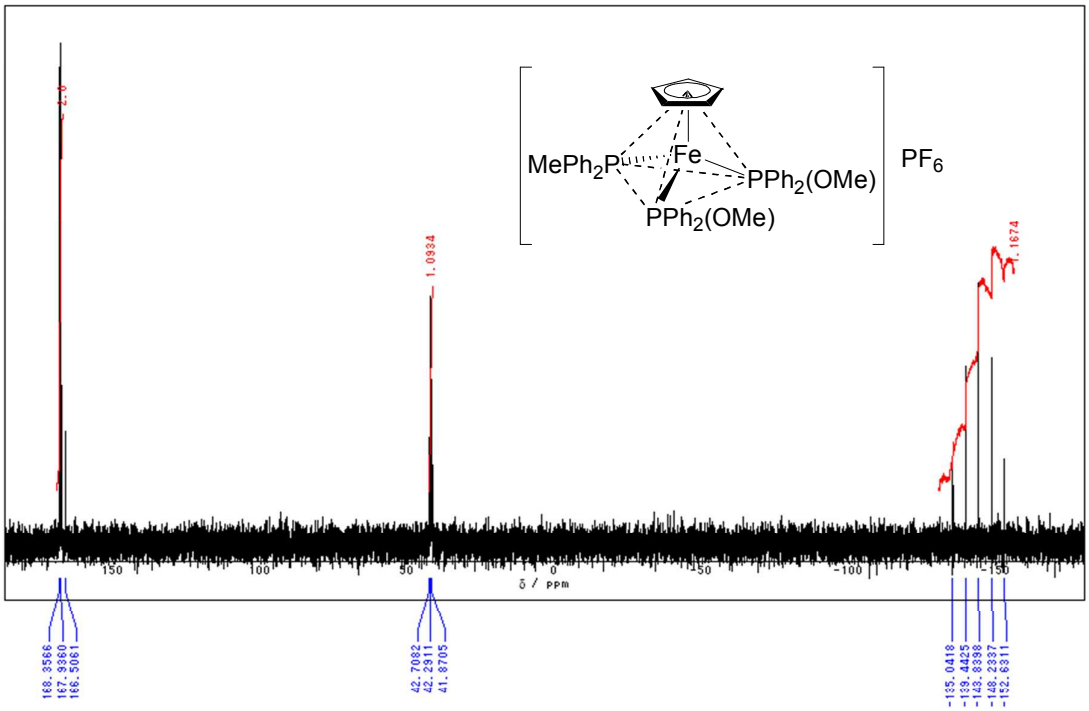

Figure S24-2. $^{31}P\{^{1}H\}$ NMR Spectrum of $[CpFe(PPh_2Me)\{PPh_2(OMe)\}_2]PF_6$ in $CDCl_3$ at 293 K.

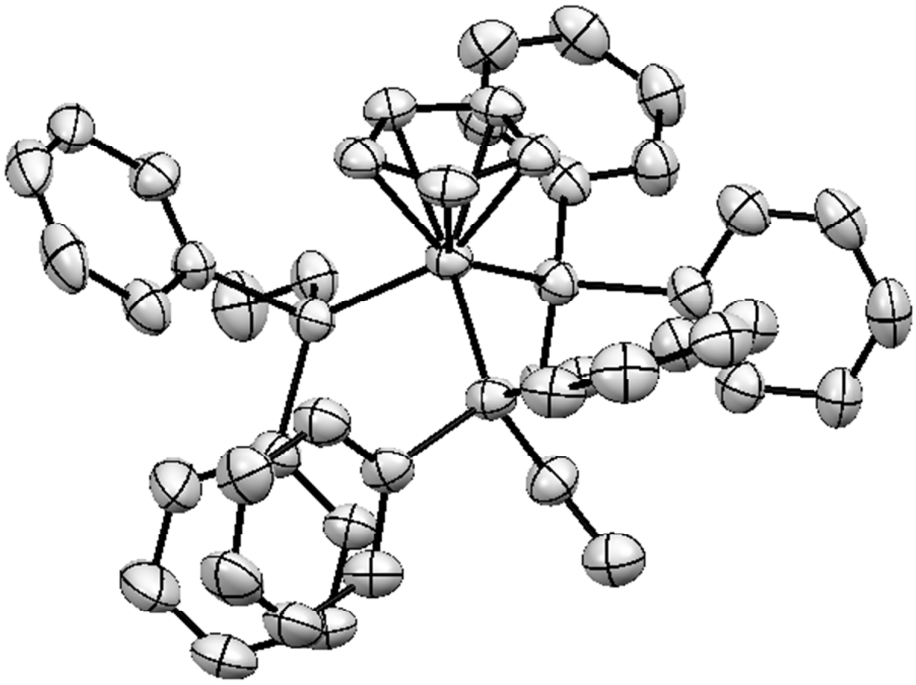

Figure S24-3. ORTEP drawing of $[CpFe(PPh_2Me)\{PPh_2(OMe)\}_2]PF_6 \cdot 2CH_2Cl_2$. Hydrogen atoms, hexafluorophosphate anion and CH_2Cl_2 molecules are omitted for clarity.

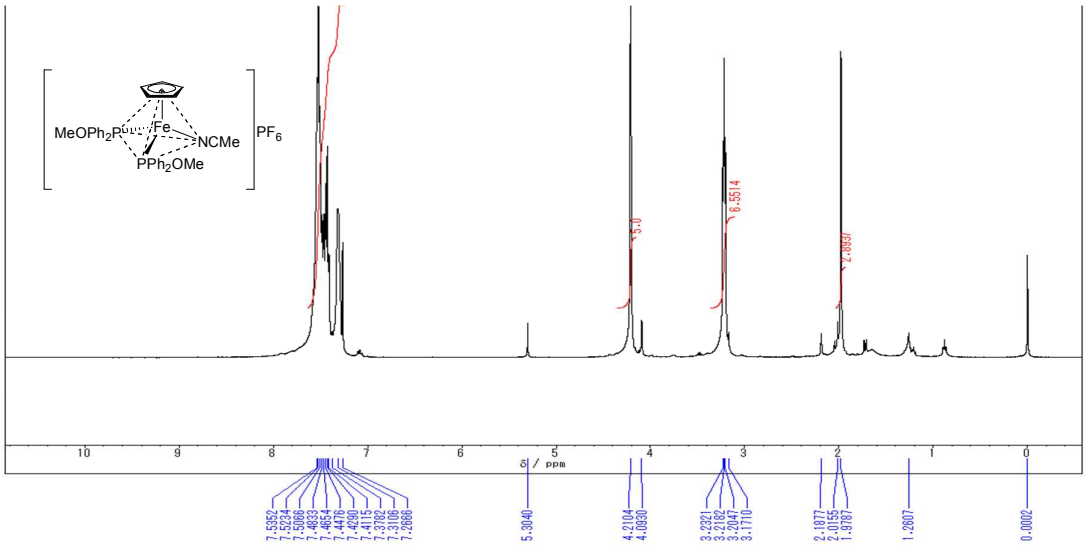

Figure S25-1. ^1H NMR Spectrum of $[CpFe\{PPh_2(OMe)\}_2NCMe]PF_6$ in $CDCl_3$ at 293 K.

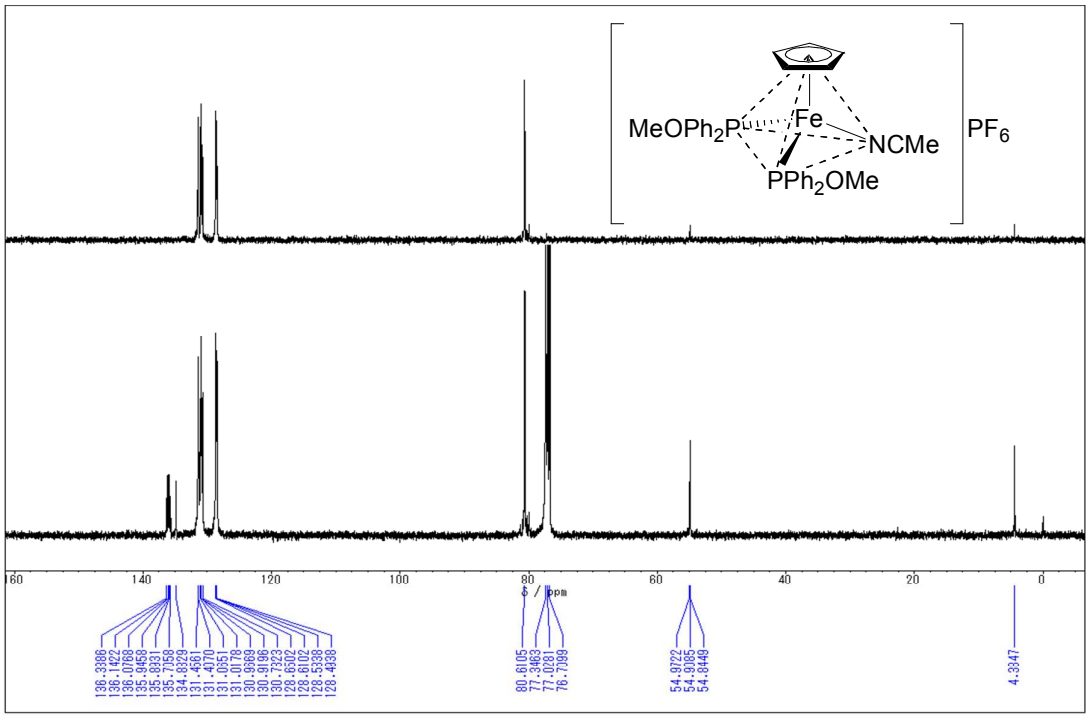

Figure S25-2. ^{13}C NMR Spectra of $[CpFe\{PPh_2(OMe)\}_2NCMe]PF_6$ in $CDCl_3$ at 293 K (top: DEPT135, bottom: decoupling).

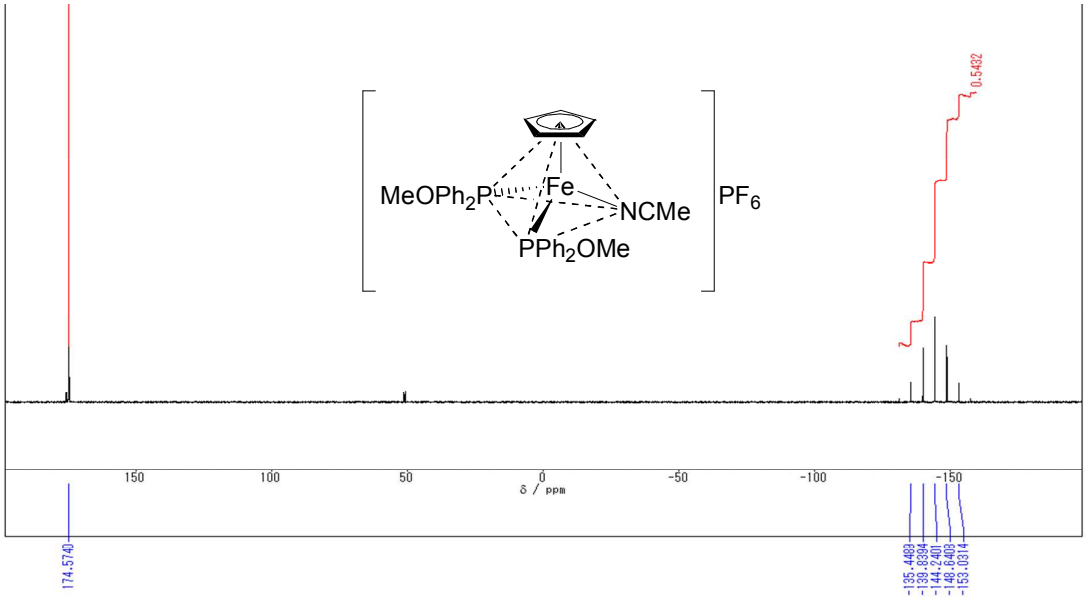

Figure S25-3. $^{31}P\{^1H\}$ NMR Spectrum of $[CpFe\{PPh_2(OMe)\}_2NCMe]PF_6$ in $CDCl_3$ at 293 K.

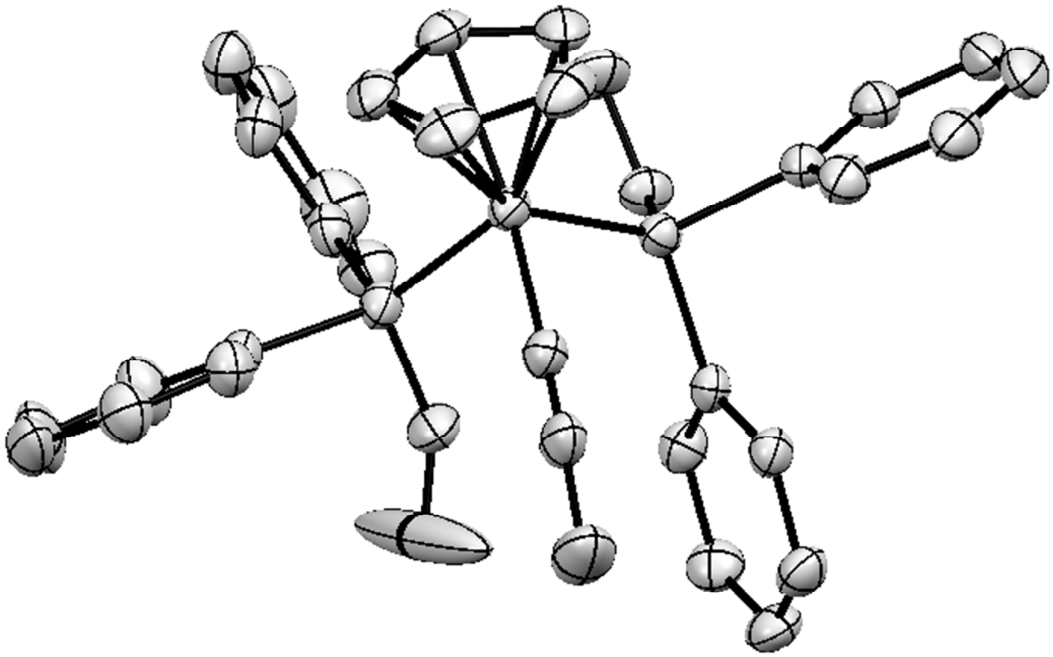

Figure S25-4. ORTEP drawing of [CpFe{$PPh_2(OMe)$}$_2$NCMe]PF_6. Hydrogen atoms and hexafluorophosphate anion are omitted for clarity.

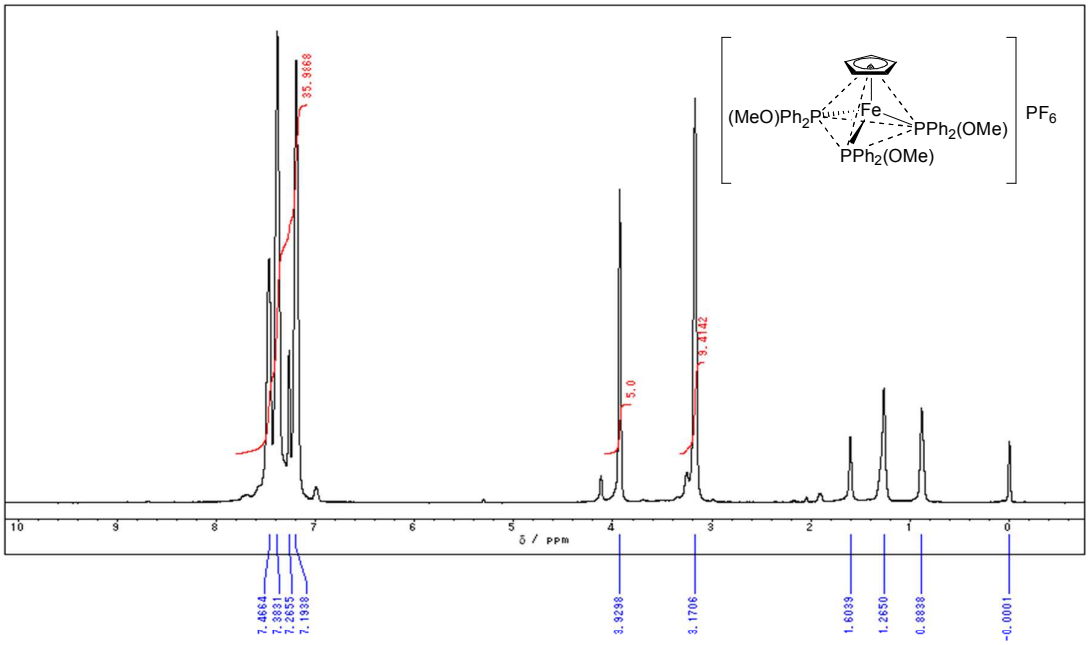

Figure S26-1. ^{1}H NMR Spectrum of [CpFe{$PPh_2(OMe)$}$_3$]PF_6 in $CDCl_3$ at 293 K.

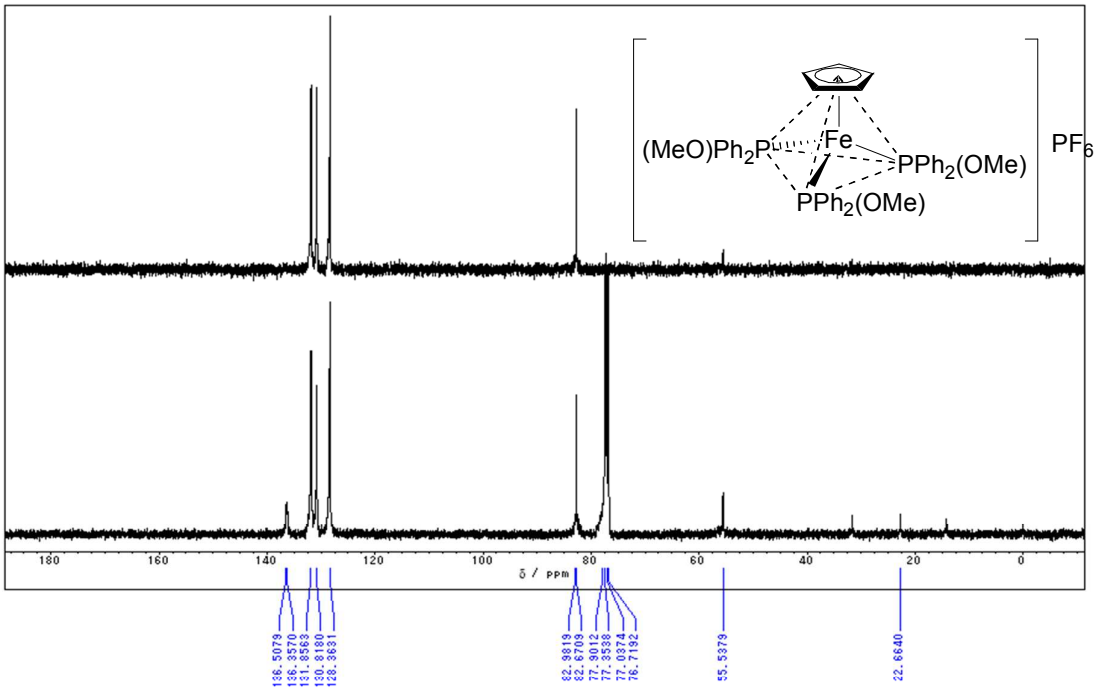

Figure S26-2. ^{13}C NMR Spectra of $[CpFe\{PPh_2(OMe)\}_3]PF_6$ in $CDCl_3$ at 293 K (top: DEPT135, bottom: decoupling).

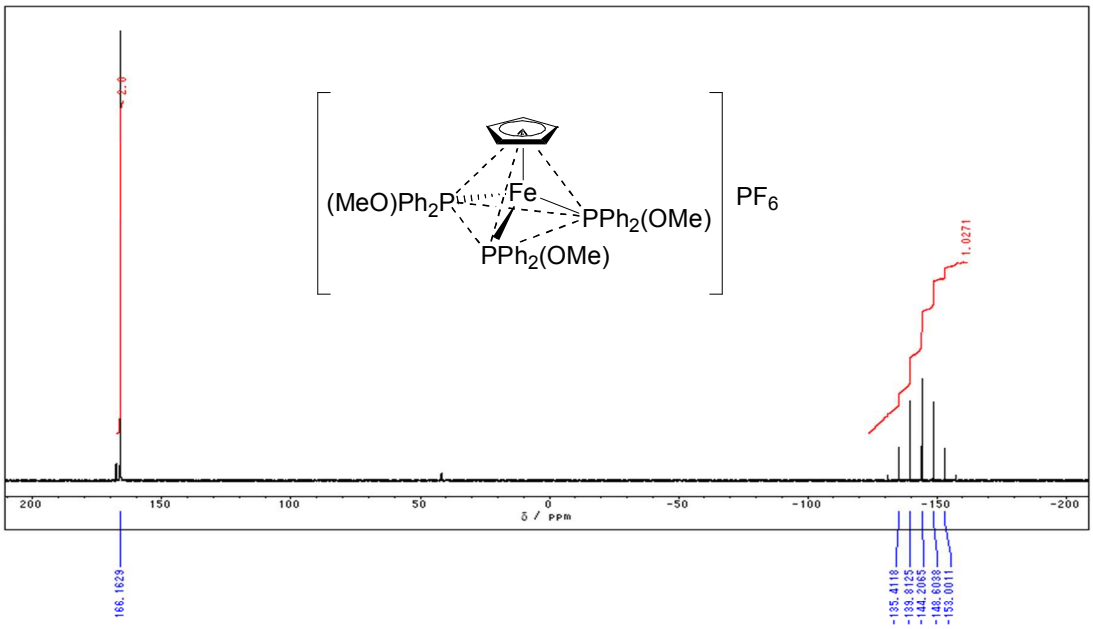

Figure S26-3. $^{31}P\{^1H\}$ NMR Spectrum of $[CpFe\{PPh_2(OMe)\}_3]PF_6$ in $CDCl_3$ at 293 K.

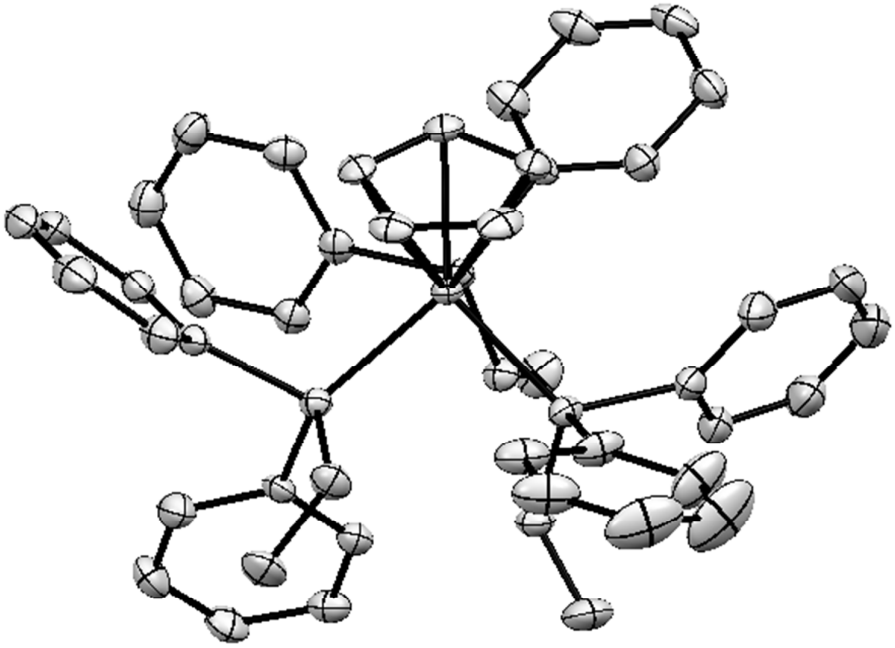

Figure S26-4. ORTEP drawing of $[CpFe\{PPh_2(OMe)\}_3]PF_6$. Hydrogen atoms, hexafluorophosphate anion, CH_2Cl_2 molecule are omitted for clarity.